Coarse-Graining Strategies for Soft Matter Simulations

Doros N. Theodorou

Computational Materials Science and Engineering Group, School of Chemical Engineering, National Technical University of Athens, Zografou Campus, 157 80 Athens, GREECE

doros@central.ntua.gr

Outline

- Need for multiscale modeling of materials.
- Potential of mean force with respect to selected degrees of freedom.
- Structural/thermodynamic coarse-graining: Force Matching, Iterative Boltzmann Inversion, Pretabulation of Interactions, Reverse Monte Carlo and Maximum Entropy methods.
- Reverse Mapping.
- Dynamical Coarse-Graining: Projection Operator Formalism.
- Langevin, Brownian, Dissipative Particle Dynamics Methods.
- Entanglement network simulations. EMSIPON.

Problems of the modern world

- Health
- Energy
- Environment
- Food

In solving these problems, a central role is played by the design of materials with prescribed properties and of processes and products based on these materials.

Contemporary materials design often involves molecular-level considerations.

> “About 10,000 years ago, humans began to domesticate plants and animals. Now it's time to domesticate molecules.”
>
> — Susan Lindquist, Whitehead Institute for Biomedical Research, Massachusetts Institute of Technology

Challenge: The behavior of materials is governed by very broad spectra of length and time scales

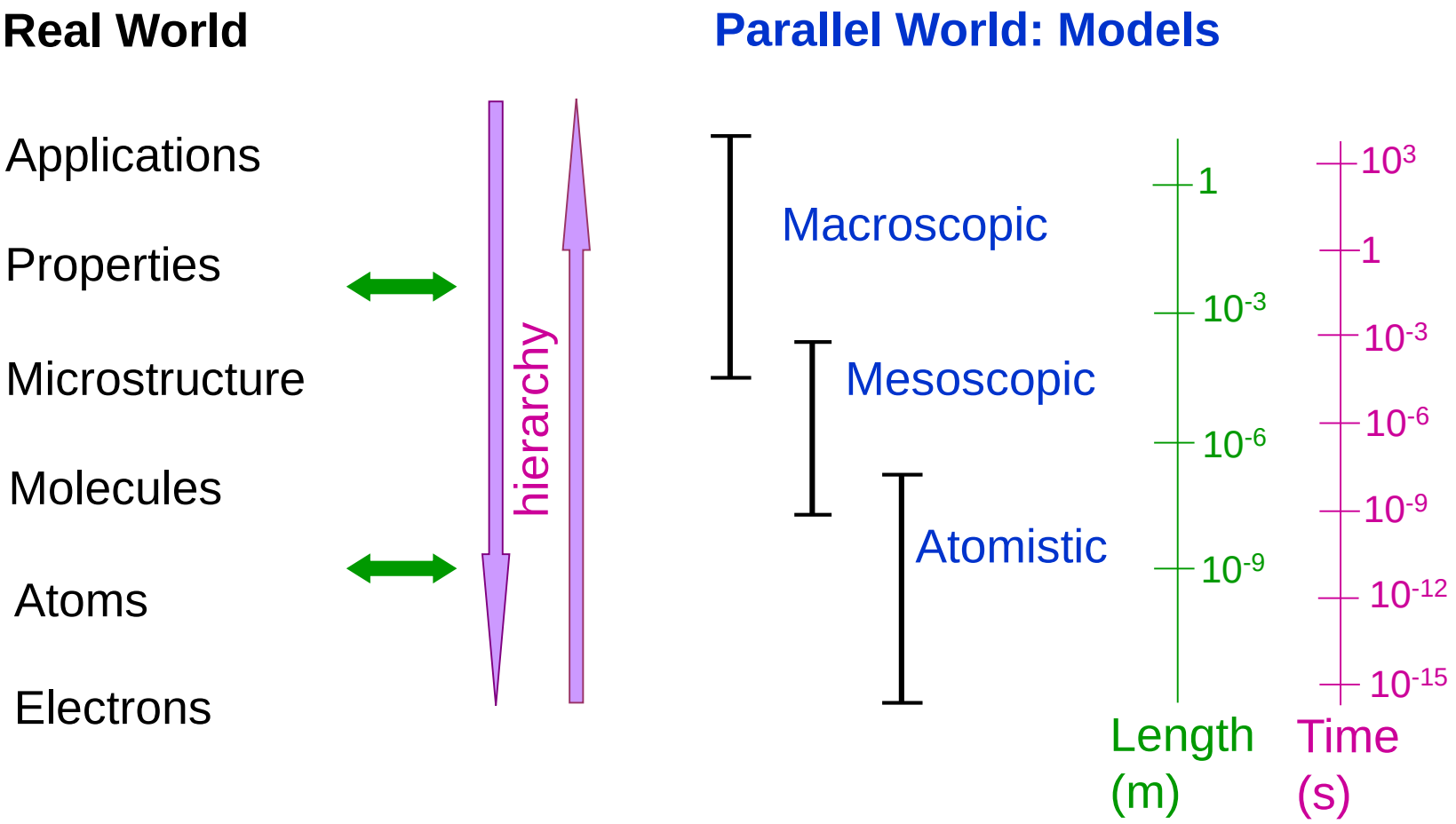

Multiscale Modeling of Materials

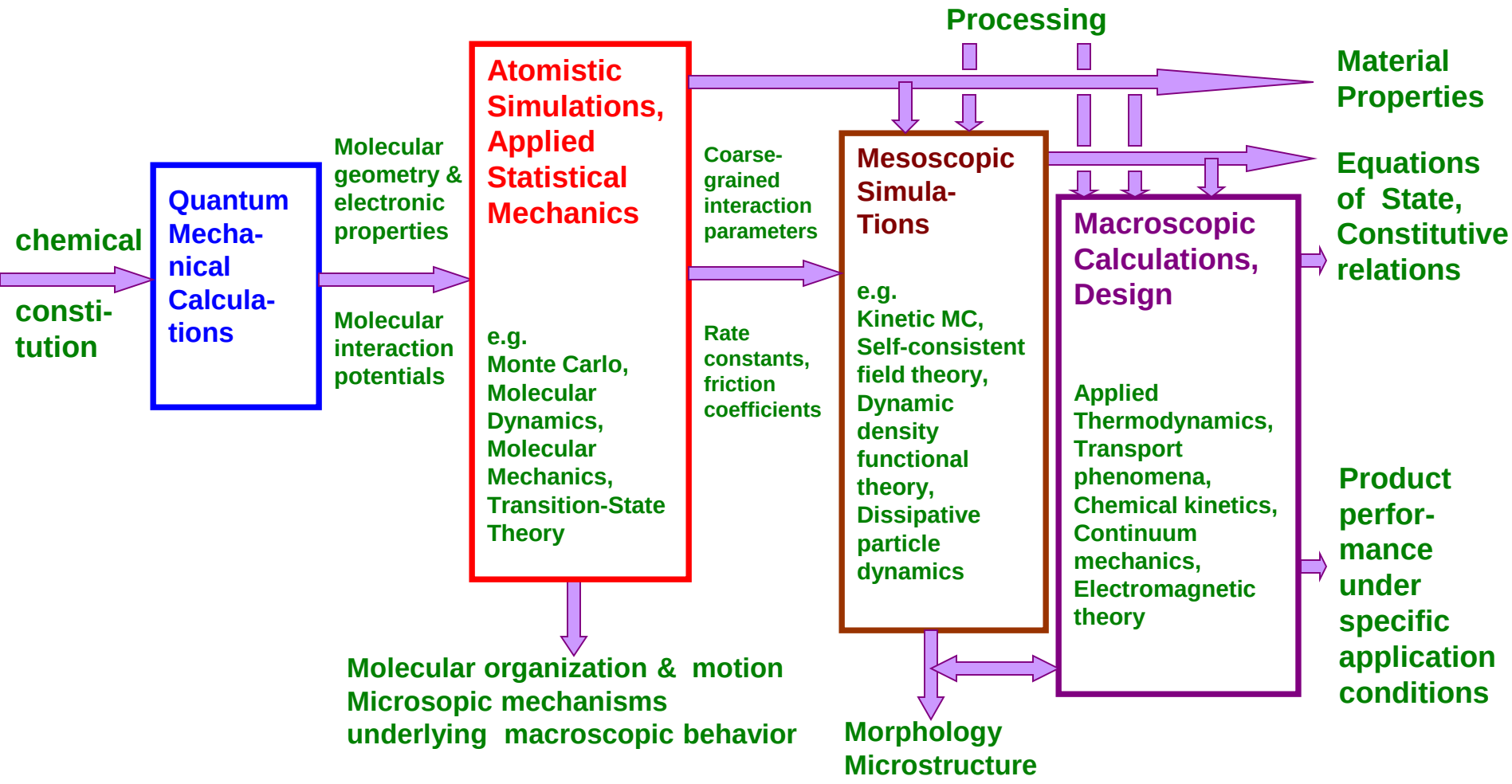

Multiscale modeling proceeds hand-in-hand with experimental measurements and guides efforts for the design of new materials.

Multiscale Modeling

Sequential

Passing parameters/functions between different levels of representation

Concurrent

e.g., AdResS

Kreis, K.; Potestio, R.; Kremer, K.; Fogarty, A.F. *J.Chem. Theory Comput.* **2016**, *12*, 4067-4081

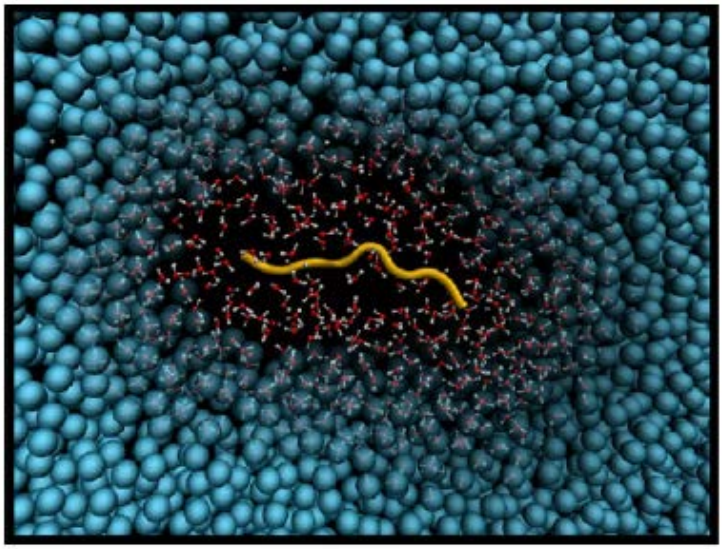

Coarse-Graining

“Top Down”

Fitting to experimental structural, thermodynamic, dynamical data.

e.g. MARTINI

Marrink, S.J.; Risselada, H.J.; Yefimov, S.; Tieleman, D.P.; de Vries, A.H. *J. Phys. Chem. B* **2004**, *108*, 750-760.

SAFT-γ-Mie

Fayaz-Torshizi, F.; Müller, E.A. *Macromol. Theory Simul*. **2022**, *31*, 2100031.

“Bottom-Up”

Effective interactions and parameters descriptive of the dynamics (friction factors, rate constants…) at the coarse-grained level derived from more fundamental levels.

Phase Diagrams of SDS and CTAB aqueous solutions

"Wet" MARTINI

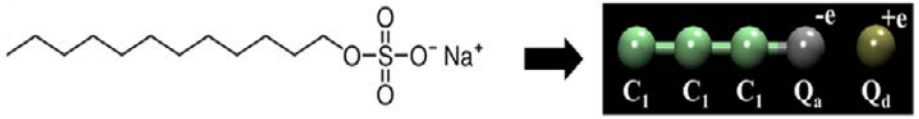

Sodium Dodecyl Sulfate (SDS)

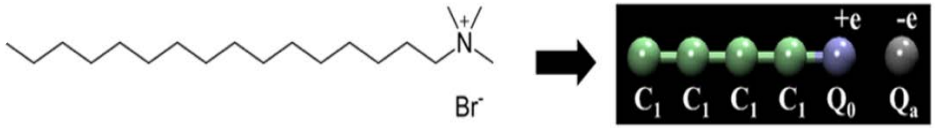

Cetyl Trimethyl Ammonium Bromide (CTAB)

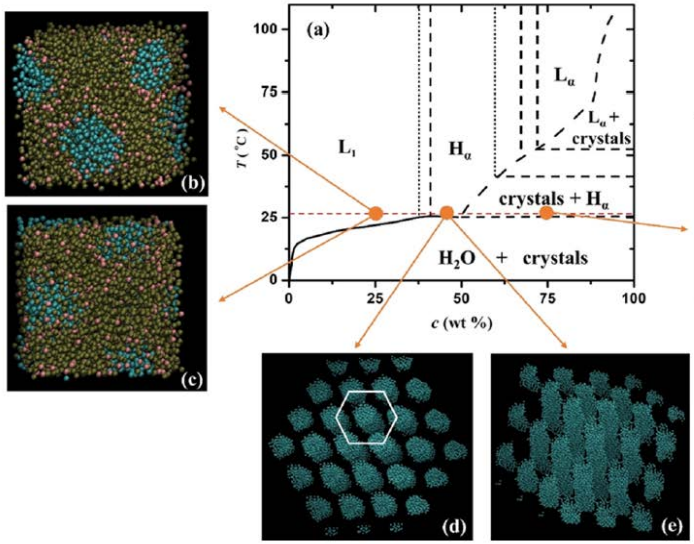

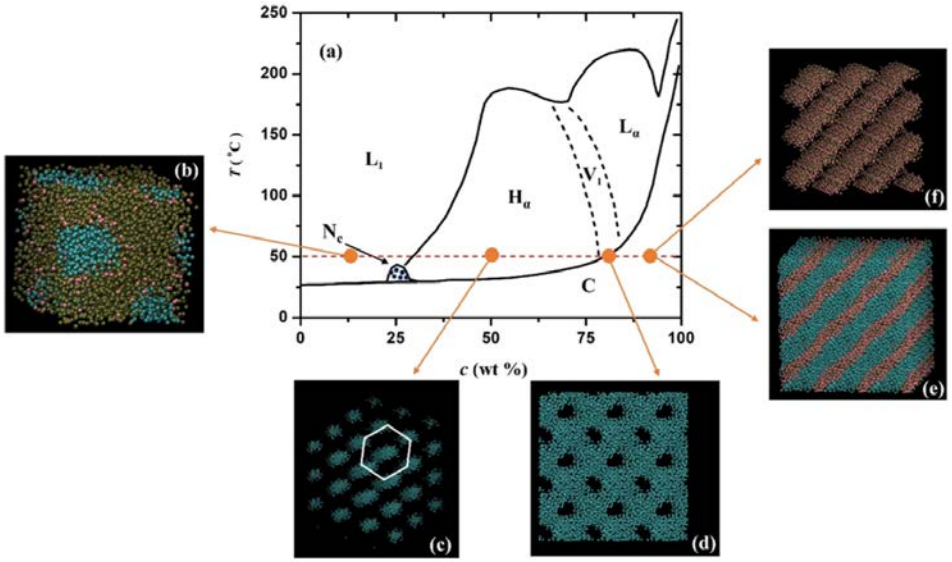

Anogiannakis, S.D.; Petris, P.C.; DNT *J. Phys. Chem. B* **2020**, *124*, 556-567.

Potential of Mean Force

Generally, if we distinguish the variables spanning the configuration space of a system into a subset of (slowly evolving) degrees of freedom, on which we want to focus, $\mathbf{R}$, and a subset of (fast) degrees of freedom, $\mathbf{r}_\mathrm{f}$:

Potential of mean force with respect to $\mathbf{R}$:

$$U_{\mathrm{mf}}(\mathbf{R}) = -k_\mathrm{B}T \ \ln \int \exp\left[-\beta \mathcal{V}(\mathbf{R}, \mathbf{r}_\mathrm{f})\right] d\mathbf{r}_\mathrm{f} \ + \text{const.}$$

Potential energy function

$U_{\mathrm{mf}}(\mathbf{R})$ is a configurational free energy, which describes effective interactions among the degrees of freedom $\mathbf{R}$, having projected out $\mathbf{r}_\mathrm{f}$.

At each $\mathbf{R}$, the $\mathbf{r}_\mathrm{f}$ are assumed to be fully equilibrated. This is physically reasonable when there is a clear time scale separation between the times governing the evolution of $\mathbf{R}$ and $\mathbf{r}_\mathrm{f}$.

Note: $$-\nabla_{\mathbf{R}_i} U_{\mathrm{mf}}(\mathbf{R}) = k_\mathrm{B}T\beta \frac{\int \left[-\nabla_{\mathbf{R}_i} \mathcal{V}(\mathbf{R}, \mathbf{r}_\mathrm{f})\right] \exp\left[-\beta \mathcal{V}(\mathbf{R}, \mathbf{r}_\mathrm{f})\right] d\mathbf{r}_\mathrm{f}}{\int \exp\left[-\beta \mathcal{V}(\mathbf{R}, \mathbf{r}_\mathrm{f})\right] d\mathbf{r}_\mathrm{f}} = \left\langle \mathbf{F}_i \right\rangle_{\mathbf{R}}$$

$$\rho(\mathbf{R}) = \frac{\int \exp\left[-\beta \mathcal{V}(\mathbf{R}, \mathbf{r}_\mathrm{f})\right] d\mathbf{r}_\mathrm{f}}{\int \exp\left[-\beta \mathcal{V}(\mathbf{R}, \mathbf{r}_\mathrm{f})\right] d\mathbf{r}_\mathrm{f} d\mathbf{R}} = C \exp\left[-\beta U_{\mathrm{mf}}(\mathbf{R})\right]$$

Example of a Potential of Mean Force

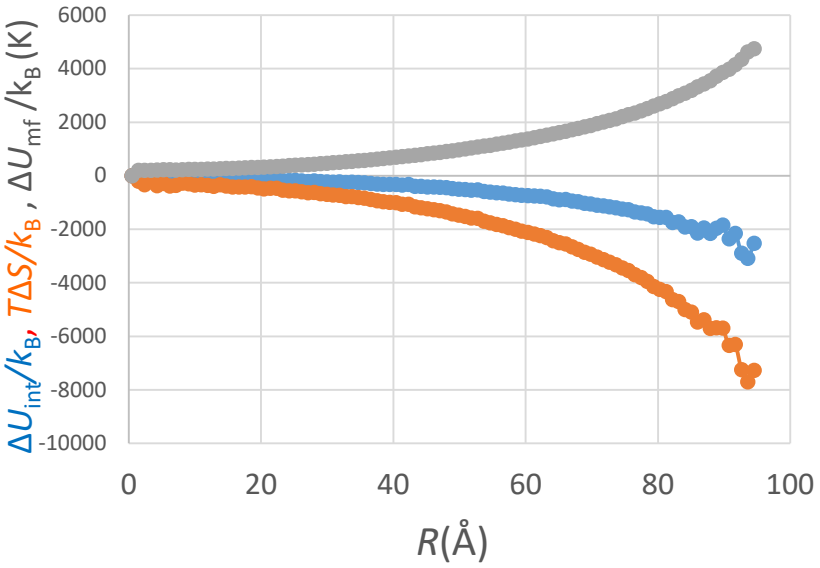

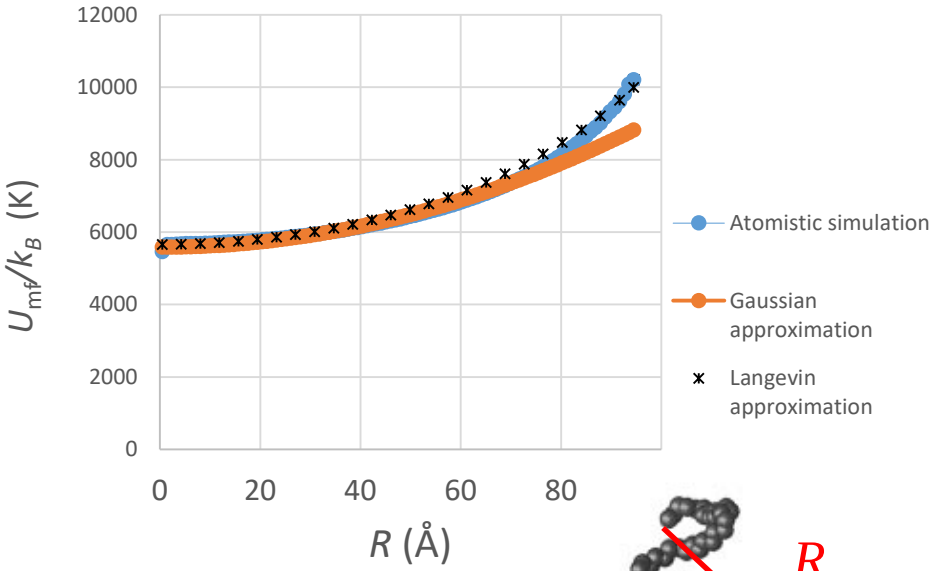

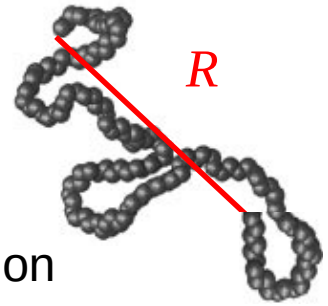

Single unperturbed C_{100} PE chain: Potential of mean force (Helmholtz energy) as a function of the end-to-end distance R:

$\Delta U_{\mathrm{mf}}(R) = U_{\mathrm{mf}}(R) - U_{\mathrm{mf}}(0)$ from united-atom Monte Carlo simulation

$T\Delta S$: Minus entropic part of ΔU_{mf}

ΔU_{int}: Internal Energy part of ΔU_{mf}

Approximations to $U_{\mathrm{mf}}(R)$ according to the Gaussian model and to the inverse Langevin model also shown.

Frangou, M. Diploma Thesis, School of Chemical Engineering, NTUA, 2016.

Potential of mean force between two spherical PS-grafted SiO_2 nanoparticles in PS melt (3D SCFT)

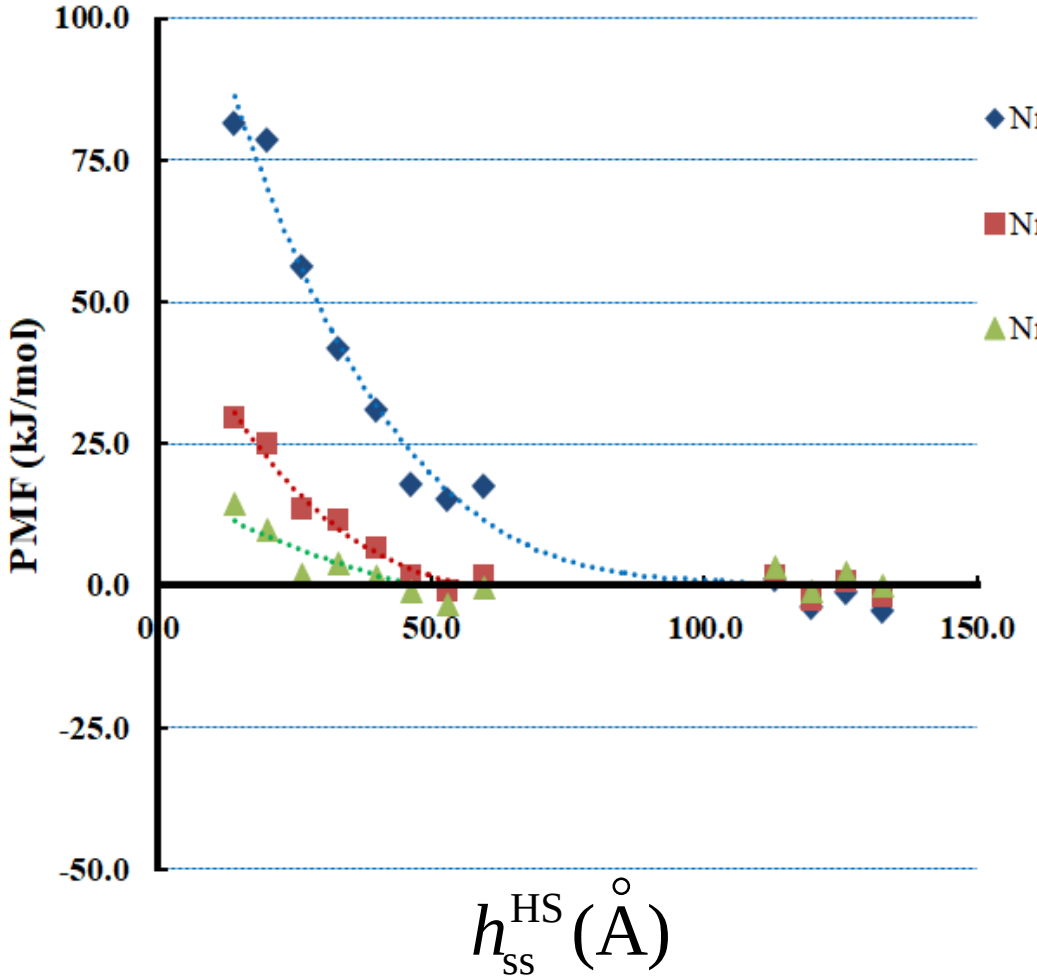

Uniformly grafted

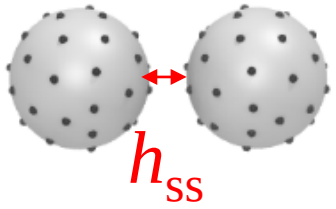

R_{NP}=2 nm

N_g=100 skel. carbons

σ_g= 0.8 chains/nm^2

T=500 K

$h_{ss}^{HS} = h_{ss} - 8\,\text{Å}$

Example of a Potential of Mean Force

Alkanes in silicalite:

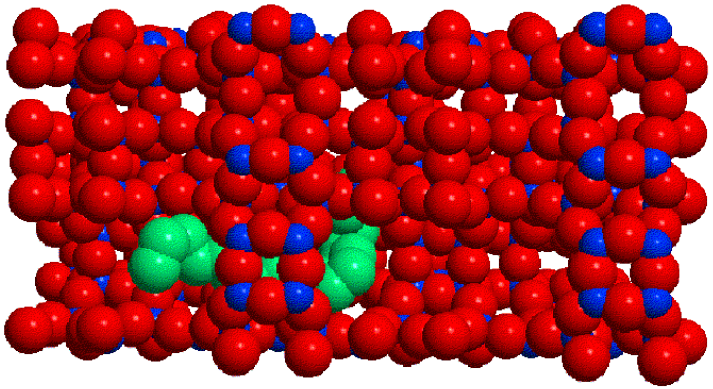

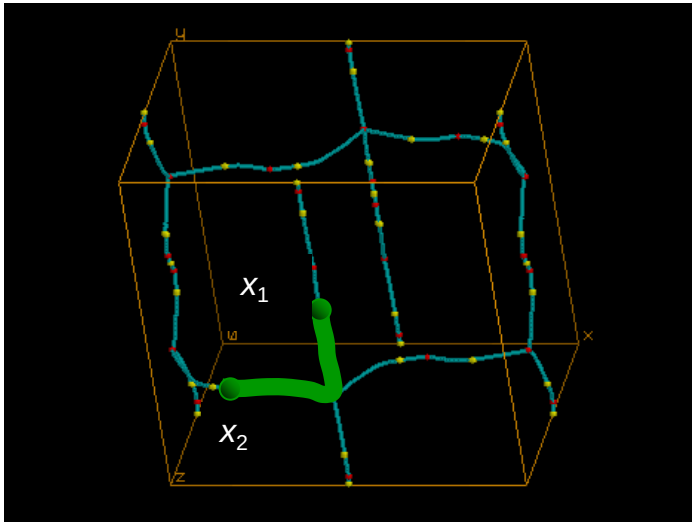

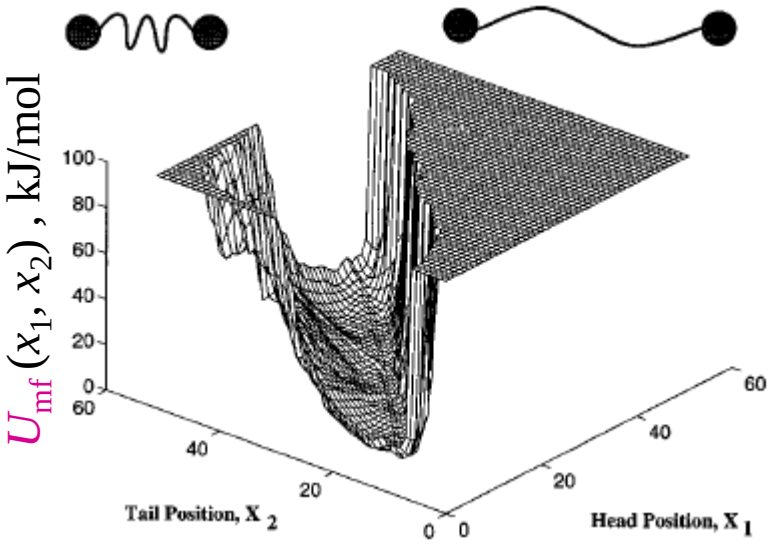

R= (x_1, x_2) : positions of chain ends along the channel segments in which they reside.

Potential of mean force $U_{mf}(x_1, x_2)$

Maginn, E.J.; Bell, A.T., DNT *J.Phys.Chem.* **100**, 7155-7173 (1996).

Configurational Coarse-Graining

Atomistic Description:

System of N_{ch} (macro)molecules, each consisting of N_{mon} particles. Configuration described by $3n$-dimensional vector $\mathbf{r}^n$, $n = N_{\mathrm{ch}}\, N_{\mathrm{mon}}$

Coarse-Grained Description:

System of N_{ch} (macro)molecules, each consisting of $N_{\mathrm{b}} = N_{\mathrm{mon}}/\lambda$ effective particles. Configuration described by $3N$-dimensional position vector $\mathbf{R}^N$, $N = N_{\mathrm{ch}}\, N_{\mathrm{b}}$.

Let $U_{\mathrm{mf}}(\mathbf{R}^N)$ be the potential of mean force with respect to the coarse-grained variables. By definition, configurational integral is given by

$$Z \equiv \int e^{-\beta \mathcal{V}\left(\mathbf{r}^n\right)} \mathrm{d}\mathbf{r}^n = \int e^{-\beta U_{\mathrm{mf}}\left(\mathbf{R}^N\right)} \mathrm{d}\mathbf{R}^N$$

Assume that $U_{\mathrm{mf}}(\mathbf{R}^N)$ is given by an additive expression of the form

$$U_{\mathrm{mf}}\left(\mathbf{R}^N\right) \approx U_\lambda^{\mathrm{CG}}\left(\mathbf{R}^N\right) = \sum_{i=1}^{N_{\mathrm{ch}}} \left(\sum_{J=2}^{N_{\mathrm{b}}} U_\lambda^{\mathrm{CG,str}}\left(\mathbf{R}_{J-1}, \mathbf{R}_J\right) + \sum_{J=2}^{N_{\mathrm{b}}-1} U_\lambda^{\mathrm{CG,bend}}\left(\mathbf{R}_{J-1}, \mathbf{R}_J, \mathbf{R}_{J+1}\right) + \sum_{J=2}^{N_{\mathrm{b}}-2} U_\lambda^{\mathrm{CG,tor}}\left(\mathbf{R}_{J-1}, \mathbf{R}_J, \mathbf{R}_{J+1}, \mathbf{R}_{J+2}\right) \right)$$
$$+ \sum_{I<J}^{N} U_\lambda^{\mathrm{CG,nb}}\left(\mathbf{R}_I, \mathbf{R}_J\right)$$

How can effective stretching, bending, torsion and nonbonded interaction potentials be determined from the atomistic force field?

A general formulation

Atomistic Description:

Coordinates $\left\{\mathbf{r}^n\right\}=\left\{\mathbf{r}_1,\mathbf{r}_2,...,\mathbf{r}_n\right\}$, momenta $\left\{\mathbf{p}^n\right\}=\left\{\mathbf{p}_1,\mathbf{p}_2,...,\mathbf{p}_n\right\}$, $\mathbf{p}_i=m_i\dot{\mathbf{r}}_i$.

Hamiltonian $h\left(\mathbf{r}^n,\mathbf{p}^n\right)=\sum_{i=1}^{n}\frac{1}{2m_i}\mathbf{p}_i^2+\mathcal{V}\left(\mathbf{r}^n\right)$

Equilibrium phase-space probability density $\rho_{rp}\left(\mathbf{r}^n,\mathbf{p}^n\right)=\rho_r\left(\mathbf{r}^n\right)\rho_p\left(\mathbf{p}^n\right)$

$$\rho_r\left(\mathbf{r}^n\right)\sim\exp\left[-\beta\mathcal{V}\left(\mathbf{r}^n\right)\right]\quad,\quad\rho_p\left(\mathbf{p}^n\right)\sim\exp\left[-\beta\sum_{i=1}^{n}\frac{\mathbf{p}_i^2}{2m_i}\right]$$

Coarse-Grained Description:

Coordinates $\left\{\mathbf{R}^N\right\}=\left\{\mathbf{R}_1,\mathbf{R}_2,...,\mathbf{R}_N\right\}$, momenta $\left\{\mathbf{P}^N\right\}=\left\{\mathbf{P}_1,\mathbf{P}_2,...,\mathbf{P}_N\right\}$, $\mathbf{P}_I=M_I\dot{\mathbf{R}}_I$

CG Hamiltonian $H\left(\mathbf{R}^N,\mathbf{P}^N\right)=\sum_{I=1}^{N}\frac{1}{2M_I}\mathbf{P}_I^2+U\left(\mathbf{R}^N\right)$

Equilibrium phase-space probability density $P_{RP}\left(\mathbf{R}^N,\mathbf{P}^N\right)=P_R\left(\mathbf{R}^N\right)P_P\left(\mathbf{P}^N\right)$

$$P_R\left(\mathbf{R}^N\right)\sim\exp\left[-\beta U\left(\mathbf{R}^N\right)\right]\quad,\quad P_P\left(\mathbf{P}^N\right)\sim\exp\left[-\beta\sum_{I=1}^{N}\frac{\mathbf{P}_I^2}{2M_I}\right]$$

Noid, W.G., Chu, J.-W., Ayton, G.S., Krishna, V., Izvekov, S., Voth, V.A., Das, A., and Andersen, H.C. *J. Chem. Phys.* **2008**, *128*, 244114.

Assume that positions and momenta of CG model are specified in terms of positions and momenta of atomistic model via the following **linear** relations:

$$\mathbf{R}^N = \mathbf{M}_\mathbf{R}\left(\mathbf{r}^n\right) \text{ or } \mathbf{R}_I = \sum_{i=1}^{n} C_{Ii}\mathbf{r}_i, \quad I = 1,2,...,N$$

$$\mathbf{P}^N = \mathbf{M}_\mathbf{P}\left(\mathbf{p}^n\right) \text{ or } \mathbf{P}_I = M_I \sum_{i=1}^{n} C_{Ii}\mathbf{p}_i / m_i, \quad I = 1,2,...,N$$

Consistency between atomistic and CG models:

$$\exp\left[-\beta U\left(\mathbf{R}^N\right)\right] \sim \int \exp\left[-\beta \mathcal{V}\left(\mathbf{r}^n\right)\right] \delta\left(\mathbf{M}_\mathbf{R}\left(\mathbf{r}^n\right) - \mathbf{R}^N\right) \mathrm{d}\mathbf{r}^n$$

$$\exp\left[-\beta \sum_{i=1}^{N} \frac{\mathbf{P}_i^2}{2M_i}\right] \sim \int \exp\left[-\beta \sum_{i=1}^{n} \frac{\mathbf{p}_i^2}{2m_i}\right] \delta\left(\mathbf{M}_\mathbf{P}\left(\mathbf{p}^n\right) - \mathbf{P}^N\right) \mathrm{d}\mathbf{p}^n$$

First consistency condition leads to:

$$U\left(\mathbf{R}^N\right) = -k_\mathrm{B} T \ln z\left(\mathbf{R}^N\right) + \text{const}$$

$$z\left(\mathbf{R}^N\right) \sim \int \exp\left[-\beta \mathcal{V}\left(\mathbf{r}^n\right)\right] \delta\left(\mathbf{M}_\mathbf{R}\left(\mathbf{r}^n\right) - \mathbf{R}^N\right) \mathrm{d}\mathbf{r}^n$$

Noid, W.G., Chu, J.-W., Ayton, G.S., Krishna, V., Izvekov, S., Voth, V.A., Das, A., and Andersen, H.C. *J. Chem. Phys.* **2008**, *128*, 244114.

Forces in CG model:

$$\mathbf{F}_I\left(\mathbf{R}^N\right)=-\frac{\partial U\left(\mathbf{R}^N\right)}{\partial \mathbf{R}_I}=\frac{k_{\mathrm{B}}T}{z\left(\mathbf{R}^N\right)}\int \exp\left[-\beta\mathcal{V}\left(\mathbf{r}^n\right)\right]\prod_{J\neq I}\delta\left(\sum_j C_{Jj}\mathbf{r}_j-\mathbf{R}_J\right)\frac{\partial}{\partial \mathbf{R}_I}\delta\left(\sum_i C_{Ii}\mathbf{r}_i-\mathbf{R}_I\right)\mathrm{d}\mathbf{r}^n$$

Definitions:

Set of atoms i **involved** in the definition of CG site I: $I_I=\left\{i\,|\,C_{Ii}\neq 0\right\},\ \ \forall I=1,2,...,N$

Set of atoms **specific** to CG site I: $S_I=\left\{i\,|\,C_{Ii}\neq 0 \text{ and } C_{Ji}=0\ \ \forall J\neq I\right\},\ \ \forall I=1,2,...,N$

Introduce set of constant coefficients $\left\{d_{Ii}\right\}$ for each site I of CG model:

$d_{Ii}\neq 0$ iff $i\in S_I$ and $\sum_{j\in S_I} d_{Ij}=1\ \ \forall I=1,2,...,N$

Using the set $\left\{d_{Ii}\right\}$ one obtains

$$\mathbf{F}_I\left(\mathbf{R}^N\right)=\left\langle \mathbb{F}_I\left(\mathbf{r}^n\right)\right\rangle_{\mathbf{R}^N} \qquad \text{where}$$

$$\mathbb{F}_I\left(\mathbf{r}^n\right)=\sum_{j\in S_I}\frac{d_{Ij}}{C_{Ij}}\mathbf{f}_j\left(\mathbf{r}^n\right)=-\sum_{j\in S_I}\frac{d_{Ij}}{C_{Ij}}\frac{\partial\mathcal{V}\left(\mathbf{r}^n\right)}{\partial\mathbf{r}_j} \qquad \text{and}$$

$$\left\langle \mathcal{A}\left(\mathbf{r}^n\right)\right\rangle_{\mathbf{R}^N}\equiv\frac{\int\mathcal{A}\left(\mathbf{r}^n\right)\exp\left[-\beta\mathcal{V}\left(\mathbf{r}^n\right)\right]\delta\left(\mathbf{M}_{\mathbf{R}}\left(\mathbf{r}^n\right)-\mathbf{R}^N\right)\mathrm{d}\mathbf{r}^n}{\int\exp\left[-\beta\mathcal{V}\left(\mathbf{r}^n\right)\right]\delta\left(\mathbf{M}_{\mathbf{R}}\left(\mathbf{r}^n\right)-\mathbf{R}^N\right)\mathrm{d}\mathbf{r}^n}$$

If no atom is involved in the definition of more than one coarse-grained sites, consistency in momentum space is ensured by

$$M_I=\left(\sum_{i\in I_I}\frac{C_{Ii}^2}{m_i}\right)^{-1}$$

Noid, W.G., Chu, J.-W., Ayton, G.S., Krishna, V., Izvekov, S., Voth, V.A., Das, A., and Andersen, H.C. *J. Chem. Phys.* **2008**, *128*, 244114.

$$\mathbf{F}_I\left(\mathbf{R}^N\right)=\left\langle \mathbb{F}_I\left(\mathbf{r}^n\right)\right\rangle_{\mathbf{R}^N}$$

$$\mathbb{F}_I\left(\mathbf{r}^n\right)=\sum_{j\in S_I}\frac{d_{Ij}}{C_{Ij}}\mathbf{f}_j\left(\mathbf{r}^n\right)=-\sum_{j\in S_I}\frac{d_{Ij}}{C_{Ij}}\frac{\partial\mathcal{V}\left(\mathbf{r}^n\right)}{\partial\mathbf{r}_j}$$

$$\left\langle \mathcal{A}\left(\mathbf{r}^n\right)\right\rangle_{\mathbf{R}^N}\equiv\frac{\int\mathcal{A}\left(\mathbf{r}^n\right)\exp\left[-\beta\mathcal{V}\left(\mathbf{r}^n\right)\right]\delta\left(\mathbf{M}_{\mathbf{R}}\left(\mathbf{r}^n\right)-\mathbf{R}^N\right)\mathrm{d}\mathbf{r}^n}{\int\exp\left[-\beta\mathcal{V}\left(\mathbf{r}^n\right)\right]\delta\left(\mathbf{M}_{\mathbf{R}}\left(\mathbf{r}^n\right)-\mathbf{R}^N\right)\mathrm{d}\mathbf{r}^n}$$

Forces in CG model: Averages of linear combinations of atomistic forces on sites specific to the CG sites.

$$M_I=\left(\sum_{i\in I_I}\frac{C_{Ii}^2}{m_i}\right)^{-1}$$

Masses of CG sites in terms of atomic masses

Variational principle for computation of many-body potential of mean force $U(\mathbf{R}^N)$:

- Consider, for each CG site I, the CG force field as a set of real continuous functions $\mathbf{G}_I\left\{\mathbf{R}^N\right\}, I=1,2,...,N \qquad \mathbf{G}_I=-\nabla_{\mathbf{R}_I}U$
- Minimize $\chi^2\left[\mathbf{G}\right]=\frac{1}{3N}\left\langle\sum_{I=1}^{N}\left|\mathbb{F}_I\left(\mathbf{r}^n\right)-\mathbf{G}_I\left(\mathbf{M}_{\mathbf{R}}\left(\mathbf{r}^n\right)\right)\right|^2\right\rangle$ with respect to the parameters of these functions. **"Force Matching"**

Noid, W.G., Chu, J.-W., Ayton, G.S., Krishna, V., Izvekov, S., Voth, V.A., Das, A., and Andersen, H.C. *J. Chem. Phys.* **2008**, *128*, 244114.

Multiscale Coarse-Graining Method (Force Matching)

Methanol Chargeless single-site CG model at molecular center of mass.
Pairwise CG potential represented by spline basis functions.

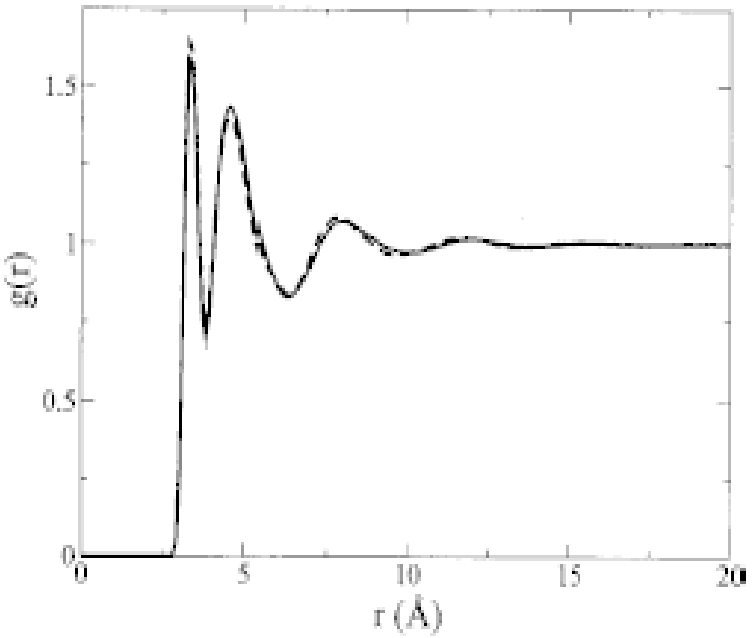

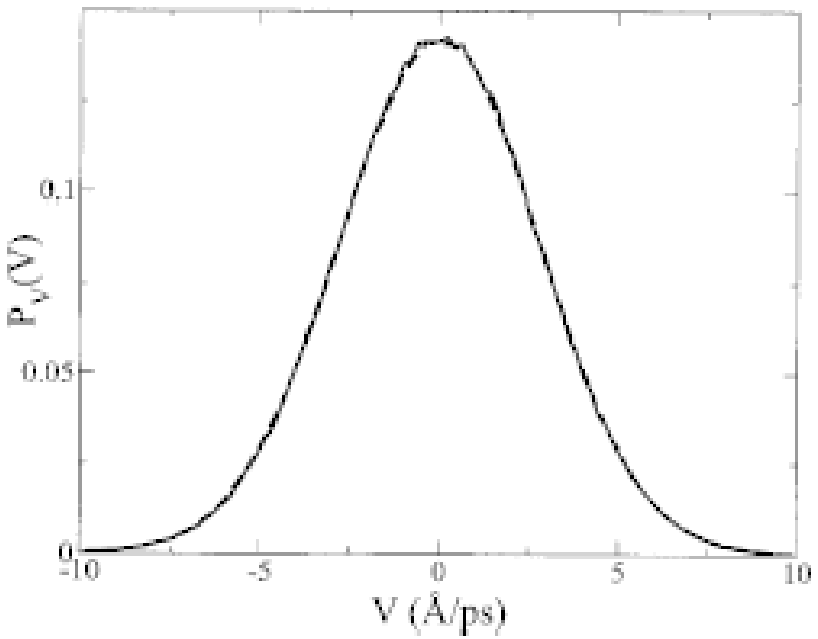

Left: Radial distribution function of CG sites as obtained from atomistic model (dashed line) and from CG model (solid line).

Right: Distribution of velocity components of CG sites as obtained from atomistic model (dashed line) and from CG model (solid line).

Noid, W.G., Liu, P., Wang,Y., Chu, J.-W., Ayton, G.S., Izvekov, S., Andersen, H.C., and Voth, G.A. *J. Chem. Phys.* **2008**, *128*, 244115.

Multiscale Coarse-Graining Method (Force Matching)

1-ethyl-3-methimidazolium nitrate ($EMIM^+ NO_3^-$)

Broken lines: Atomistic. Solid lines: Coarse-grained

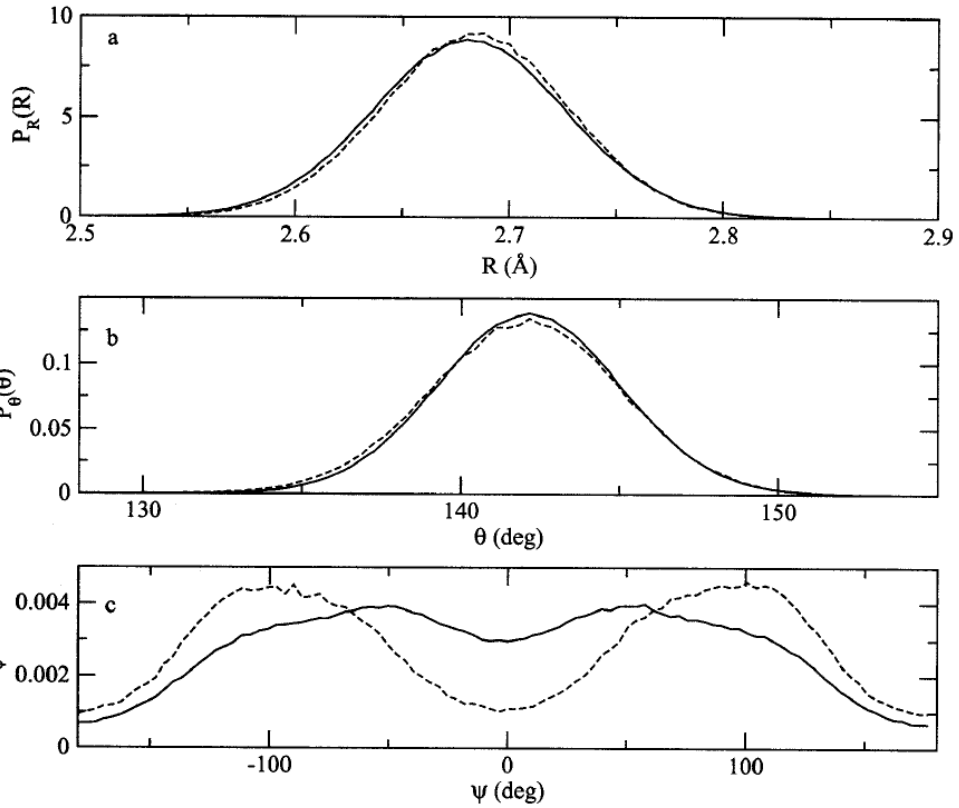

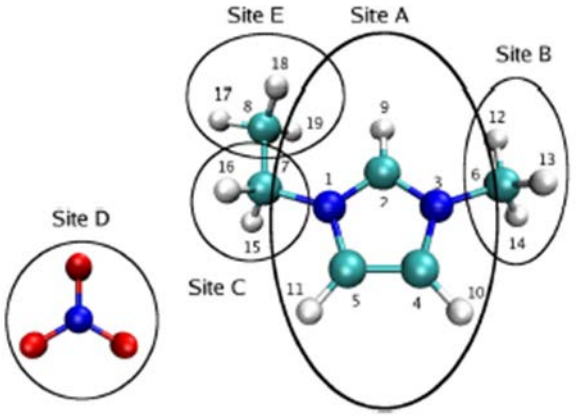

A-C effective bond lengths.

B-A-C valence angles.

B-A-C-E dihedral angles.

Noid, W.G., Liu, P., Wang,Y., Chu, J.-W., Ayton, G.S., Izvekov, S., Andersen, H.C., and Voth, G.A. *J. Chem. Phys.* **2008**, *128*, 244115.

Iterative Boltzmann Inversion Method

Match structure. Coarse-grained effective potentials derived through an iterative process using an oligomeric reference system.

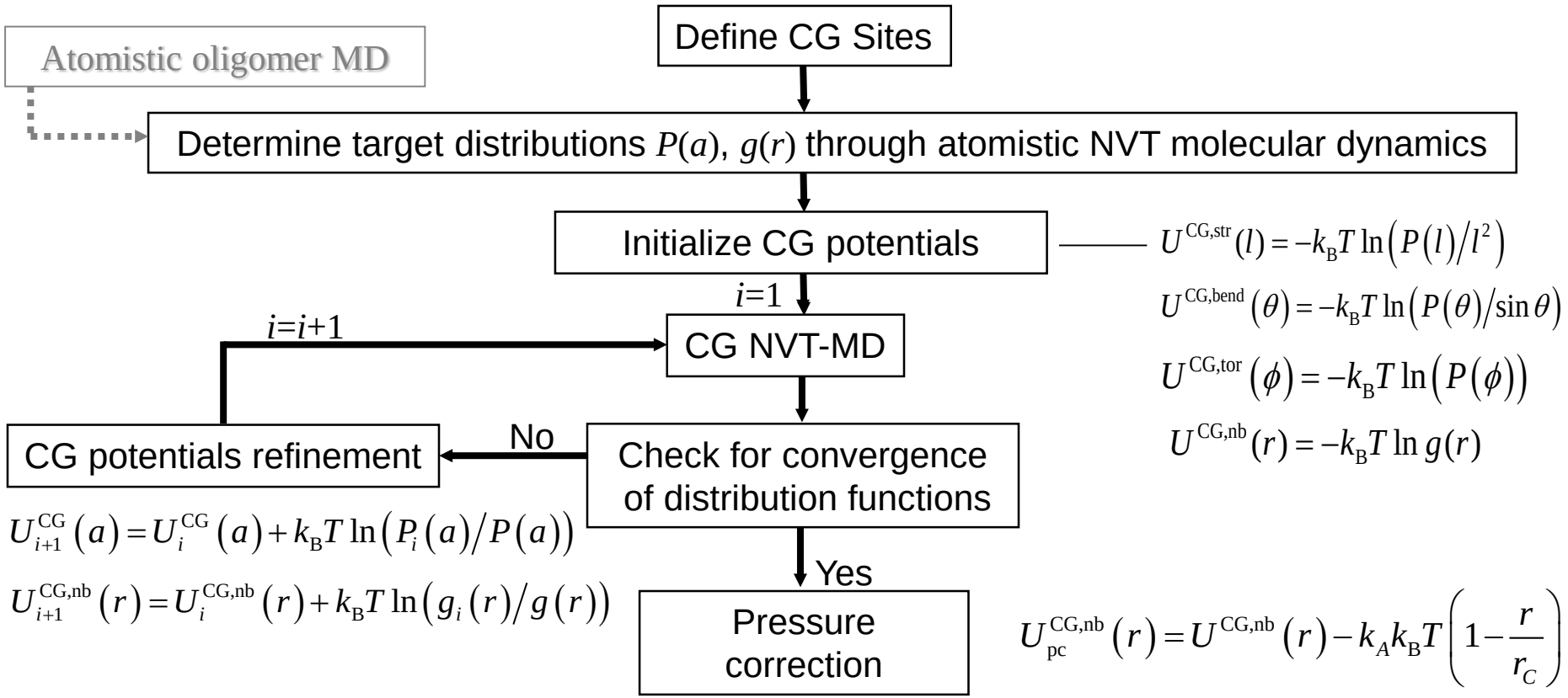

W. Schommers, Phys. Rev. A **1983**, *28*, 3599.

Reith, D.; Pütz, M.; Müller-Plathe, F. *J. Comp. Chem.* **2003**, *24*, 1624.

IBI-Based Coarse Graining of Poly(Ethylene Terephthalate)

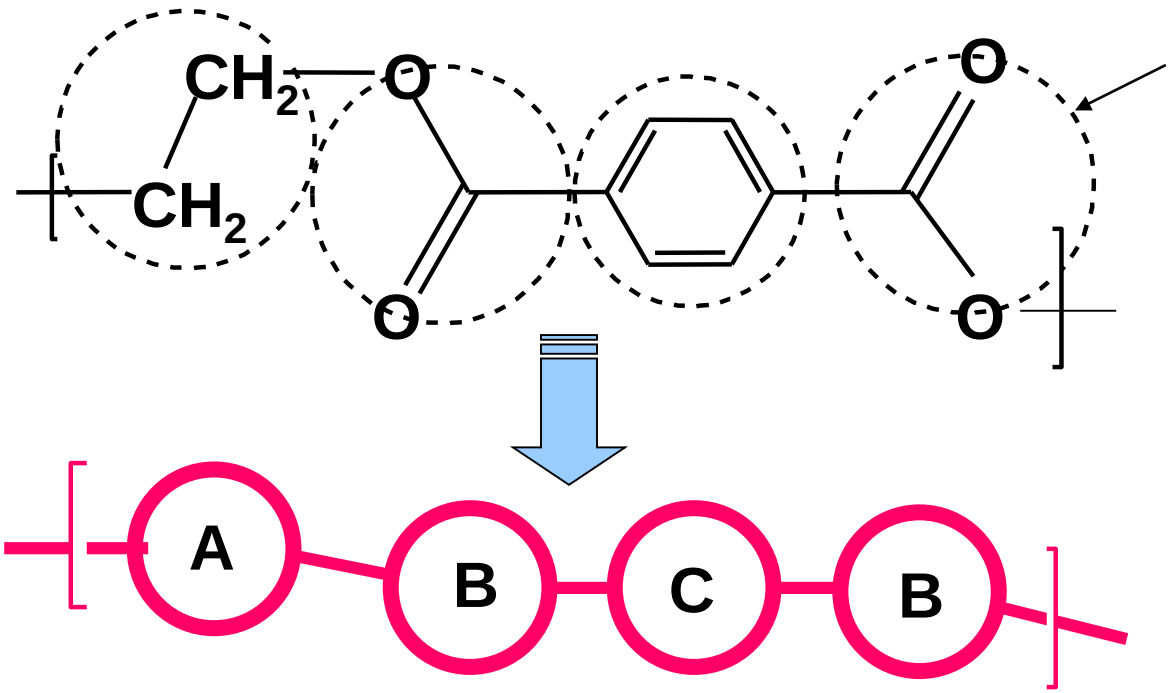

United Atom Model
42 d.o.f./monomer

6 bond types
7 angle types
6 torsion types
1 out of plane type
20 unique non-bonded pairs

Coarse-Grained Model
9 d.o.f./monomer

2 bonds A-B, B-B
2 angles A-B-B, B-A-B
2 torsions A-B-B-A, B-A-B-B
6 unique non-bonded pairs

Kamio, K.; Moorthi, K.; DNT. *Macromolecules* **2007**, *40*, 710-722.

Coarse-Grained Effective Potentials: PET

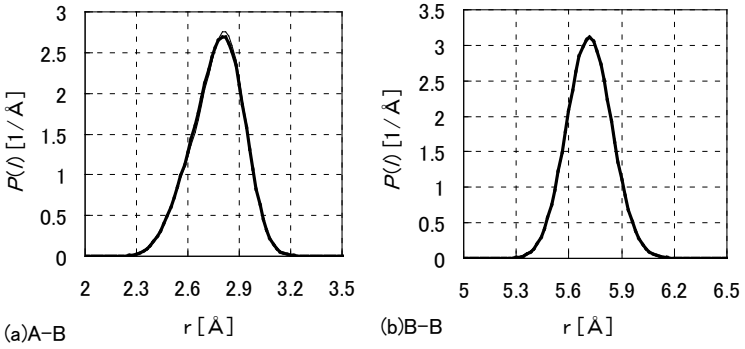

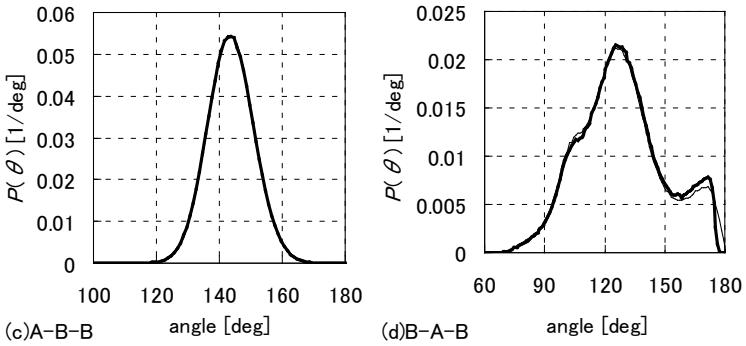

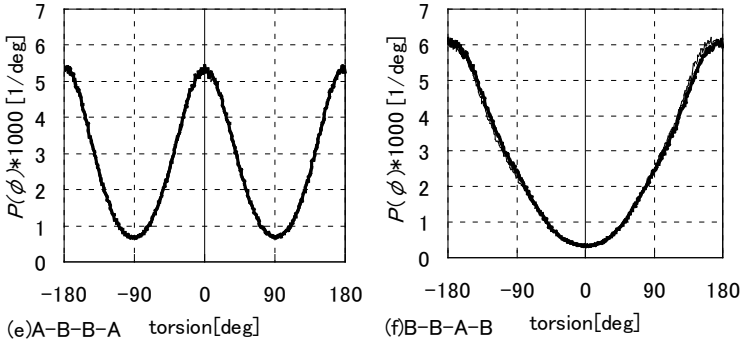

Intramolecular distributions

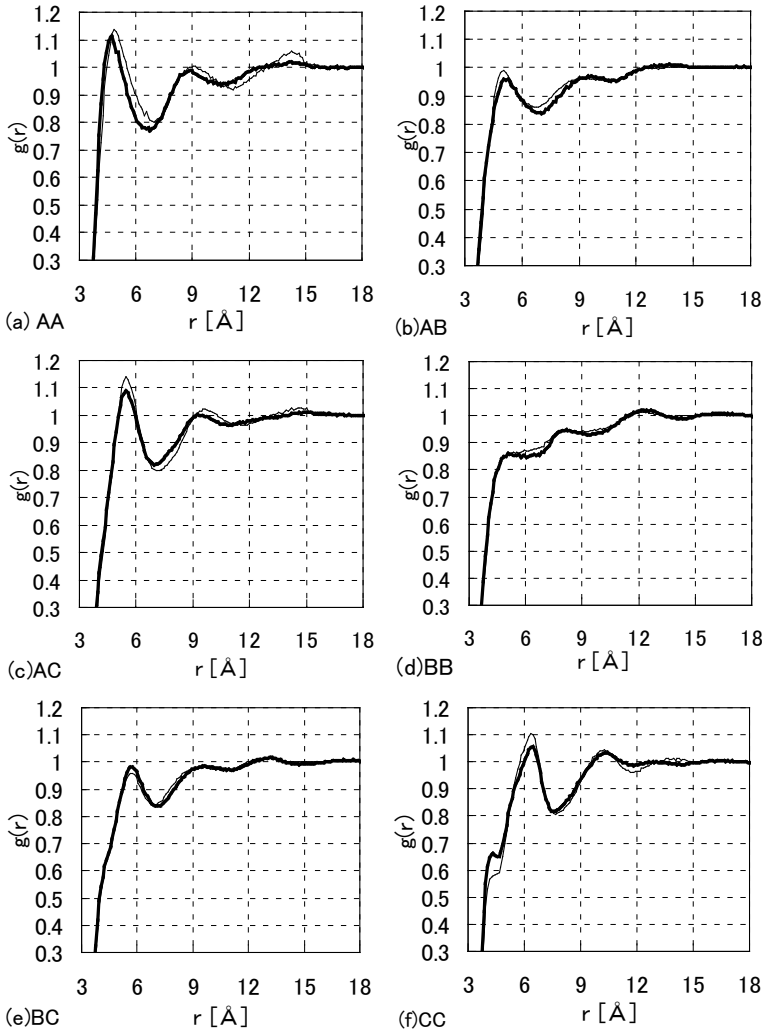

Intermolecular distributions

Thin: Target
Bold: CG

Upon convergence, distribution functions of the CG dimer system are in good agreement with the target distributions derived from atomistic simulation

PET Melt Properties from Connectivity-Altering CG MC Simulation

1 atm, 450 K, degree of polymerization =100

Density

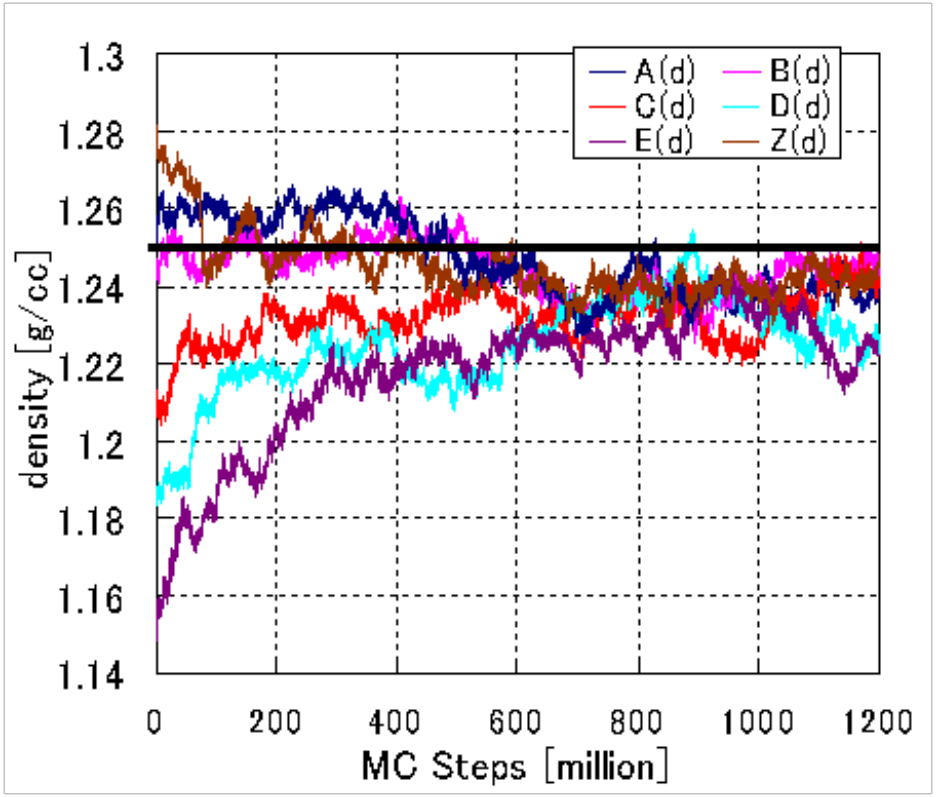

CG MC: $\rho = 1.24 \pm 0.01$ g/cm^3.

Experiment: $\rho = 1.25$ g/cm^3

Mean squared end-to-end distance of subchains

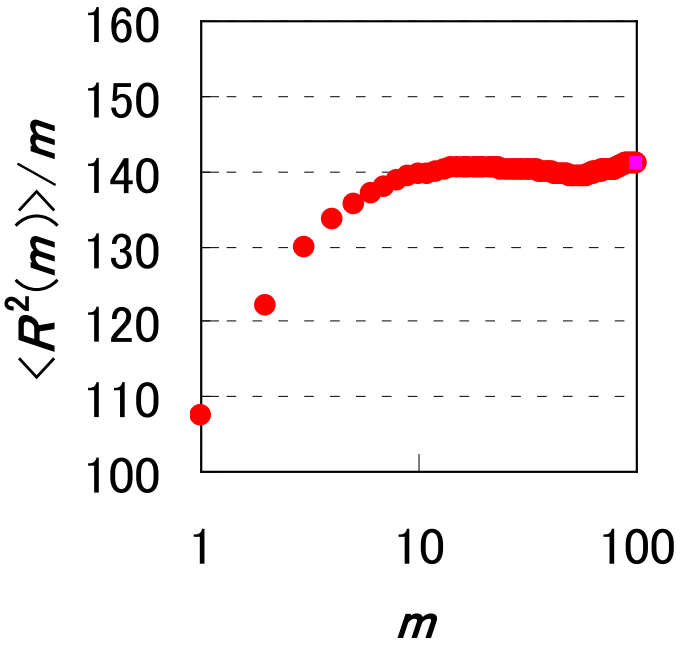

Asymptotic value $\langle R^2(m)\rangle/m = 140$ Å^2, or $\langle R^2\rangle/M = 0.68$Å^2 /(g mol^{-1}).

Neutron scattering [Guilmer et al. (1986)]: $\langle R^2\rangle/M = 0.61$-$0.69$ Å^2 /(g mol^{-1}).

Coarse-graining molecular models: Atactic Polystyrene

Iterative Boltzmann Inversion (IBI)

D. Reith, M. Pütz, and F. Müller-Plathe, *J. Comp. Chem.* **2003**, *24*, 1624;
Spyriouni, T.; Tzoumanekas, C.; DNT; Müller-Plathe, F.; Milano G. *Macromolecules* **2007**, *40*, 3876.

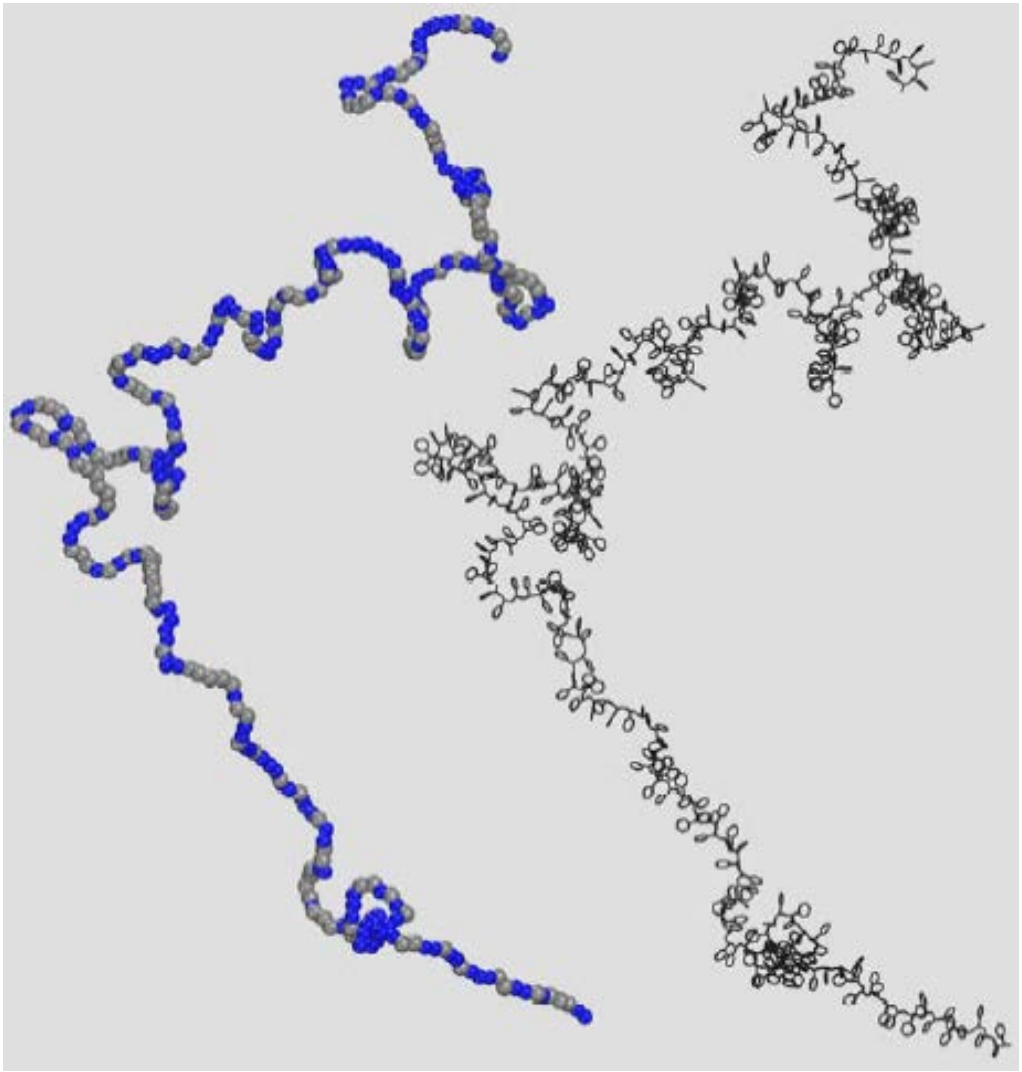

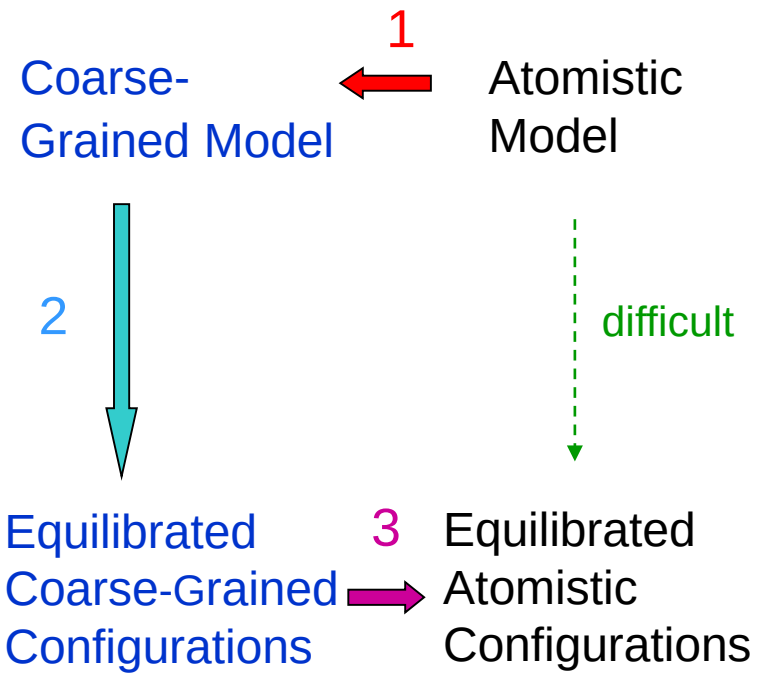

1. Coarse-graining (IBI)

2. Equilibration at coarse-grained level (using connectivity-altering MC)

3. Reverse-Mapping

Coarse-grained simulations of monodisperse aPS melts

T=500 K and 413 K, *p* = 1 bar
chain length 9 to 2000 repeat units

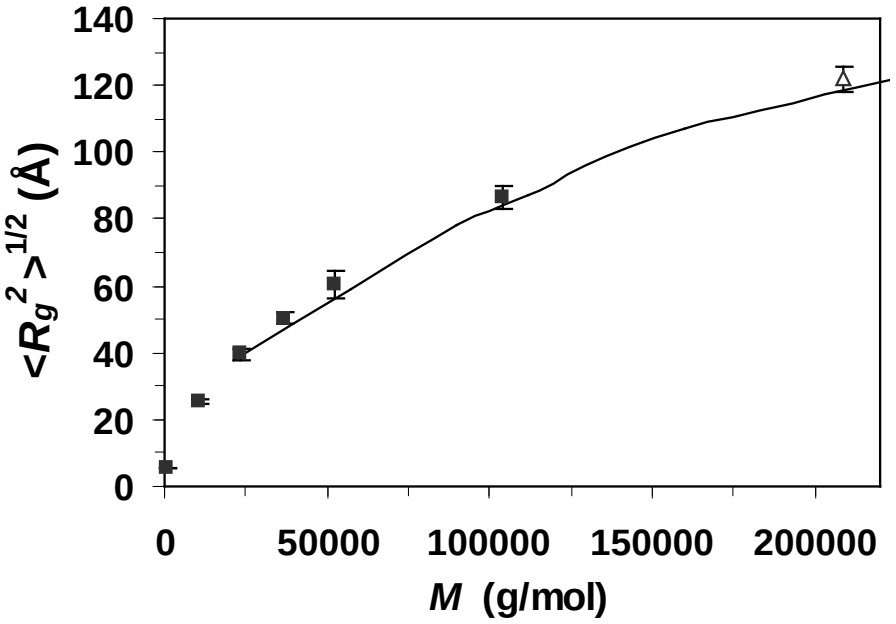

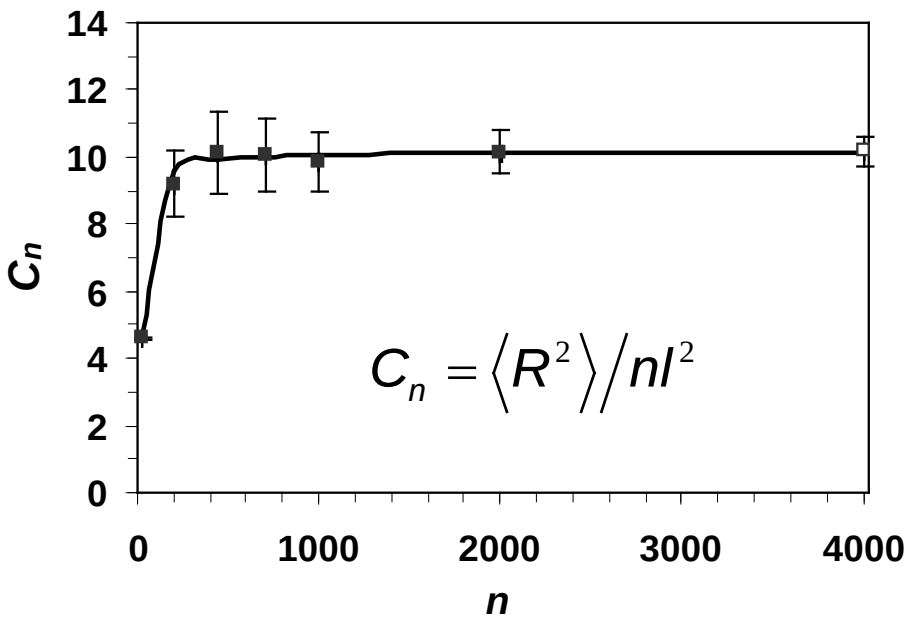

Points: simulation
line: SANS (Cotton et al., 1974)

Points: simulation
line: freely rotating chain model

T. Spyriouni, C. Tzoumanekas, DNT, F. Müller-Plathe, G. Milano
Macromolecules **2007**, *40*, 3876.

Reverse Mapping for PS

- Energy-weighted Geometric Reconstruction:
  - CH_2 carbons placed at CG sites.
  - CH and connected aromatic carbons grown simultaneously using equilibrium bond angles.
  - Rest of the ring positioned as a planar object at a pre-selected torsion angle.
  - Selection among 100 candidate reconstructed configurations based on Boltzmann factor of energy increment, avoiding improbable torsion angles.
- Structure optimization via MC:
  - Rotation of PS monomers around CH_2–CH_2 axes.
  - Configurationally biased regrowth of monomers.
  - Rotation of rings.
  - MC starts with full intramolecular and soft intermolecular potentials. Intermolecular potentials increased to full strength in 5 steps.
- Energy minimization of resulting united-atom PS:
  - Soft potentials for pushing apart overlapping atoms
  - LJ interactions gradually switched on (from 80% to 100%)

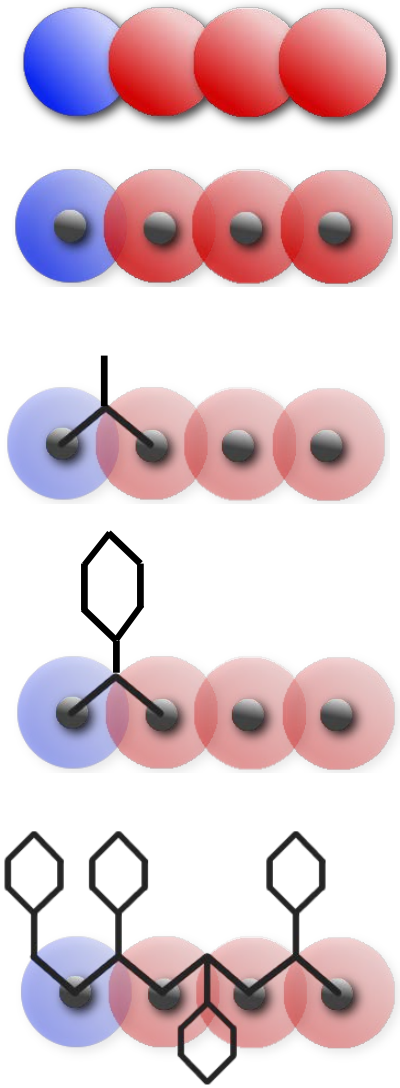

Vogiatzis, G.G.; DNT *Macromolecules* **2014**, *47,* 387.

aPS Reverse mapping: Torsion angle distributions

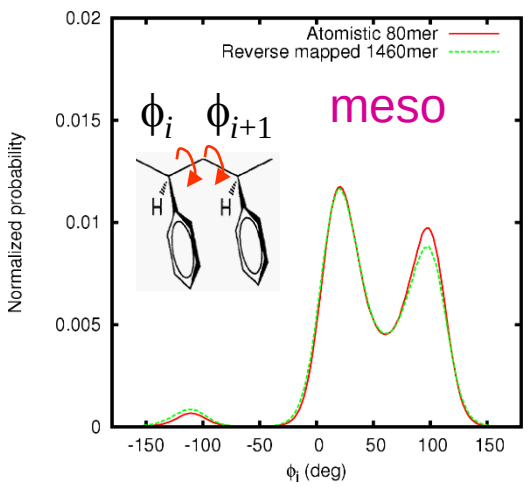

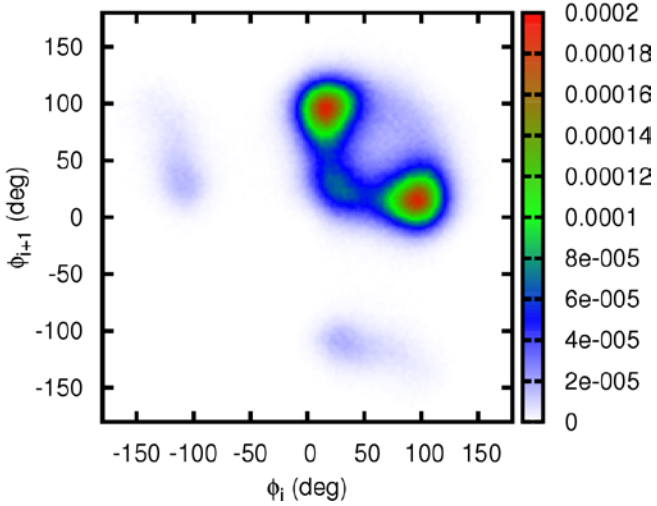

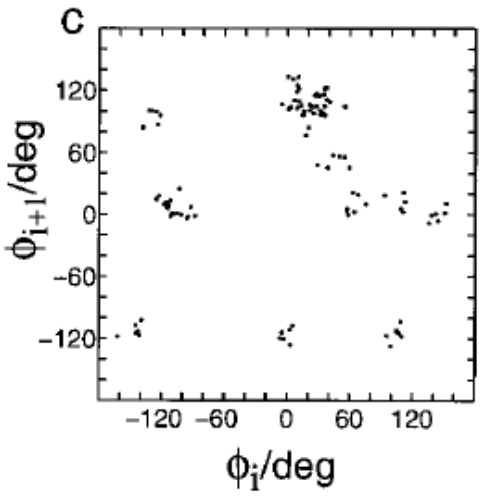

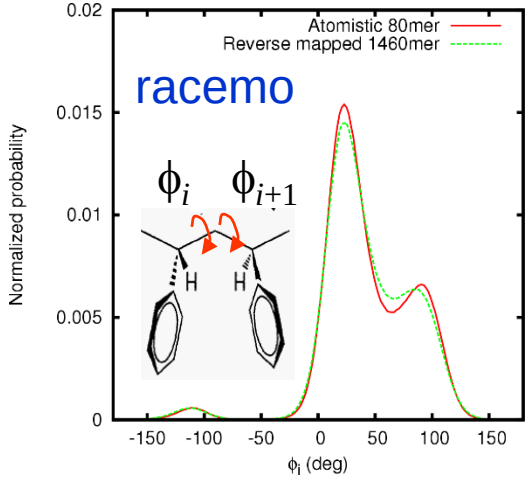

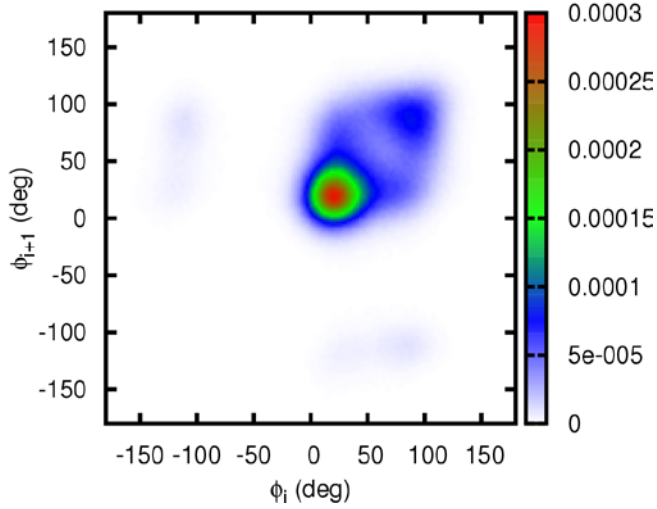

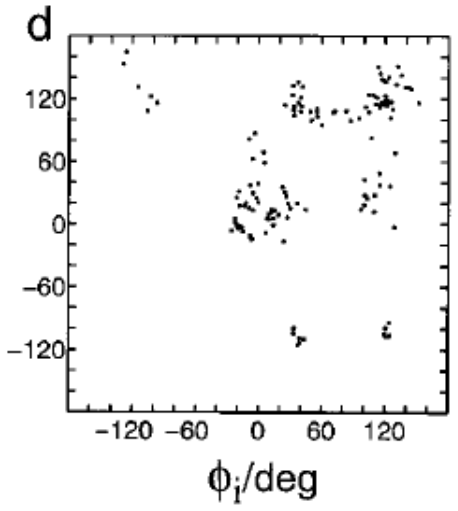

Vogiatzis, G.G.; DNT *Macromolecules* **2014**, *47,* 387.

Robyr, P.; Gan, Z.; Suter, U.W. *Macromolecules* **1998**, *31*, 8918.

aPS: Reverse mapping to atomistic level

Reverse mapping to united atom model of
Lyulin, A.V.; Michels, M.A.J. *Macromolecules* **2002**, *35*,1463.

WAXS pattern

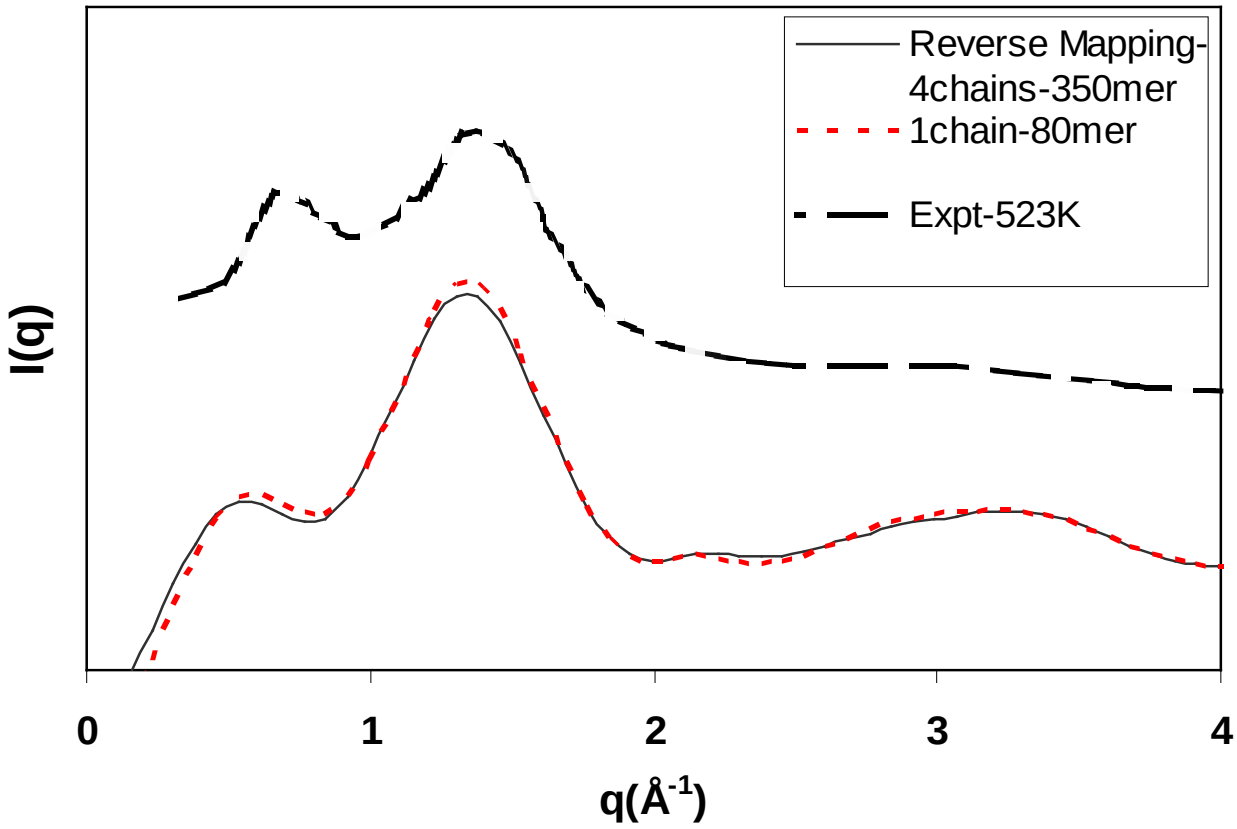

T. Spyriouni, C. Tzoumanekas, DNT, G. Milano, F. Müller-Plathe, *Macromolecules* **2007**, *40*, 3876-3885.

Coarse-graining via Pretabulation of Interactions Between Molecular Pairs

- Atomistic calculation of the intramolecular potential for each pair of coarse-grained moieties, scanning all variables determining the pair relative configuration
- Tabulation of the calculated potential values (accounting for symmetries)
- Application of multi-dimensional interpolation methods for the evaluation of the potential during run time

Example :
Liquid Benzene

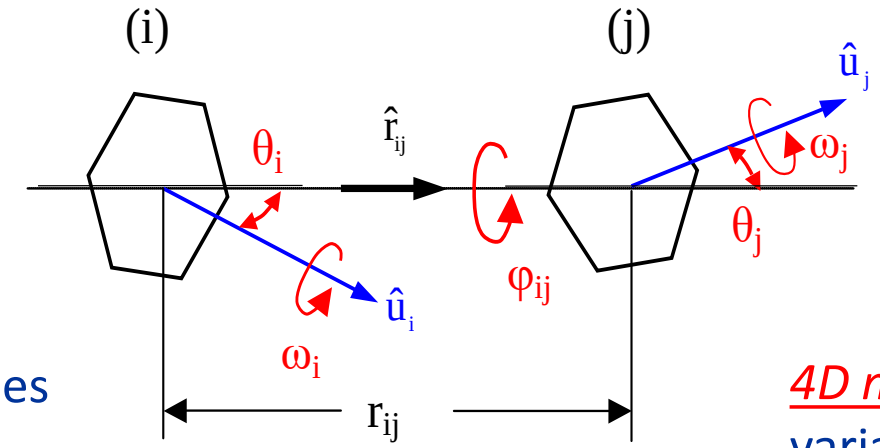

6D model – Six variables determining relative position and orientation : $r_{ij},\theta_i,\theta_j,\varphi_{ij},\omega_i,\omega_j$

4D model – Four variables determining relative position and orientation : $r_{ij},\theta_i,\theta_j,\varphi_{ij}$

$$U_{\mathrm{mf},ij}(r_{ij},\theta_i,\theta_j,\phi_{ij}) = -k_{\mathrm{B}}T \ln\left\{\frac{9}{\pi^2}\int_0^{\pi/3} \mathrm{d}\omega_i \int_0^{\pi/3} \mathrm{d}\omega_j \exp\left[-\mathcal{V}_{ij}^0(r_{ij},\theta_i,\theta_j,\phi_{ij},\omega_i,\omega_j)\right]\right\}$$

Zacharopoulos, N.; Vergadou, N.; DNT *J.Chem.Phys.* **2005,** *122*, 244111.

Liquid Benzene – Comparison of Atomistic and Coarse-grained Simulations

Atomistic MD

(flexible molecules, COMPASS force field)

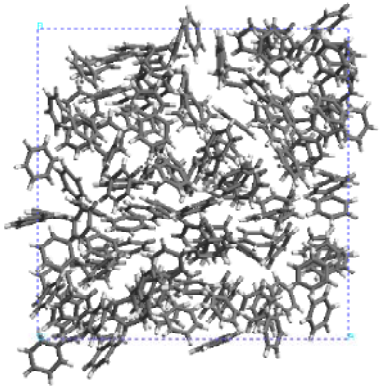

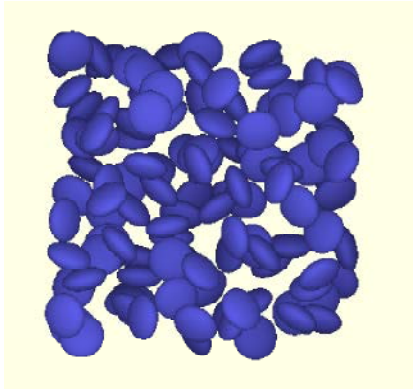

Coarse-grained MC

(4D model)

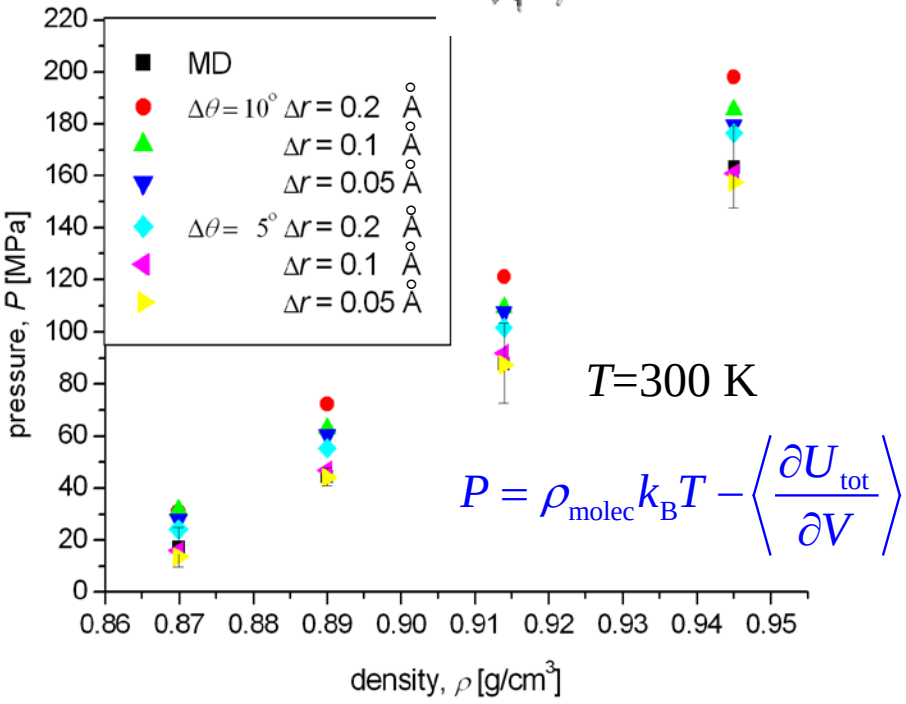

$$P = \rho_{\text{molec}} k_B T - \left\langle \frac{\partial U_{\text{tot}}}{\partial V} \right\rangle$$

Structure – PDF between COM

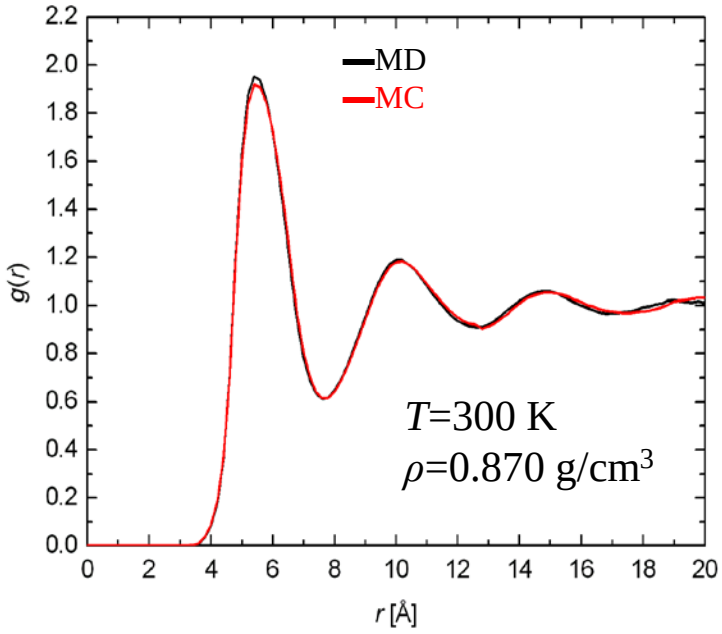

Zacharopoulos, N.; Vergadou, N.; DNT *J.Chem.Phys.* **2005,** *122*, 244111.

Liquid Benzene – Comparison of Atomistic and Coarse-grained Simulations

Atomistic MD

(flexible molecules, COMPASS force field)

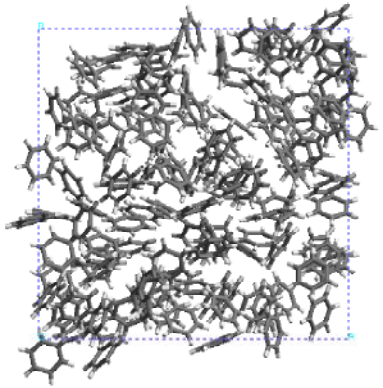

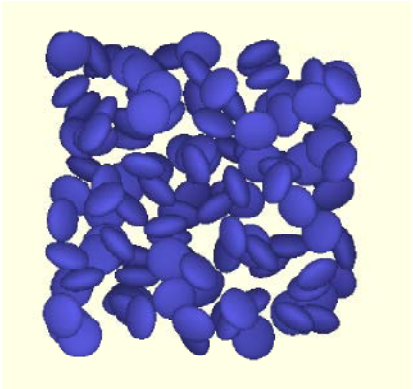

Coarse-grained MC

(4D model)

Orientational Correlation between unit normal vectors on different molecules

$$P_2(r) = \frac{1}{2}\left[3\left\langle \cos^2(\hat{\mathbf{u}}_i \cdot \hat{\mathbf{u}}_j) \right\rangle_{r_{ij}=r} - 1 \right]$$

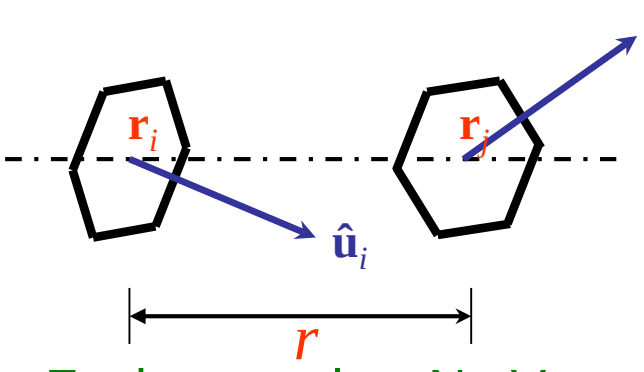

$\hat{\mathbf{u}}_i // \hat{\mathbf{u}}_j$: P_2=+1

$\hat{\mathbf{u}}_i \perp \hat{\mathbf{u}}_j$: P_2=–1/2

$\hat{\mathbf{u}}_i, \hat{\mathbf{u}}_j$ random: $\langle P_2 \rangle$=0

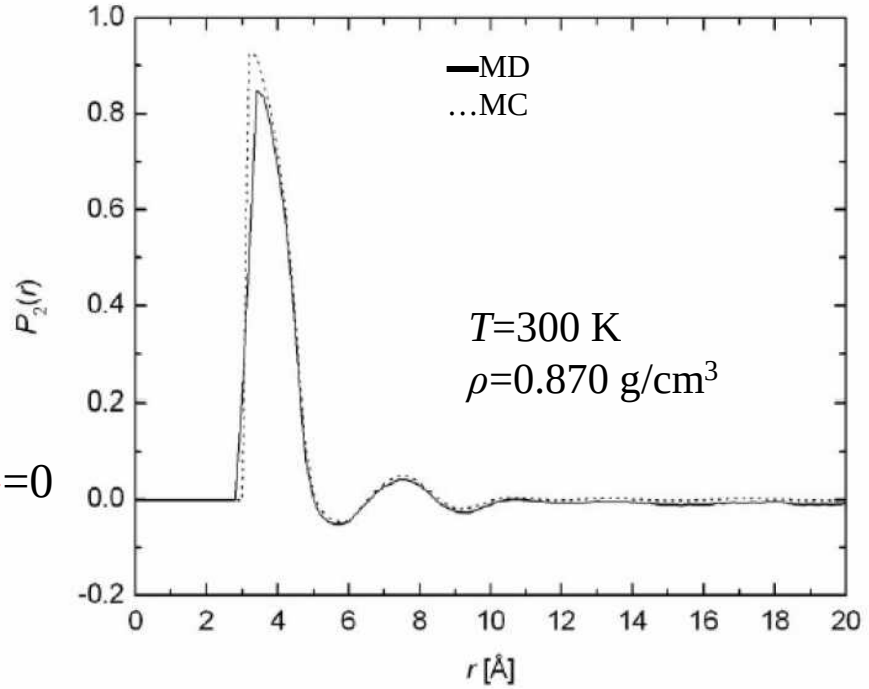

Zacharopoulos, N.; Vergadou, N.; DNT *J.Chem.Phys.* **2005,** *122*, 244111.

Other Coarse-Graining Algorithms

Inverse Monte Carlo

Lyubartsev, A.P., and Laaksonen, A. *Phys. Rev. E* **1995**, *52*, 3730-3737.
Lyubartsev, A.P., and Laaksonen, A. *Lect. Notes Phys.* **2004**, *640*, 219-244.

Optimizes the effective pair potential to reproduce $g(r)$'s between coarse-grained centers as computed from atomistic simulation. A Newton-Raphson scheme is used to optimize the potential, represented by a set of tabulated values as a step-wise function of distance.

Relative entropy minimization

Shell, S. *J. Chem. Phys.* **2008**, *129*, 144108 (2008).
Chaimovitch, A., and Shell, S. *J. Chem. Phys.* **2011**, *134*, 094112.

Coarse-grained effective potential defined by a condition designed to provide minimum entropy change between the atomistically represented and the coarse-grained system and thereby minimize the information loss associated with the coarse-graining process.

Public domain software for coarse-graining:
Denis Andrienko et al., MPIP https://www.votca.org/

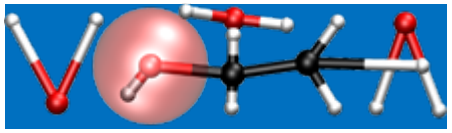

Dynamical Coarse-Graining: The Projection Operator Formalism

Atomistic description: $3n$ generalized coordinates $\mathbf{q}(t)$
$3n$ generalized momenta $\mathbf{p}(t)$
Hamiltonian $\mathcal{H}(\mathbf{q},\mathbf{p})$

Hamilton's equations of motion:

$$\frac{\mathrm{d}}{\mathrm{d}t}\begin{bmatrix}\mathbf{q}\\ \mathbf{p}\end{bmatrix}=\begin{bmatrix}\dfrac{\partial}{\partial\mathbf{p}}\\ -\dfrac{\partial}{\partial\mathbf{q}}\end{bmatrix}\mathcal{H}$$

Liouville equation for the probability density in phase space $\rho(\mathbf{q},\mathbf{p},t)$:

$$\frac{\partial\rho}{\partial t}+\sum_{i=1}^{n}\left(\frac{\partial\mathcal{H}}{\partial\mathbf{p}_i}\cdot\frac{\partial}{\partial\mathbf{q}_i}-\frac{\partial\mathcal{H}}{\partial\mathbf{q}_i}\cdot\frac{\partial}{\partial\mathbf{p}_i}\right)\rho=0 \quad \text{or} \quad \frac{\partial\rho}{\partial t}+\mathrm{i}L\rho=0$$

$\mathrm{i}L$: classical Liouville operator

For any function of the phase space point $\mathcal{A}(\mathbf{q},\mathbf{p})$:

$$\dot{\mathcal{A}}=\frac{\mathrm{d}\mathcal{A}}{\mathrm{d}t}=\sum_{i=1}^{n}\left(\frac{\partial\mathcal{A}}{\partial\mathbf{q}_i}\cdot\frac{\mathrm{d}\mathbf{q}_i}{\mathrm{d}t}+\frac{\partial\mathcal{A}}{\partial\mathbf{p}_i}\cdot\frac{\mathrm{d}\mathbf{p}_i}{\mathrm{d}t}\right)=\sum_{i=1}^{n}\left(\frac{\partial\mathcal{H}}{\partial\mathbf{p}_i}\cdot\frac{\partial}{\partial\mathbf{q}_i}-\frac{\partial\mathcal{H}}{\partial\mathbf{q}_i}\cdot\frac{\partial}{\partial\mathbf{p}_i}\right)\mathcal{A}=\mathrm{i}L\mathcal{A}$$

Projections of observables in phase space

Consider first a set of (not necessarily orthogonal or normalized) reference vectors $\{\mathbf{a}_1, \mathbf{a}_2, ..., \mathbf{a}_N\}$ in $\mathbb{R}^n$ and an arbitrary vector $\mathbf{x}$ in $\mathbb{R}^n$.
How can one best represent $\mathbf{x}$ as a linear combination of $\{\mathbf{a}_1, \mathbf{a}_2, ..., \mathbf{a}_N\}$?

Determine coefficients $\{c_1, c_2, ..., c_N\}$ such that

$$\left(\mathbf{x} - c_1\mathbf{a}_1 - c_2\mathbf{a}_2 - ... - c_N\mathbf{a}_N\right)^2 = \min.$$

$$\begin{bmatrix} \mathbf{a}_1\cdot\mathbf{a}_1 & \mathbf{a}_1\cdot\mathbf{a}_2 & \cdots & \mathbf{a}_1\cdot\mathbf{a}_N \\ \mathbf{a}_2\cdot\mathbf{a}_1 & \mathbf{a}_2\cdot\mathbf{a}_2 & \cdots & \mathbf{a}_2\cdot\mathbf{a}_N \\ \vdots & \vdots & \ddots & \vdots \\ \mathbf{a}_N\cdot\mathbf{a}_1 & \mathbf{a}_N\cdot\mathbf{a}_2 & \cdots & \mathbf{a}_N\cdot\mathbf{a}_N \end{bmatrix} \begin{bmatrix} c_1 \\ c_2 \\ \vdots \\ c_N \end{bmatrix} = \begin{bmatrix} \mathbf{x}\cdot\mathbf{a}_1 \\ \mathbf{x}\cdot\mathbf{a}_2 \\ \vdots \\ \mathbf{x}\cdot\mathbf{a}_N \end{bmatrix}$$

Matrix $(\mathbf{a}\cdot\mathbf{a})$

or $$c_j = \sum_{i=1}^{N} \left(\mathbf{a}\cdot\mathbf{a}\right)^{-1}_{ji} \left(\mathbf{x}\cdot\mathbf{a}_i\right)$$

Projection of $\mathbf{x}$ onto the set of reference vectors $\{\mathbf{a}_1, \mathbf{a}_2, ..., \mathbf{a}_N\}$:

$$P\mathbf{x} = \sum_{j=1}^{N} \left(\sum_{i=1}^{N} \left(\mathbf{a}\cdot\mathbf{a}\right)^{-1}_{ji} \left(\mathbf{x}\cdot\mathbf{a}_i\right) \right) \mathbf{a}_j$$

Projections of observables in phase space

For a n-particle system at equilibrium, characterized by a time-independent normalized phase-space probability density $\rho^{\mathrm{eq}}(\mathbf{q}, \mathbf{p})$, we think of all observables as constituting a Hilbert space, i.e. as a vector space equipped with a scalar product. For two observables, $\mathcal{A}$ and $\mathcal{B}$, we define the scalar product as the correlation function:

$$\left\langle \mathcal{A}, \mathcal{B} \right\rangle = \int \mathcal{A}(\mathbf{q},\mathbf{p})\,\mathcal{B}(\mathbf{q},\mathbf{p})\,\rho^{\mathrm{eq}}(\mathbf{q},\mathbf{p})\,\mathrm{d}\mathbf{q}\mathrm{d}\mathbf{p}$$

Given an arbitrary observable $\mathcal{X}$ and a set of reference observables $\left\{\mathcal{A}_1, \mathcal{A}_2, ..., \mathcal{A}_N\right\}$, we define the projection of $\mathcal{X}$ on the reference observables as

Projection operator P

$$P\mathcal{X} = \sum_{j=1}^{N}\left(\sum_{i=1}^{N}\left\langle \mathcal{A}, \mathcal{A}\right\rangle^{-1}_{ji}\left\langle \mathcal{X}, \mathcal{A}_i\right\rangle\right)\mathcal{A}_j$$

Inverse of matrix of equilibrium correlations between the $\mathcal{A}_i$'s

Projection operator orthogonal to P

$$Q = 1 - P$$

Projection onto a subset of (slow) variables

Observables $\{\mathcal{A}_1, \mathcal{A}_2, ..., \mathcal{A}_N\}$ can be shown to evolve according to:

$$\dot{\mathcal{A}}_k(t) = \sum_{j=1}^{N} \mathrm{i}\,\Omega_{kj}\,\mathcal{A}_j(t) + \int_0^t \mathrm{d}s \sum_{j=1}^{N} M_{kj}(s)\,\mathcal{A}_j(t-s) + R_k(t), \quad k = 1, 2, ..., N$$

Mori-Zwanzig equation

where

$$\mathrm{i}\Omega_{kj} = \sum_{i=1}^{N} \left\langle \mathcal{A}, \mathcal{A} \right\rangle^{-1}_{ji} \left\langle \dot{\mathcal{A}}_k, \mathcal{A}_i \right\rangle$$

Frequency Matrix

$$R_k(t) = e^{\mathrm{i}QLt} Q\ \mathrm{i}L\mathcal{A}_k(0)$$

Random Force

Part of $\dot{\mathcal{A}}_k$ that is initially orthogonal to all $\mathcal{A}_i$ and evolves so as to remain orthogonal to them at all subsequent times.

If set $\{\mathcal{A}_1, \mathcal{A}_2, ..., \mathcal{A}_N\}$ includes all the slow dynamics, then $R_k(t)$ will fluctuate rapidly around 0 and $M_{kj}(s)$ will quickly decay to 0 at long times.

$$M_{kj}(s) = -\sum_{i=1}^{N} \left\langle \mathcal{A}, \mathcal{A} \right\rangle^{-1}_{ji} \left\langle R_i(s), R_k(0) \right\rangle$$

Memory Matrix

Projection onto a subset of (slow) variables

Correlation functions: $C_{kl}(t) = \left\langle \mathcal{A}_k(t), \mathcal{A}_l(0) \right\rangle \equiv \left\langle \mathcal{A}_k(t)\, \mathcal{A}_l(0) \right\rangle$

Postmultiplying both sides of the Mori-Zwanzig equation by $\mathcal{A}_l(0)$ and ensemble averaging, we obtain

$$\dot{C}_{kl}(t) = \sum_{j=1}^{N} \mathrm{i}\,\Omega_{kj} C_{kl}(t) + \int_0^t \mathrm{d}s \sum_{j=1}^{N} M_{kj}(s) C_{jl}(t-s) \qquad k,l = 1,2,\ldots,N$$

The correlation matrix obeys a similar equation to the Mori-Zwanzig, involving the frequency matrix and the memory matrix, but without the random force term.

Nakajima, S. *Progr. Theor. Phys*. **1958**, *20*, 948-959.
Zwanzig, R. *J. Chem. Phys*. **1960**, *33*, 1338-1341.
Zwanzig, R. *Phys. Rev*. **1961**, ***124***, 983-992.
Mori, H. *Progr. Theor. Phys.* **1965**, *33*, 423-455.
Kawasaki, K. J. *Phys. A. Math. Nucl. Gen*. **1973**, *6*, 1289-1295.
Hijón, C., Español, P., Vanden-Eijnden, E., and Delgado-Buscalioni, R. *Faraday Discuss*. **2010**, *144*, 301-322.

Markovian approximation

Equations of motion for slow observables (Mori-Zwanzig):

$$\dot{\mathcal{A}}_k(t) = \sum_{j=1}^{N} \mathrm{i}\,\Omega_{kj}\,\mathcal{A}_j(t) + \int_0^t \mathrm{d}s \sum_{j=1}^{N} M_{kj}(s)\,\mathcal{A}_j(t-s) + R_k(t), \quad k = 1, 2, \ldots, N$$

Fast degrees of freedom, projected out of the description, manifest themselves through the memory term and the random force term.

If there is a clear time scale separation between the slow variables $\{\mathcal{A}_1, \mathcal{A}_2, \ldots, \mathcal{A}_N\}$ and the remaining variables of the system, the autocorrelation functions $\langle R_i(s)\, R_k(0)\rangle$ of the random forces and, therefore, the memory matrix elements $M_{kj}(s)$ decay to zero over times much shorter than t.
Memory term in Mori-Zwanzig equation can be approximated by

$$\int_0^t \mathrm{d}s \sum_{j=1}^{N} M_{kj}(s)\,\mathcal{A}_j(t-s) \approx \sum_{j=1}^{N} \left(\int_0^t \mathrm{d}s M_{kj}(s) \right) \mathcal{A}_j(t) \approx \sum_{j=1}^{N} \left(\int_0^\infty \mathrm{d}s M_{kj}(s) \right) \mathcal{A}_j(t)$$

$$= -\sum_{j=1}^{N} \xi_{kj}\,\mathcal{A}_j(t), \text{ with } \quad \xi_{kj} = -\int_0^\infty \mathrm{d}s\, M_{kj}(s) = \sum_{i=1}^{N} \int_0^\infty \mathrm{d}s \left\langle \mathcal{A}, \mathcal{A} \right\rangle_{ji}^{-1} \left\langle R_i(s), R_k(0) \right\rangle$$

dissipative matrix

Example: free Brownian particle in solvent

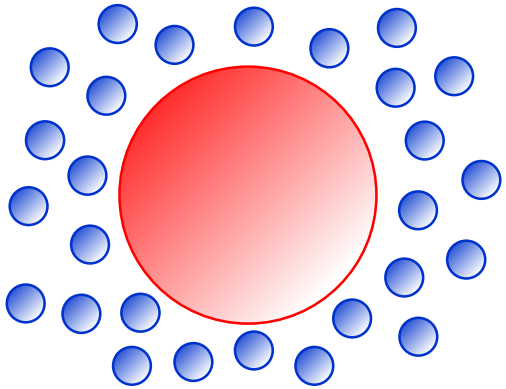

Choose 3 components of the momentum of the particle as the slow degrees of freedom:

$$\mathcal{A}_k \to p_k, \quad k = 1,2,3$$

$$\left\langle \mathcal{A}_i, \mathcal{A}_j \right\rangle \to \left\langle p_i, p_j \right\rangle = \left\langle p_i^2 \right\rangle \delta_{ij} = m k_{\mathrm{B}} T \delta_{ij}$$

$$\left\langle \mathcal{A}, \mathcal{A} \right\rangle^{-1}_{ji} \to \frac{1}{\left\langle p_i^2 \right\rangle} \delta_{ji} = \frac{1}{m k_{\mathrm{B}} T} \delta_{ji}$$

$$\mathrm{i}\Omega_{kj} = \sum_{i=1}^{N} \left\langle \mathcal{A}, \mathcal{A} \right\rangle^{-1}_{ji} \left\langle \dot{\mathcal{A}}_k, \mathcal{A}_i \right\rangle \to \sum_{i=1}^{3} \frac{1}{m k_{\mathrm{B}} T} \delta_{ji} \left\langle \dot{p}_k, p_i \right\rangle = \frac{1}{m k_{\mathrm{B}} T} \left\langle \dot{p}_k, p_j \right\rangle = 0$$

$R_k(0) = F_k(0)$ Total force initially exerted by solvent molecules on particle

$R_k(t) = F_{\mathrm{o}k}(t)$ Total force that would be exerted by solvent molecules on particle if initially the force on it were $F_k(0)$ and the whole system evolved between times 0 and t in such a way that the particle remained stationary.

$$M_{kj}(s) = -\sum_{i=1}^{N} \frac{1}{m k_{\mathrm{B}} T} \delta_{ji} \left\langle F_{\mathrm{o}i}(s) F_k(0) \right\rangle_{\mathrm{o}} = -\frac{1}{m k_{\mathrm{B}} T} \left\langle F_k(0) F_{\mathrm{o}j}(s) \right\rangle_{\mathrm{o}}$$

Example: free Brownian particle in solvent

Mori-Zwanzig equation: $\dot{\mathbf{p}}(t) = -\int_0^t \mathrm{d}s \, \frac{1}{3mk_\mathrm{B}T} \left\langle \mathbf{F}(0) \cdot \mathbf{F}_\mathrm{o}(s) \right\rangle_\mathrm{o} \mathbf{p}(t-s) + \mathbf{F}_\mathrm{o}(t)$

Markovian approximation: $\dot{\mathbf{p}}(t) = -\underbrace{\left\{ \int_0^\infty \mathrm{d}s \, \frac{1}{3mk_\mathrm{B}T} \left\langle \mathbf{F}(0) \cdot \mathbf{F}_\mathrm{o}(s) \right\rangle_\mathrm{o} \right\}}_{\xi} \mathbf{p}(t) + \mathbf{F}_\mathrm{o}(t)$

$m\dot{\mathbf{v}}(t) = -m\xi\mathbf{v}(t) + \mathbf{R}(t)$ Langevin equation for free Brownian particle (1908)

A stochastic differential equation.

Langevin force $\mathbf{R}(t)$ is known only through its statistical properties:

$\left\langle \mathbf{R}(t) \right\rangle = \mathbf{0}$

$\left\langle \mathbf{R}(t) \cdot \mathbf{v}(t) \right\rangle = 0$

$\left\langle R_\alpha(t) \cdot R_\beta(0) \right\rangle = 2 m k_\mathrm{B} T \, \xi \, \delta_{\alpha\beta} \, \delta(t)$

$\zeta = m\xi$ = friction factor.
Usually estimated from particle diameter d and solvent viscosity η as
$\zeta = 3 \pi \eta d$ (Stokes, 1851).

Particle self-diffusivity
$D_\mathrm{s} = k_\mathrm{B}T/\zeta$ (Einstein, 1905).

Langevin equation: Brownian particle in an external field

$$m\dot{\mathbf{v}}(t) = \mathbf{F}(\mathbf{r}) - m\xi\,\mathbf{v}(t) + \mathbf{R}(t)$$

External force due to field

Friction force

Langevin (random) force

$$\langle \mathbf{R}(t) \rangle = \mathbf{0}$$

$$\langle \mathbf{R}(t) \cdot \mathbf{v}(t) \rangle = 0$$

$$\langle R_\alpha(t) \cdot R_\beta(0) \rangle = 2 m k_{\mathrm{B}} T \xi \delta_{\alpha\beta} \delta(t)$$

$$\mathbf{F}(\mathbf{r}) = -\nabla_{\mathbf{r}} U(\mathbf{r})$$

How does one integrate this stochastic differential equation numerically? (Langevin Dynamics)

Generalized Langevin Equation

For a generalization of the projection operation formalism to non-Hamiltonian systems with an arbitrary number of coarse-grained variables, see Xiang, J.; Kim, K.S. *J. Chem. Phys*. **2011**, *134*, 044132.
The potential of mean force with respect to the coarse-grained variables appears in the resulting formulation.

A scheme for Langevin equation integration

Stochastic equations of motion:

$$\dot{\mathbf{r}}_i = \mathbf{v}_i$$

$$\dot{\mathbf{v}}_i = -m_i^{-1}\nabla_{\mathbf{r}_i} U(\mathbf{r}) - \xi \mathbf{v}_i + \sigma m_i^{-1/2}\dot{\mathbf{W}}_i$$

"BAOAB Scheme"

1. $\mathbf{v}_{k+1/4} = \mathbf{v}_k - \frac{\Delta t}{2}\mathbf{M}^{-1}\nabla U(\mathbf{r}_k)$
2. $\mathbf{r}_{k+1/2} = \mathbf{r}_k + \frac{\Delta t}{2}\mathbf{v}_{k+1/4}$
3. $\mathbf{v}_{k+3/4} = a_1\mathbf{v}_{k+1/4} + \sqrt{1-a_1^2}\,(\beta\mathbf{M})^{-1/2}\boldsymbol{\psi}_{k+1/2}$
4. $\mathbf{r}_{k+1} = \mathbf{r}_{k+1/2} + \frac{\Delta t}{2}\mathbf{v}_{k+3/4}$
5. $\mathbf{v}_{k+1} = \mathbf{v}_{k+3/4} - \frac{\Delta t}{2}\mathbf{M}^{-1}\nabla U(\mathbf{r}_{k+1})$

Definitions:

$$\dot{\mathbf{W}}_i = \mathbf{R}_i(t)/(2m_i\xi k_{\mathrm{B}}T)^{1/2}$$

$$\sigma^2 = 2\xi k_{\mathrm{B}}T$$

$$\mathbf{M} = \mathrm{diag}(m_1, m_2, ..., m_N)$$

$$\boldsymbol{\psi}_{k+1/2} \sim \mathcal{N}(0,1)^{3N}$$

$$a_1 = e^{-\xi\Delta t}$$

$$\beta = 1/(k_{\mathrm{B}}T)$$

Fass, J.; Sivak, D.A.; Crooks, G.E.; Beauchamp, K.A.; Leimkuhler, B.; Chodera, J.D. *Entropy* **2018**, *20*, *318.*

Example: Langevin Dynamics of a Free Brownian Particle

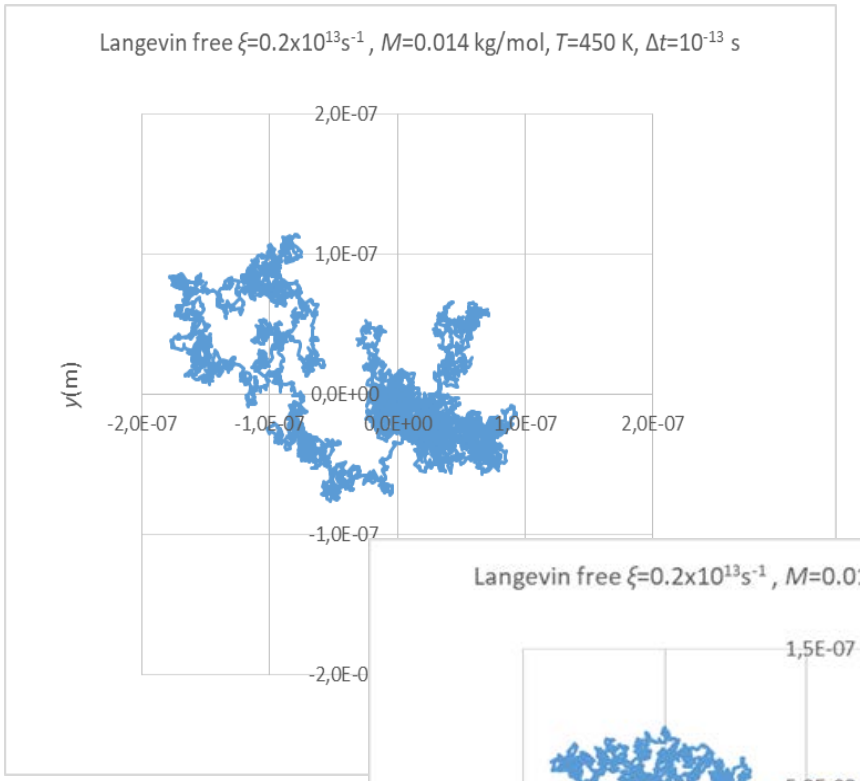

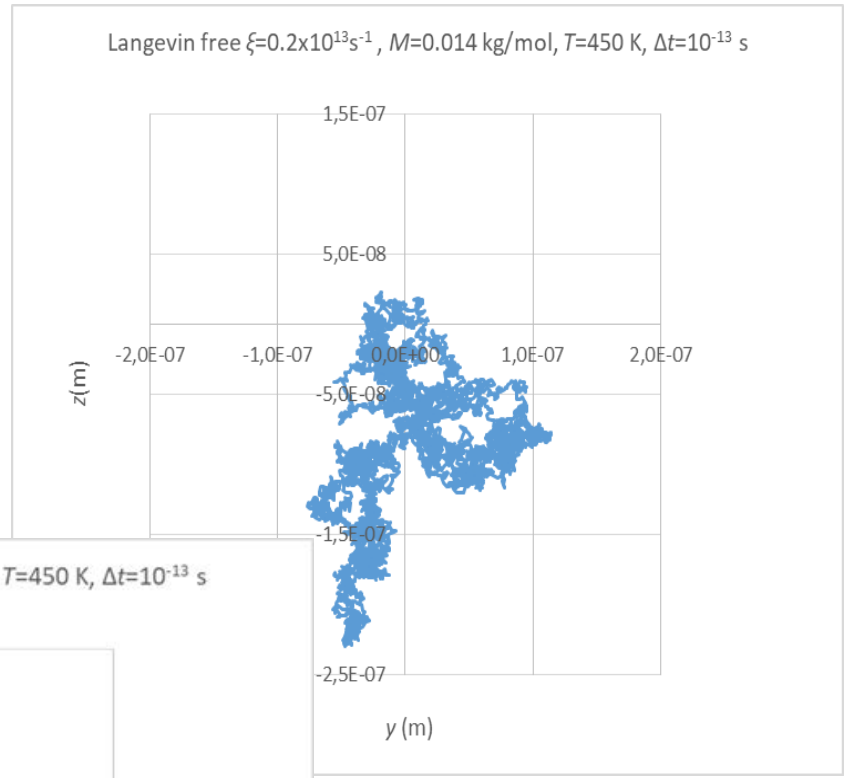

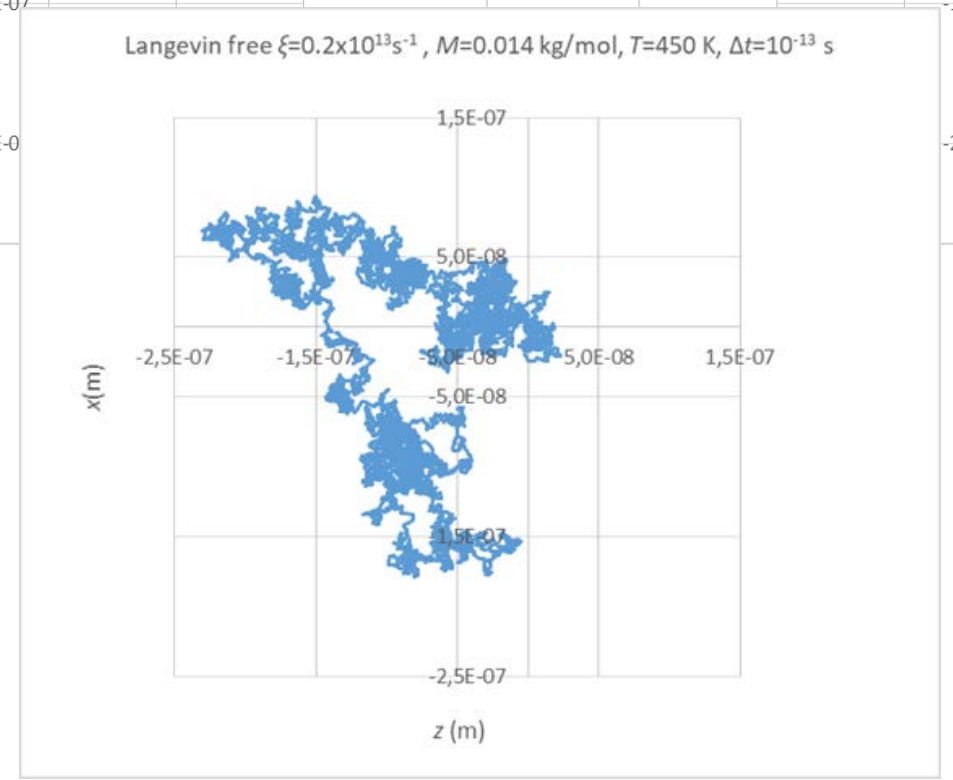

Example: Langevin Dynamics of a Free Brownian Particle

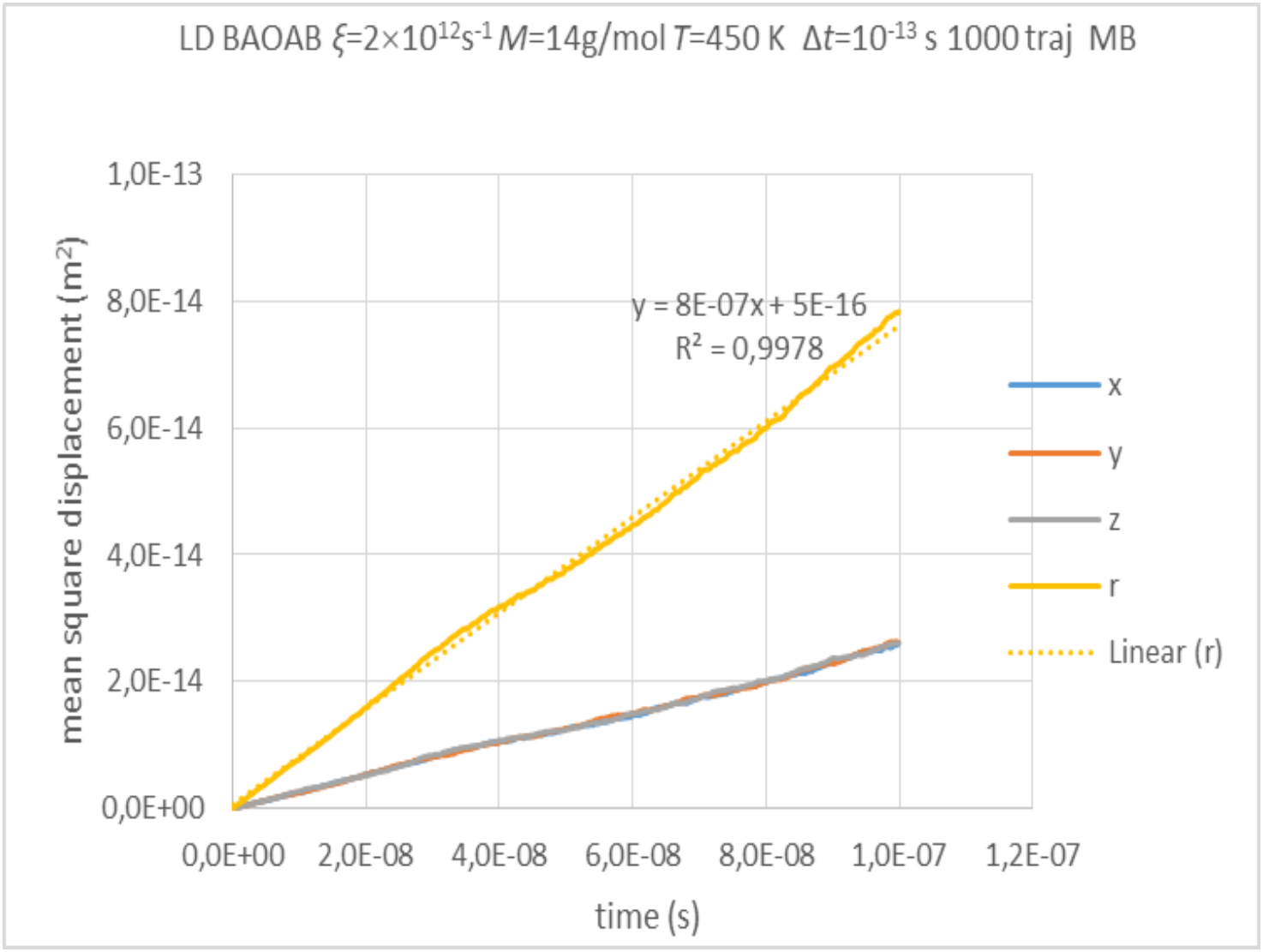

$$D_{\mathrm{s,sim}} = \frac{7.82\times10^{-14}}{6\times9.98\times10^{-8}}\frac{\mathrm{m}^2}{\mathrm{s}} = 0.131\times10^{-6}\frac{\mathrm{m}^2}{\mathrm{s}} \qquad D_{\mathrm{s,theory}} = \frac{RT}{\xi M} = 0.134\times10^{-6}\frac{\mathrm{m}^2}{\mathrm{s}}$$

Example: Langevin Dynamics of a Free Brownian Particle

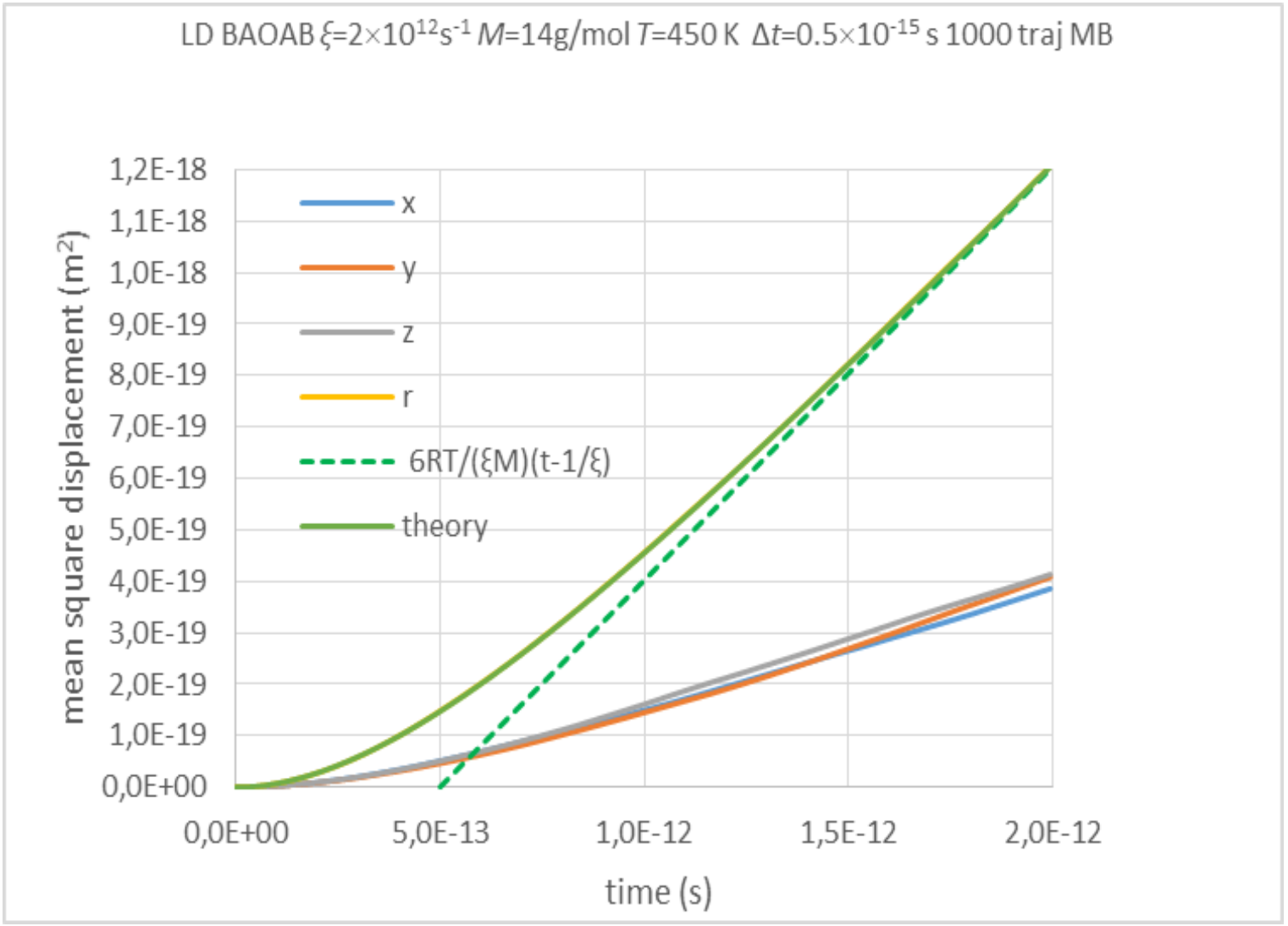

theory: $$\left\langle r^2 \right\rangle = 6D_s\left(t - \frac{1}{\xi} + \frac{1}{\xi}\exp(-\xi t)\right)$$

Example: Langevin Dynamics of a Free Brownian Particle

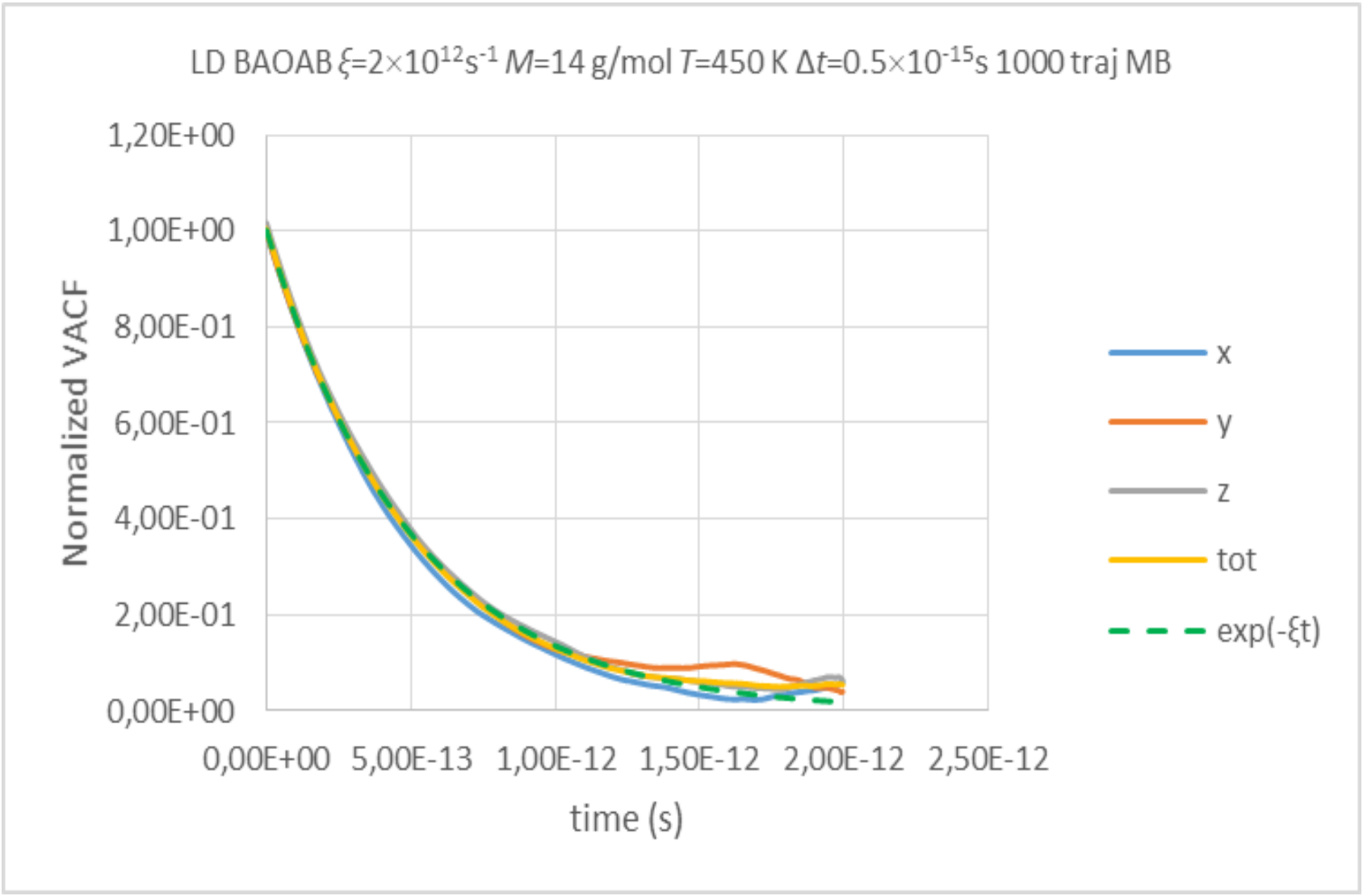

Example: Langevin Dynamics of a Free Brownian Particle

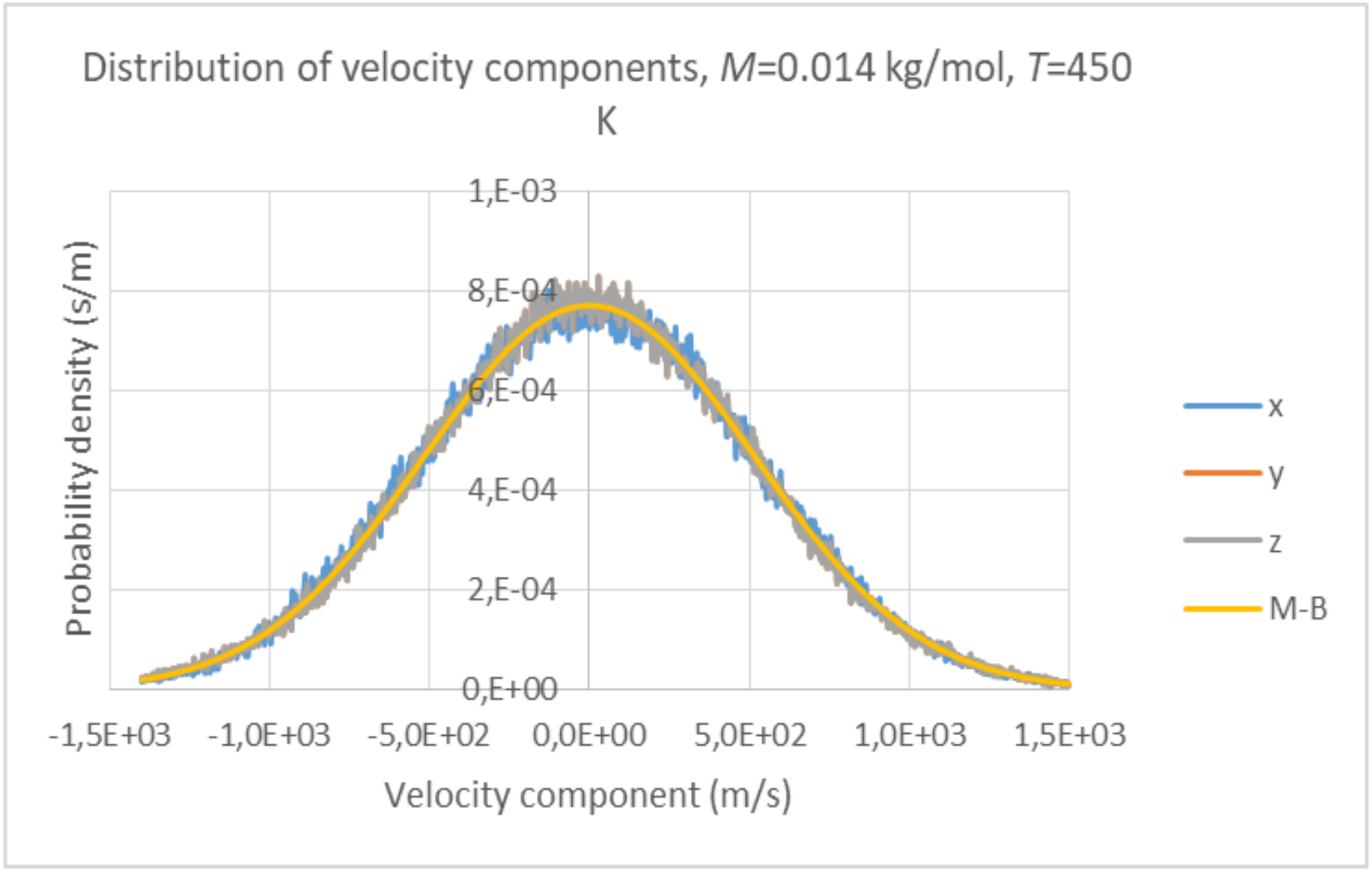

Example: Langevin Dynamics of a Free Brownian Particle

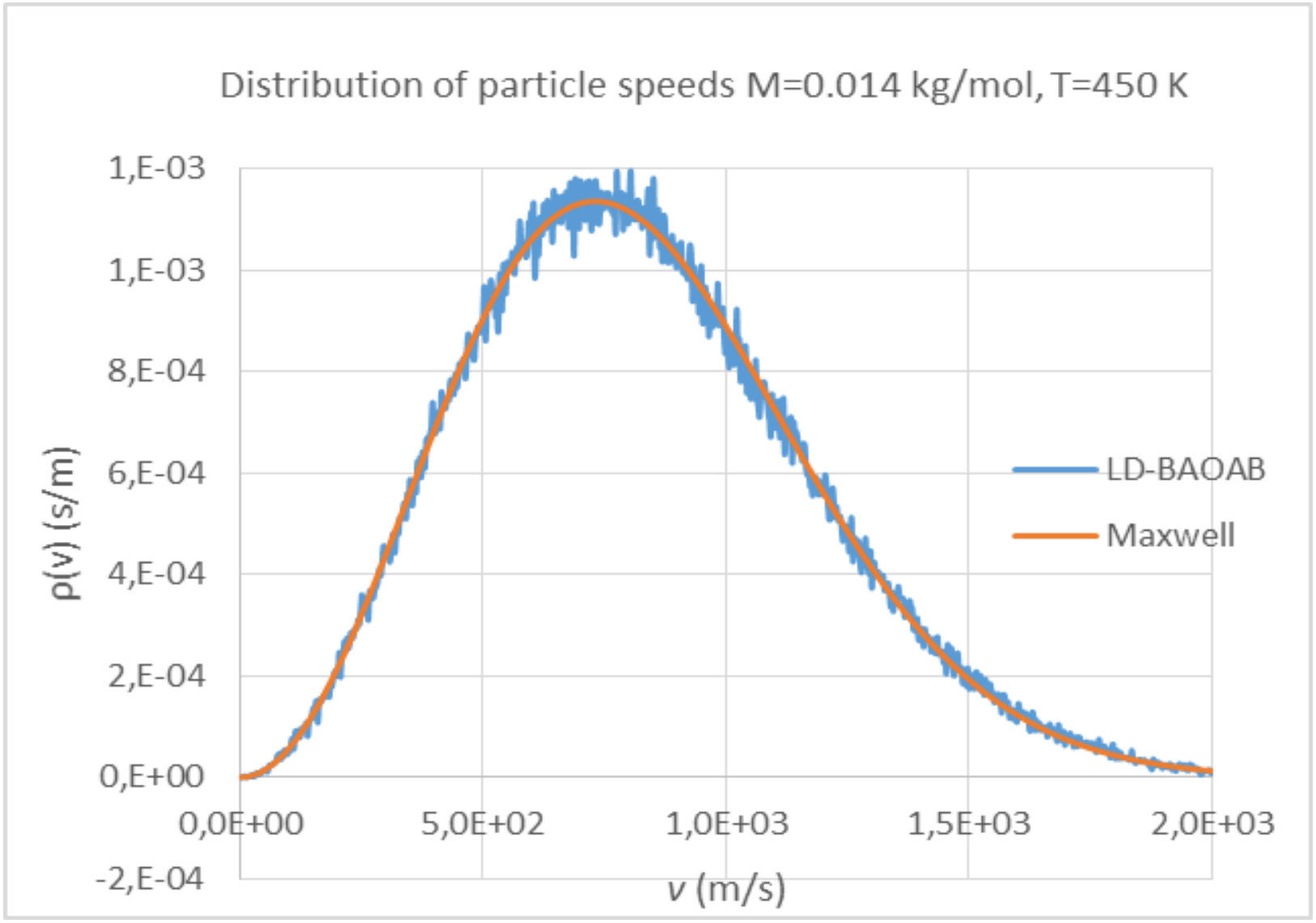

Position Langevin Equation – Brownian Dynamics

$$m\,\dot{\mathbf{v}}(t) = \mathbf{F}(\mathbf{r}) - m\,\xi\,\mathbf{v}(t) + \mathbf{R}(t)$$

External force due to field

Friction force

Langevin (random) force

$$\mathbf{F}(\mathbf{r}) = -\nabla_{\mathbf{r}} U(\mathbf{r})$$

$$\langle \mathbf{R}(t) \rangle = \mathbf{0}$$

$$\langle \mathbf{R}(t) \cdot \mathbf{v}(t) \rangle = 0$$

$$\langle R_\alpha(t) \cdot R_\beta(0) \rangle = 2\,m\,k_{\mathrm{B}}\,T\,\xi\,\delta_{\alpha\beta}\,\delta(t)$$

If we are interested in tracking the evolution of the system over time intervals $\Delta t >> 1/\xi$, we can neglect the inertial term on the left-hand side:

$$\left| m\,\dot{\mathbf{v}}(t) \right| \sim \left| m\,\mathbf{v}/\Delta t \right| << \left| m\,\mathbf{v}\,\xi \right| = \left| -m\,\xi\,\mathbf{v}(t) \right|$$

Under these conditions, we say that we study Brownian motion in the high friction limit. The motion is described by a position Langevin equation:

$$\dot{\mathbf{r}}(t) = \frac{1}{m\,\xi}\mathbf{F}(\mathbf{r}) + \mathbf{r}'(t) \quad \text{where } \mathbf{r}'(t) = \frac{1}{m\xi}\mathbf{R}(t) \text{ is a random velocity process}$$

$$\langle r'_\alpha(t) \rangle = 0 \qquad \langle r'_\alpha(t)\, r'_\beta(0) \rangle = 2\frac{k_{\mathrm{B}}T}{m\,\xi}\delta_{\alpha\beta}\delta(t) = 2D_{\mathrm{s}}\,\delta_{\alpha\beta}\,\delta(t) \qquad (\alpha,\beta = 1,2,3)$$

Brownian Dynamics

For a system of interacting Brownian particles, integration over time step Δt can be performed using the equations

$$\mathbf{r}_i\left(t+\Delta t\right)=\mathbf{r}_i\left(t\right)+\sum_j \frac{\mathbf{D}_{ij}\left(\boldsymbol{r}\right)}{k_{\mathrm{B}}T}\cdot\mathbf{F}_j\left(\mathbf{r}\right)\Delta t+\nabla_{\mathbf{r}_j}\cdot\mathbf{D}_{ij}\left(\mathbf{r}\right)\Delta t+\Delta\mathbf{r}_i^{\mathrm{G}}$$

$\Delta r_{i\alpha}^{\mathrm{G}}$ sampled from a multivariate Gaussian distribution with

Mean $\left\langle \Delta r_{i\alpha}^{\mathrm{G}} \right\rangle = 0 \quad \left(i=1,2,...,N;\ \alpha=1,2,3\right)$ and

Covariance matrix $\left\langle \Delta r_{i\alpha}^{\mathrm{G}} \Delta r_{j\beta}^{\mathrm{G}} \right\rangle = 2D_{ij,\alpha\beta}\Delta t \ \left(i,j=1,2,...,N;\ \alpha,\beta=1,2,3\right)$

For a set of dilute Brownian particles of diameter d moving in a solvent of viscosity η, the diffusivity tensors are well approximated by

$$\mathbf{D}_{ij}\left(\mathbf{r}\right)=\begin{cases}\dfrac{k_{\mathrm{B}}T}{3\pi\eta d}\mathbf{1}\,, & \text{if } i=j\\[2ex] \dfrac{k_{\mathrm{B}}T}{8\pi\eta r_{ij}}\left(\mathbf{1}+\dfrac{\mathbf{r}_{ij}\mathbf{r}_{ij}}{r_{ij}^2}\right), & \text{if } i\neq j\end{cases}$$

Hydrodynamic interactions
Oseen tensor

Brownian Dynamics/Transition State Theory Study of Long Alkane Diffusion in Silicalite-1

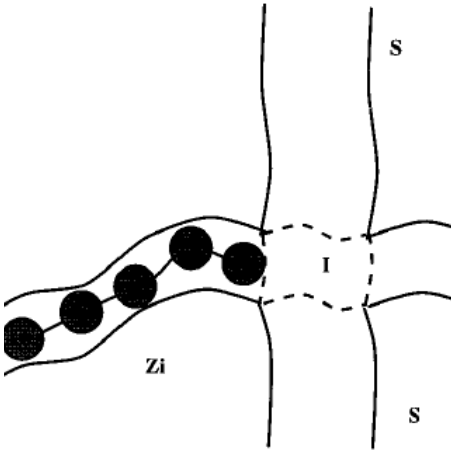

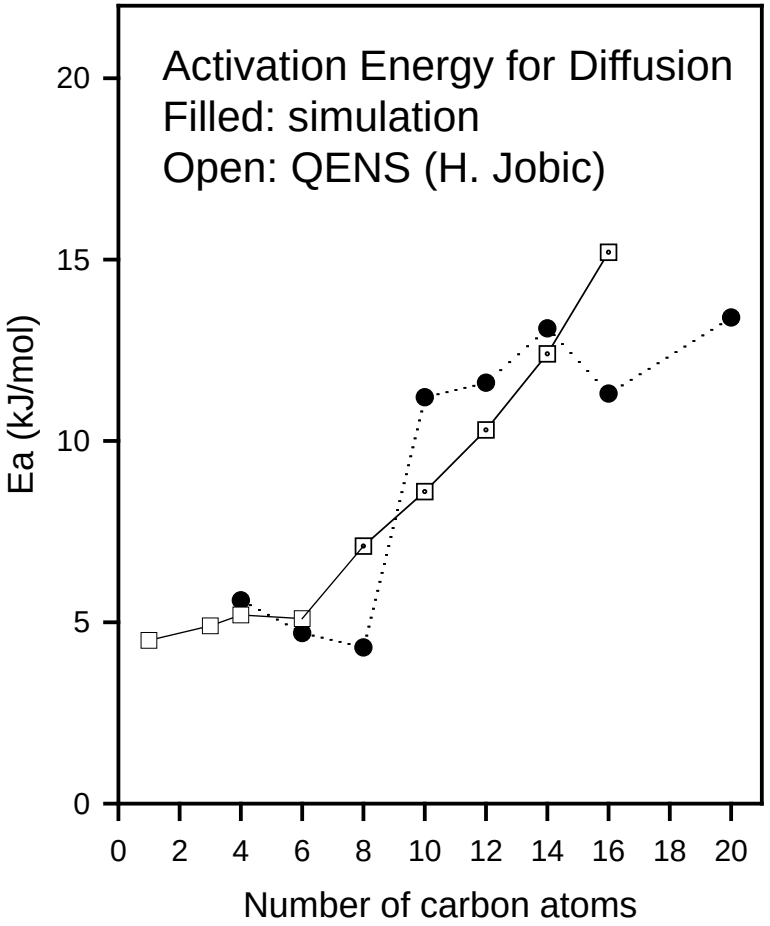

- Potential of mean force $U(x_1, x_2)$ in each macrostate extracted from configurational bias Monte Carlo Integration (CBMCI).
- Contribution to friction matrix in each environment estimated by fitting chain midpoint and contour length time auto-correlation functions from short-time MD.
- Rate constants for transitions between macrostates calculated by TST using CBMCI and piecewise planar representations of the dividing surfaces.

Maginn, E.J.; Bell, A.T.; DNT *J. Phys. Chem*. **1996**, *100*, 7155-7173.

Dissipative Particle Dynamics

Model = set of point particles that move and interact with each other with three types of pairwise forces:

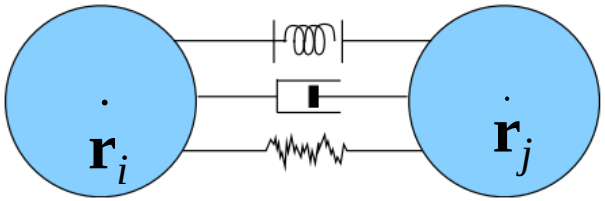

$$\mathbf{r}_{ij} = \mathbf{r}_i - \mathbf{r}_j$$

$$r_{ij} = \left|\mathbf{r}_{ij}\right|$$

$$\mathbf{e}_{ij} = \frac{\mathbf{r}_{ij}}{r_{ij}}$$

$$\mathbf{F}_i = \sum_{j \neq i} \left(\mathbf{F}_{ij}^{\mathrm{C}} + \mathbf{F}_{ij}^{\mathrm{D}} + \mathbf{F}_{ij}^{\mathrm{R}} \right)$$

1) A **conservative** force derived from a potential

$$\mathbf{F}_{ij}^{\mathrm{C}} = a_{ij} \left(1 - \frac{r_{ij}}{r_{\mathrm{c}}} \right) \mathbf{e}_{ij}$$

2) A **dissipative** force that reduces the radial velocity differences

$$\mathbf{F}_{ij}^{\mathrm{D}} = -\zeta_{ij} \omega_{\mathrm{D}} \left(\mathbf{e}_{ij} \cdot \mathbf{v}_{ij} \right) \mathbf{e}_{ij}$$

3) A **stochastic** force directed along the line joining the centers of the particles

$$\mathbf{F}_{ij}^{\mathrm{R}} = \sigma_{ij} \omega_{\mathrm{R}} \psi_{ij} \mathbf{e}_{ij}$$

ψ_{ij}: Gaussian white noise that is symmetric ($\psi_{ij} = \psi_{ji}$) and satisfies

$$\langle \psi_{ij}(t) \rangle = 0, \quad \langle \psi_{ij}(t)\, \psi_{kl}(t') \rangle = (\delta_{ik}\delta_{jl} + \delta_{il}\delta_{jk})\, \delta(t - t')$$

Fluctuation-dissipation

$$\left[\omega_{\mathrm{R}}\left(r_{ij}\right) \right]^2 = \omega_{\mathrm{D}}\left(r_{ij}\right)$$

$$\sigma_{ij}^2 = 2\zeta_{ij} k_{\mathrm{B}} T$$

Forces vanish beyond a cutoff distance r_{c}.
Total momentum is conserved,
hydrodynamics is respected, T = const.

Hoogerbrugge and Koelman, *Europhys. Lett.* **1992**, *19*, 155.
Español and Warren, *Europhys. Lett.* **1995**, *30*, 191.

Coarse-graining of poly(SPE) antifouling polymers

Atomistic

Molecular Dynamics

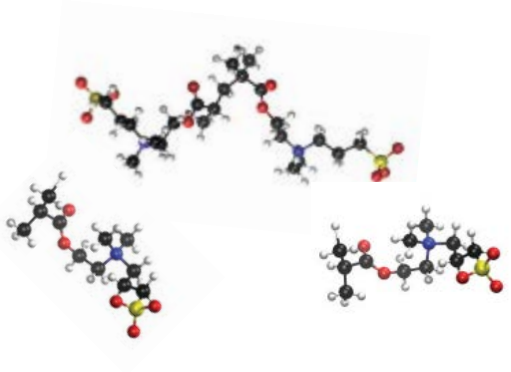

(fs – μs; Å – 10 nm)

Examine

low to moderate molar masses

Assess

- Short- and long-range structure, conformations
- Dynamics
- Thermodynamics

Mapping

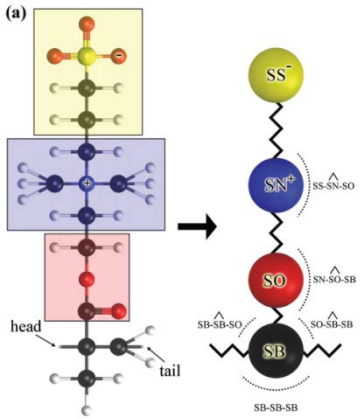

Parameterization Procedure

Bonded interactions

-Matching of strand and strand/angle distributions

Nonbonded interactions

-Matching g_{ij}s

Dynamics

-Friction factor

Mesoscopic

Dissipative Particle Dynamics (DPD)

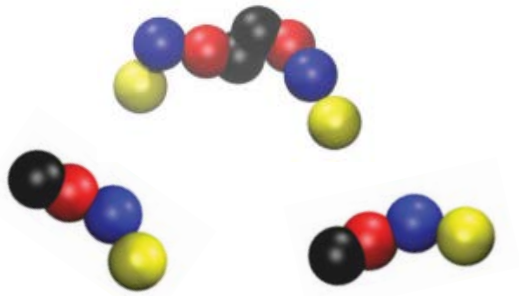

(ps - 10 ms; nm – μm)

Reproduce

atomistic results

Access high molar mass regime

Predict

- Long-range structure and conformations
- Surface-foulant potential of mean force

Coarse-graining of water and DPD units

Coarse-graining : $N_m = 5$ water molecules per bead

Size of water bead : $r_c = \sqrt[3]{3N_m \frac{M_{H_2O}}{N_{Avo}\rho_{H_2O}}} = 7.66$ Å

Repulsion strength : $a_{ij} = 135.868$ (units of $k_B T/r_c$)
(reproduces experimental compressibility of H_2O)

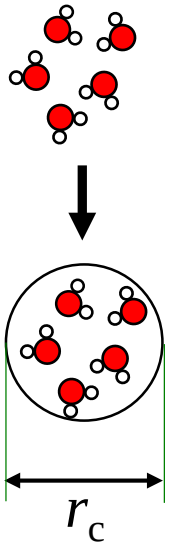

- DPD → limited ability to reproduce the dynamical properties of water.[1,2]
- The mobilities are compared to experimental D_{H20}, following literature approach to convert DPD time unit into physical time.

×500 longer time step than MD ($dt_{MD} = 0.001$ ps)

Speedup: 3-5 orders of magnitude[1]

Simulation time step : $dt = 0.023$ ps

Effective time step : $dt^{renorm} = dt \frac{D^{exp}_{H_2O}}{N_m D^{sim}_{H_2O}} = 0.496$ ps

[1]Groot, R. D.; Rabone, K.L. *Biophys. J.* **2001**, *81*(2): 725–736

[2]Lee M- T. et al. J. *Chem. Theory Comput*. **2015**, *11*(9), 4395-4403

Coarse-graining of SPE polymers

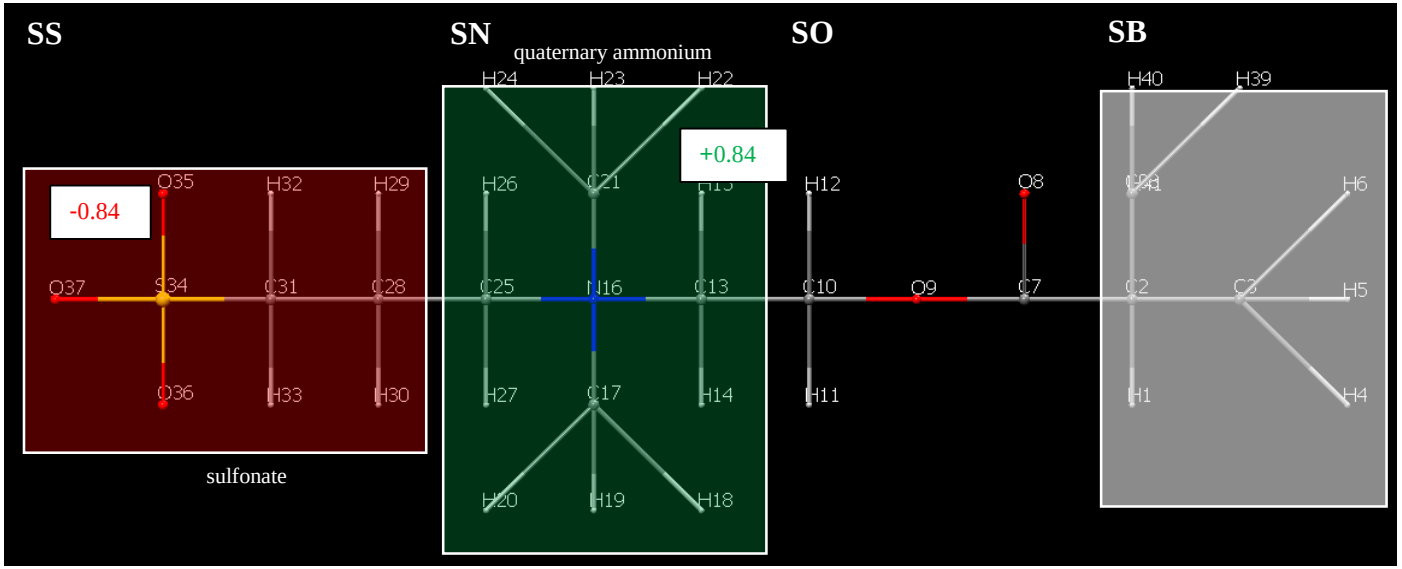

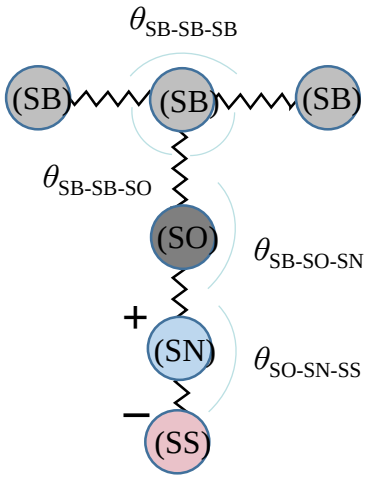

Starting atomistic representation: OPLS

Beads mapped to the centers-of-mass:

$$\mathbf{r}_{\mathrm{cg},j} = \frac{\sum_{\text{all atoms } i \text{ belonging to bead } j} M_i \mathbf{r}_i}{\sum_{\text{all atoms } i \text{ belonging to bead } j} M_i}$$

Charge set to $|q| = 0.84$ e (based on atomistic OPLS). Charge smeared over sphere of radius $0.25\, r_c$.

Lee, M. T.; Vishnyakov, A.; Neimark, A. V. *J. Chem. Phys*. **2016**, *144* (1), 1–12.

Warren, P. B.; Vlasov, A. *J. Chem. Phys.* **2014**, *140*, 084904.

Derivation of DPD bonded coefficients

Starting point: 0.1 μs atomistic MD of two SPE8 chains in water, 10.4% w/w.

Automatic regression of the the strand-length and angle distributions with harmonic effective bonded potentials for use in DPD simulations.

Annealing optimization scheme that finds *all* the optimal strand and angle coefficients *at the same time* that best reproduce the distributions from MD *in the presence of all interactions*.

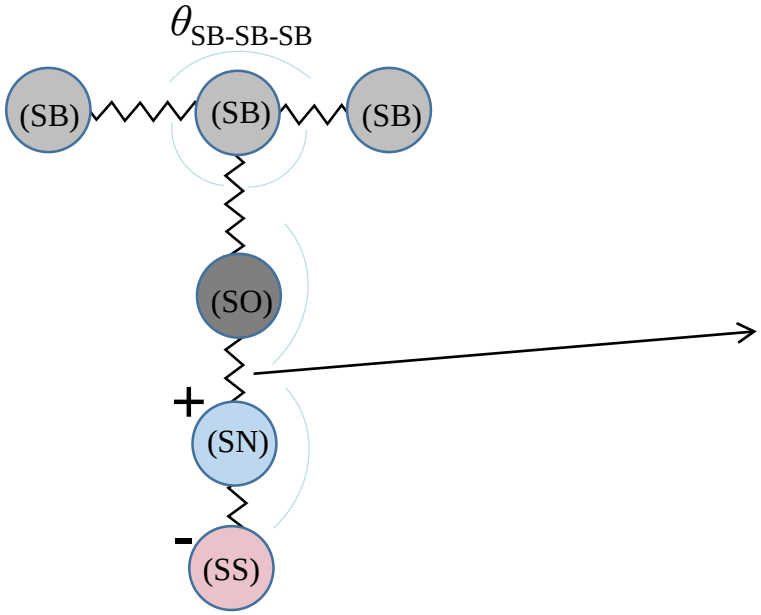

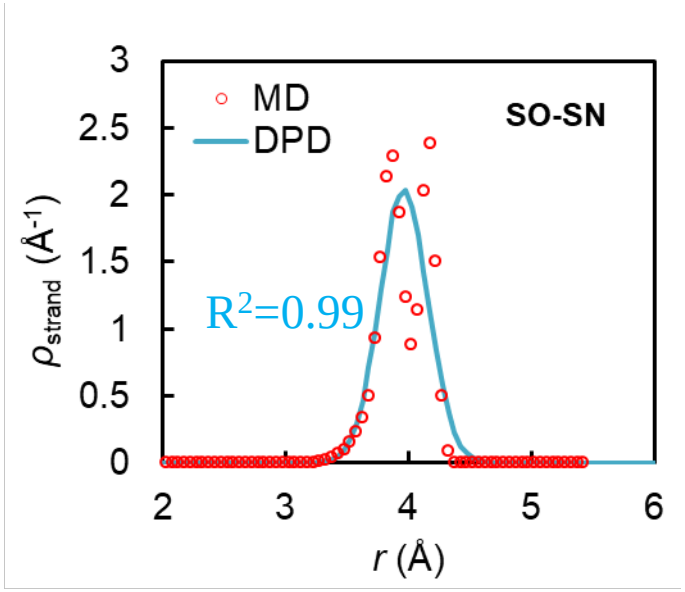

Example: SO-SN *strand length*

Nonbonded Interactions

Optimization of a_{ij} coefficients[1] for all the possible interactions with the target to minimize the following objective function:

$$\mathrm{MSSE} = \frac{1}{n_{\mathrm{pairs}}} \sum_{\mathrm{pairs}\ ij} \sum_{r=0}^{r_{\max}} \left(g_{ij}^{\mathrm{DPD}}(r) - g_{ij}^{\mathrm{MD}}(r) \right)^2$$

Involves integrals of squared deviations between atomistic and DPD-based g_{ij}'s over distances commensurate with or smaller than the saturation distance of the pair distribution functions.

15 a_{ij} parameters needed for the description of all the interactions.
($n_{\mathrm{SPE\text{-}SPE}} = 10$, $n_{\mathrm{SPE/W}} = 5$)

a_{ij} coefficients to be optimized:

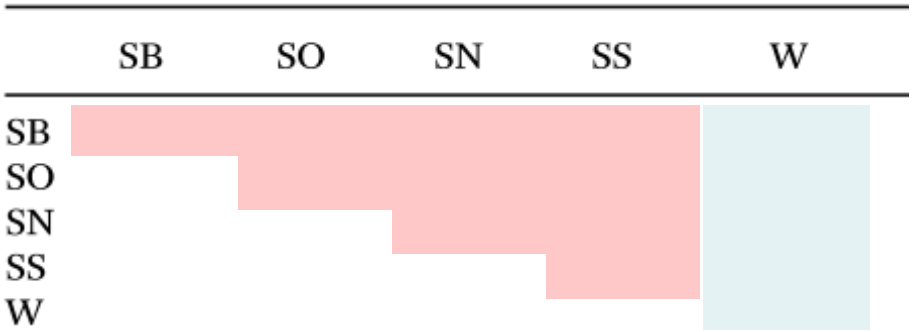

1. Groot, R. D.; Warren, P. B. J. *Chem. Phys*. **1997**, *107* (11), 4423–4435.

Nonbonded interactions

Objective function optimized as follows:

1. ~5000 iterations with bounded random sampling [a_{min}=10, a_{max} = 180]
2. ~3000 iterations with multidimensional Bayesian optimization[1] having as an input the 5000 previous iterations.

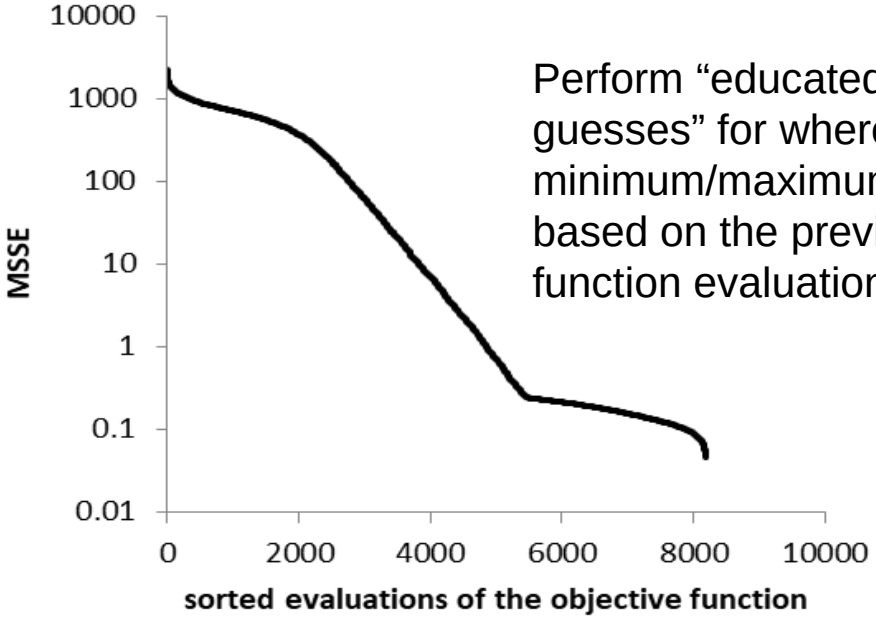

Perform "educated guesses" for where a minimum/maximum exists based on the previous function evaluations.

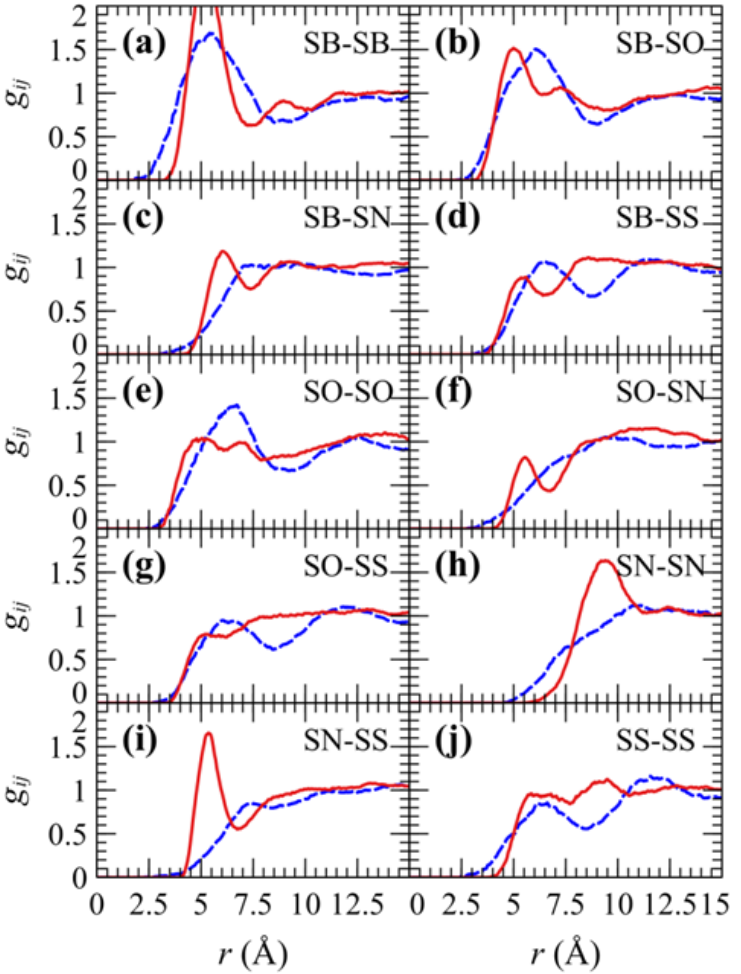

Example pair radial distribution functions from atomistic MD (blue) and DPD (red).

[1] https://github.com/fmfn/BayesianOptimization

[2] https://machinelearningmastery.com/what-is-Bayesian-optimization/

[3] https://arxiv.org/abs/1807.02811

Investigation of SPE chains in bulk solution

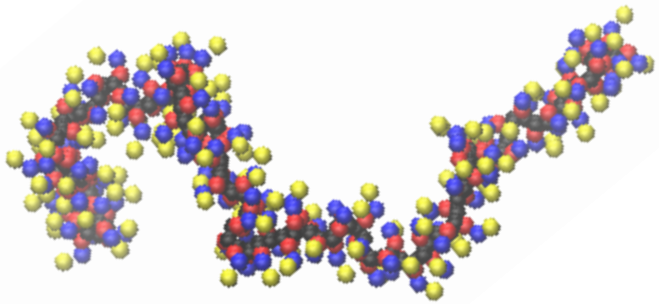

SPE_{128}

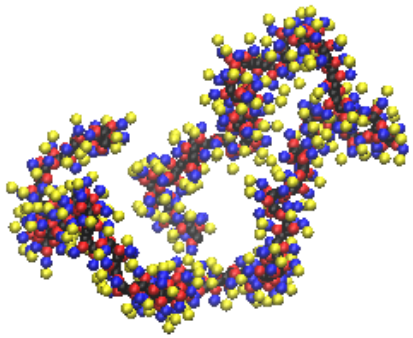

SPE_{256}

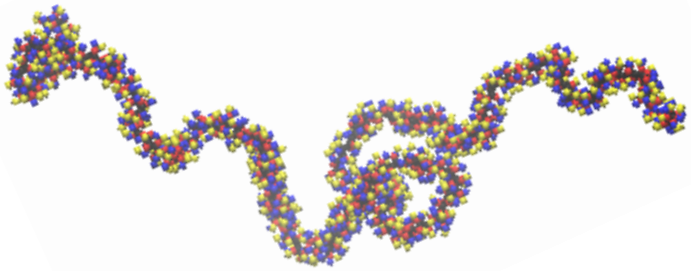

SPE_{512}

Structural features of Atomistic and Mesoscopic SPEs

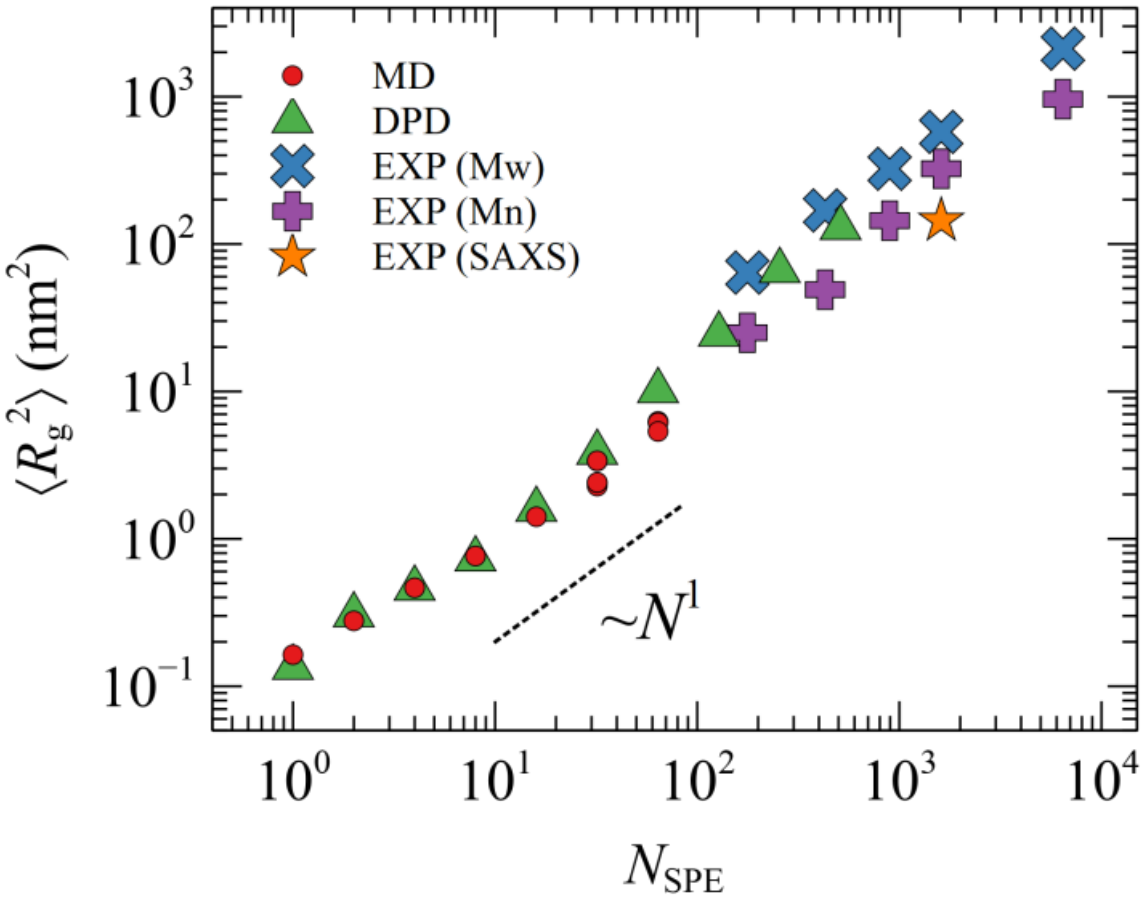

Mean square radius of gyration from MD (●), DPD calculations (▲) and experimental data[1] (×, + and ★). Experimental data derived from the correlation $R_g = aM_\alpha{}^b$ with $a = 0.69$ nm and $b = 0.48$, with M_α being either the weight- (M_w, ×) or number (M_n, +) average molar mass.

[1]Mary, P.; Bendejacq, D. D.; Labeau, M.-P.; Dupuis, P. *J. Phys. Chem. B* **2007**, *111*, 7767.

Mesoscopic Investigation of SPE brushes

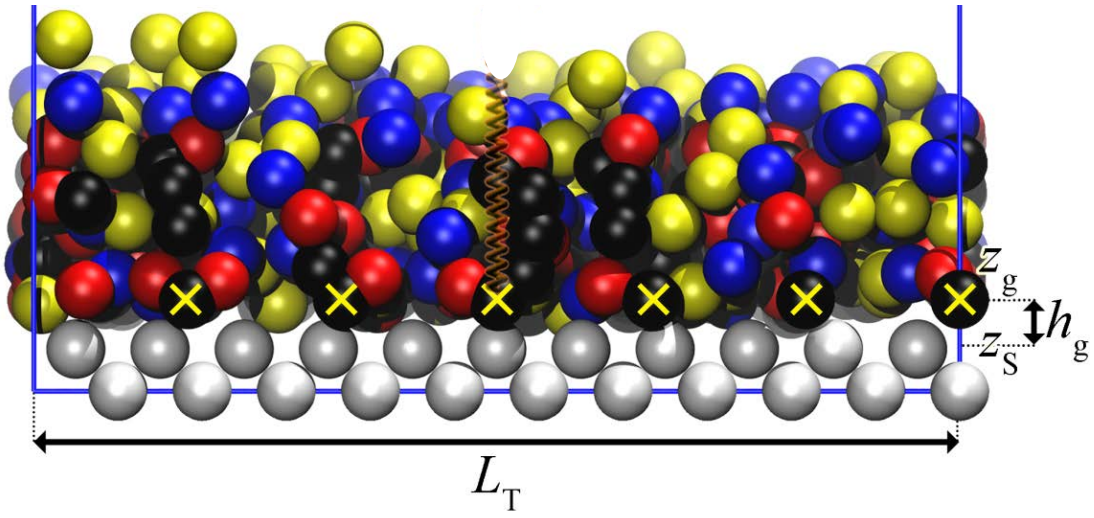

Area/chain = 1.44 nm^2. SB (black), SO (red), SN (blue), SS (yellow) and wall beads (white) shown. Wall beads and grafted beads (SB beads marked with $\times$) remain immobile throughout the simulation. z_S : position of wall surface. h_g: grafted point-wall surface distance.

Polyamide membrane surface modeled as periodic FCC lattice (white beads).

Initially, SPE chains grafted periodically with the same areal densities and chain lengths as in Xiang et. al.'s work[1] for validation purposes.

Additional simulations[2] over a broader parameter space spanning various degrees of polymerization (N_{SPE} = 5-20) and areas per chain (0.64-37 nm^2).

[1]Xiang et al. *Langmuir* **2018**, *34*, 2245−2257

[2]Sgouros, A.P.; Knippenberg, S.; Guillaume, M.; DNT *Soft Matter* **2021**, *17*, 10873

SPE brush density profiles

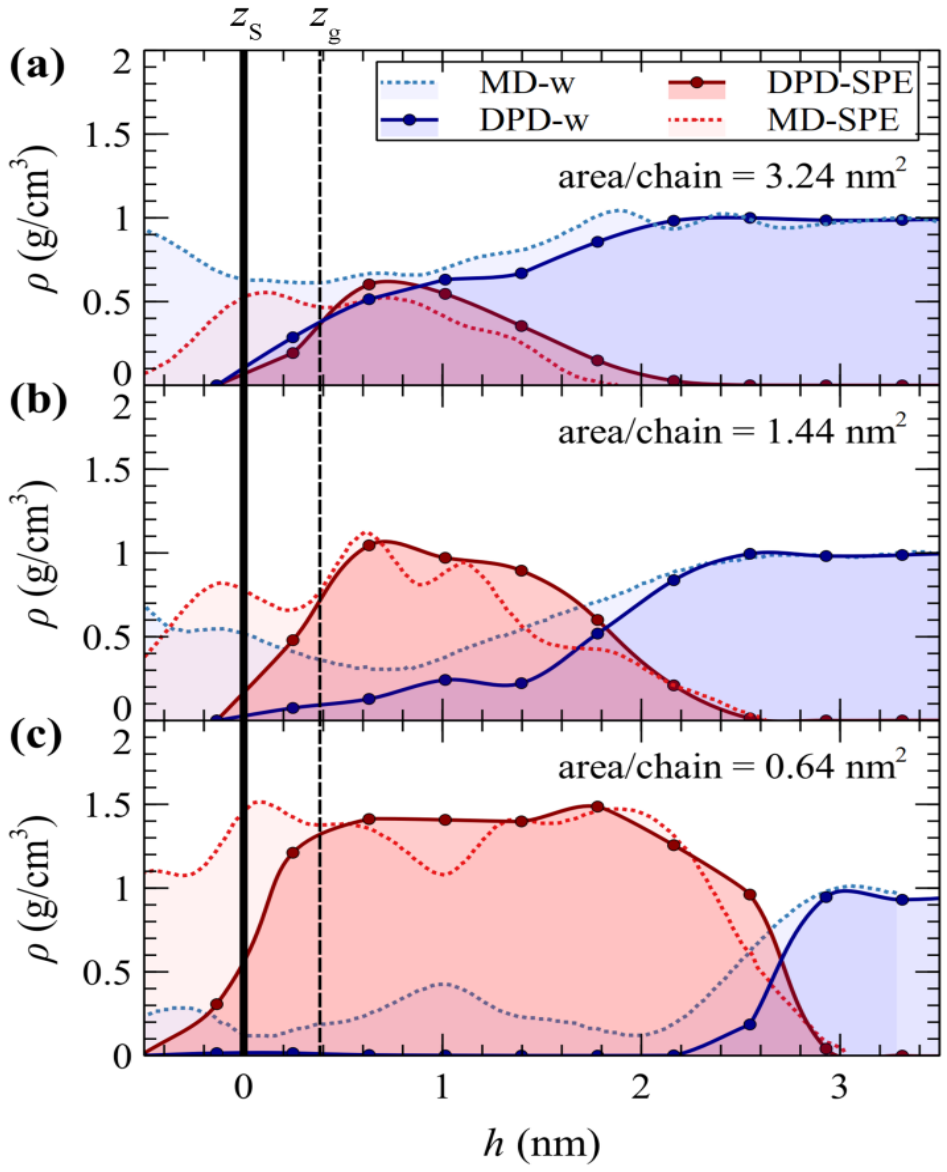

Density profiles of SPE (red) and water (blue) from DPD (solid lines)[2] and atomistic MD[1] (dotted lines). 5 SPE units per grafted chain.

Area/chain = **(a)** 3.24 nm^2
(b) 1.44 nm^2
(c) 0.64 nm^2.

Solid vertical line: effective position of the wall, z_S.

Dashed line: position of grafting points, z_g, in DPD.

Bin width $0.5r_{DPD} \sim 0.383$ nm.

[1]Xiang et al. *Langmuir* **2018**, *34*, 2245

[2]Sgouros, A.P.; Knippenberg, S.; Guillaume, M.; DNT *Soft Matter* **2021**, *17*, 10873

Mean force on approaching foulant

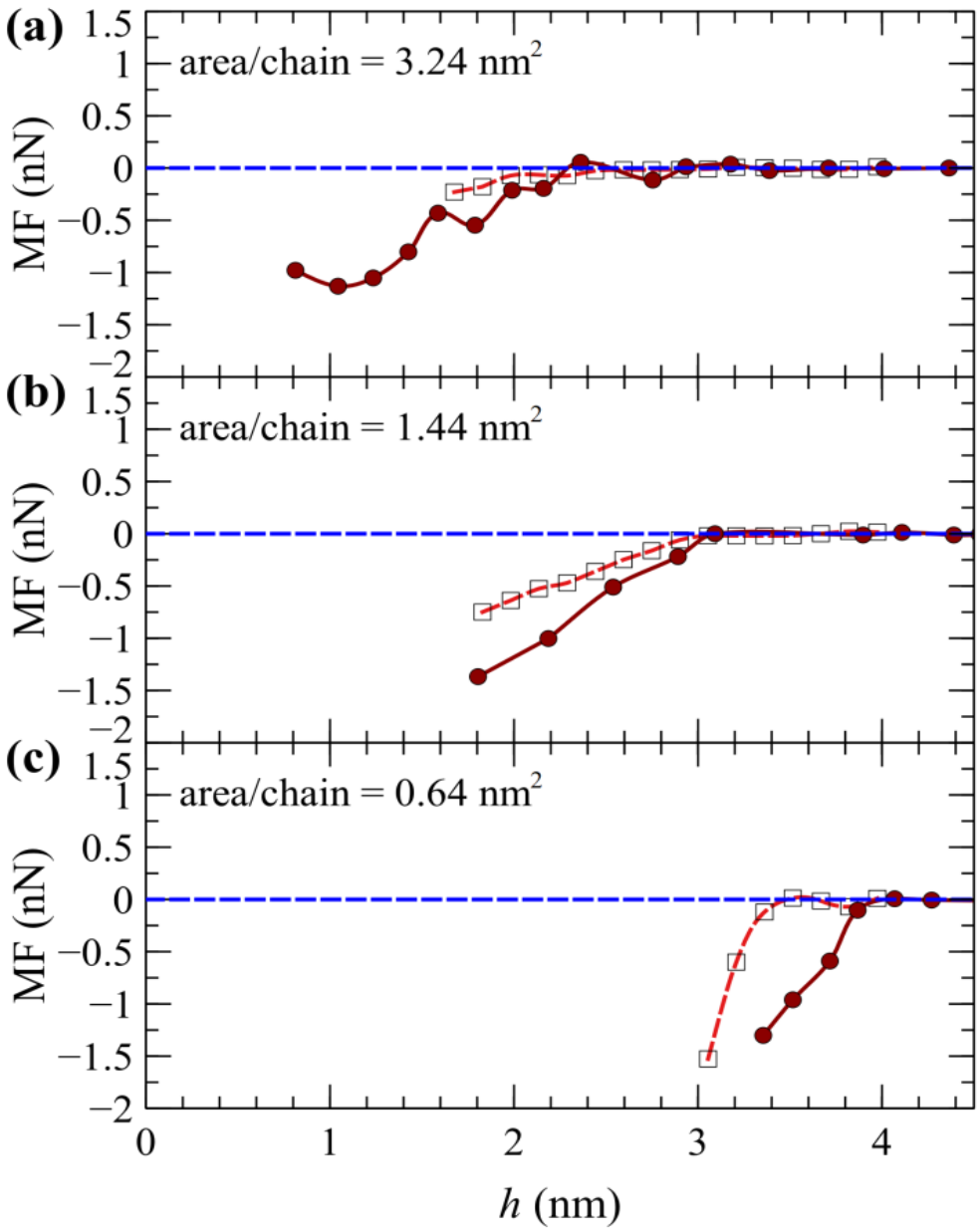

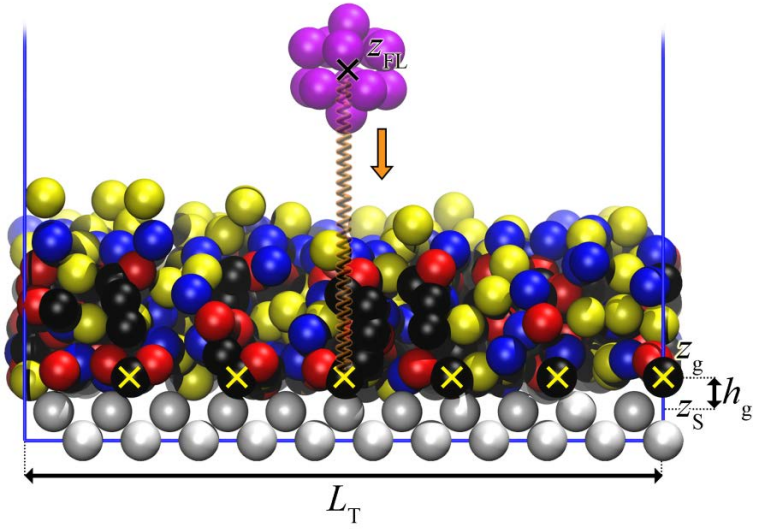

Umbrella Sampling (Weighted Histogram Analysis Method)

Foulant modeled as icosahedron with radius of gyration 0.73 nm

Filled circles: atomistic MD, Xiang et al., *Langmuir* **2018**, *34*, 2245.

Open squares: DPD, Sgouros, A.P.; Knippenberg, S.; Guillaume, M.; DNT *Soft Matter* **2021**, *17*, 10873

Entanglement network-based mesoscopic simulations of polymer melts

short chains
(unentangled)

long chains
(entangled)

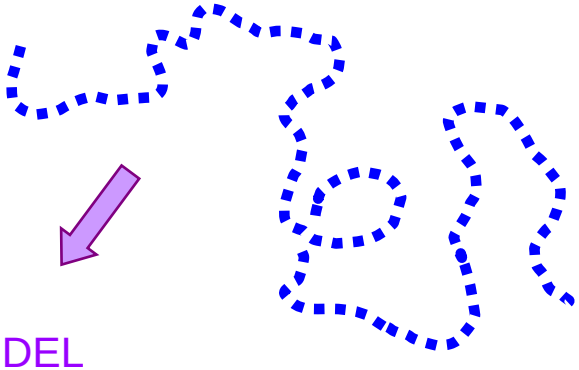

ROUSE MODEL

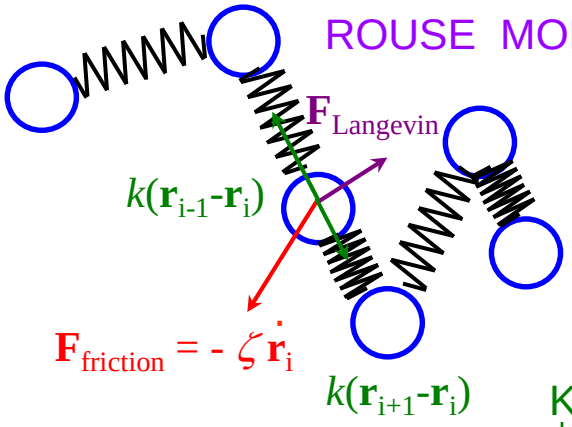

Kuhn length

Parameters $k=3k_BT/b^2$, ζ

REPTATION MODEL

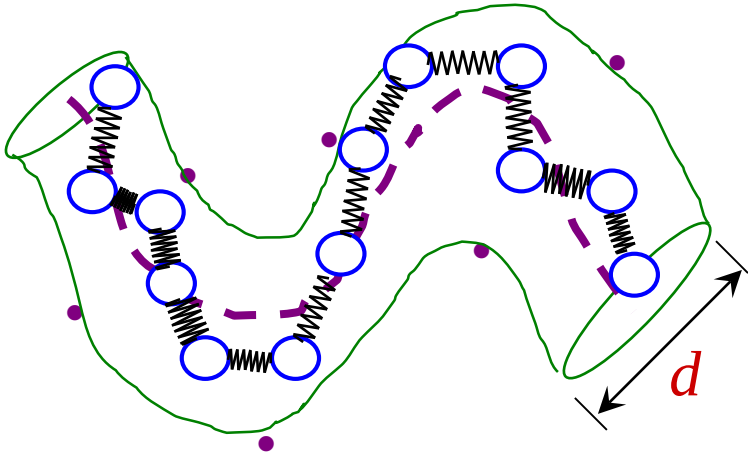

Additional parameter $d \approx a_{pp}$

Rouse, P. E. *J. Chem. Phys*. **1953**, *21*, 1272.

de Gennes, P.G. *Scaling Concepts in Polymer Physics*, Cornell University Press: Ithaca, NY, 1979.

Doi, M.; Edwards, S.F. *The Theory of Polymer Dynamics*, Clarendon Press: Oxford, 1986.

Mesoscopic Entanglement Network Representation

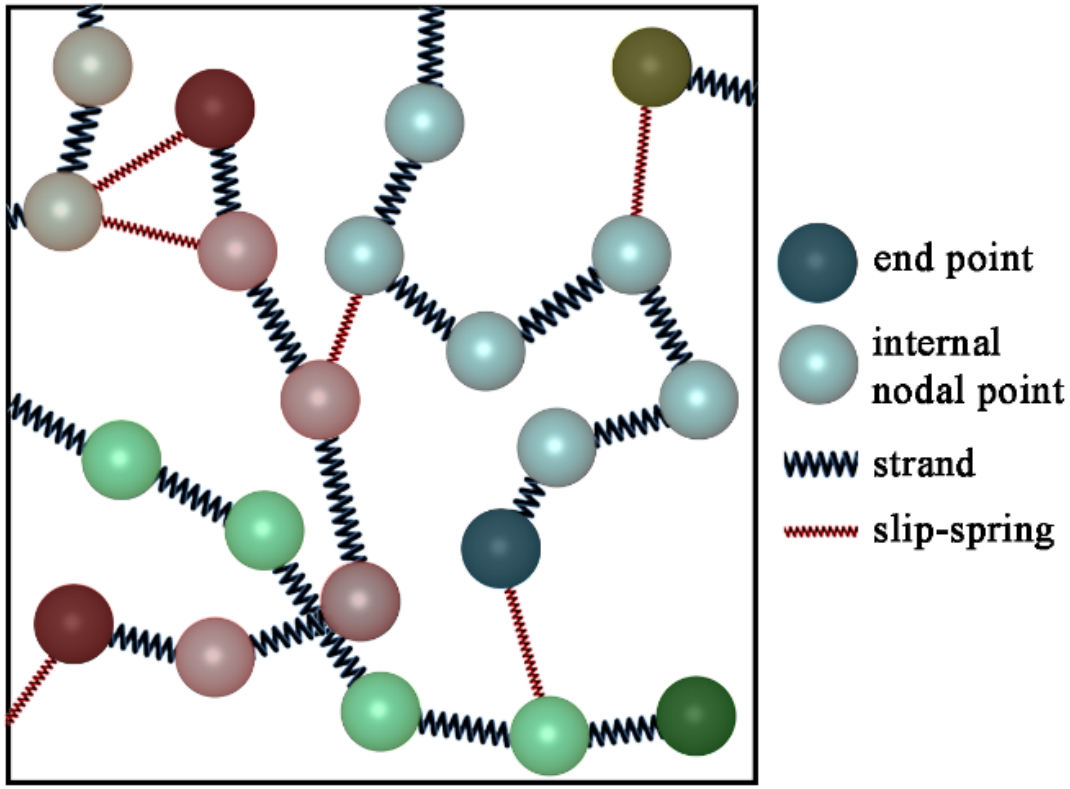

Nodal point or “bead”:
5-10 Kuhn segments

PE:
n=52 C atoms/bead

cis-1,4 PI:
22 -CH_2-$CH(CH_3)$=CH-CH_2- units/bead

Ensemble canonical with respect to polymer chains,
canonical or grand canonical with respect to slip-springs
Concentration of slip-springs regulated via activity z_{activ}

$$z_{activ} = \langle n_{ss} \rangle / \left\langle \sum_{i>j} e^{-A_{ss}\left(|\mathbf{r}_i - \mathbf{r}_j|\right)/(k_B T)} \right\rangle$$

Chappa et al. *Phys. Rev. Lett.* **2012**, *109*, 148302.

Mesoscopic Helmholtz energy function

$$A = A_{\text{strands}} + A_{\text{angles}} + A_{\text{nonbonded}} + A_{\text{entanglements}} + A_{\text{compensating}}$$

$A_{\text{strands}} + A_{\text{angles}}$: Effective stretching and bending potentials, contributed by pairs and triplets of beads along a chain. Incorporate subchain entropic elasticity.

$A_{\text{nonbonded}}$: Excluded volume and van der Waals attractive interactions. Functional integral of a nonbonded Helmholtz energy function, which depends on local density and is derived from an equation of state. Computed by spatial discretization.

$A_{\text{entanglements}}$: Free energy of the slip-springs.

$A_{\text{compensating}}$: Removes perturbations in chain conformations caused by the slip springs.
(Chappa et al. *Phys. Rev. Lett.* **2012**, *109*, 148302).

Simulation canonical wrt polymer, grand canonical wrt slip-springs (activity z_{activ})

Intramolecular Helmholtz Energy

Potential of mean force for stretching of strands

From equilibrium atomistic simulations

$$A_{\text{strand}}(\mathbf{r}) = -k_{\text{B}}T \ln \frac{\rho_{\text{strand}}(r)}{4\pi r^2}$$

$$\mathbf{F}_{\text{strand}}(\mathbf{r}) = -\nabla_{\mathbf{r}} A_{\text{strand}}$$

Very well described by L_{301}^{-1} approximation proposed by M. Kröger for inverse Langevin function.

J. Non-Newtonian Fluid Mech. **2015**, *223*, 77.

Deviates from Gaussian at high extensions.

Bending potential of mean force

$$A_{\text{angle}}(\theta) = k_{\text{a}}(\theta - \pi)^2$$

Fitted to effective bond angle distributions between strands.

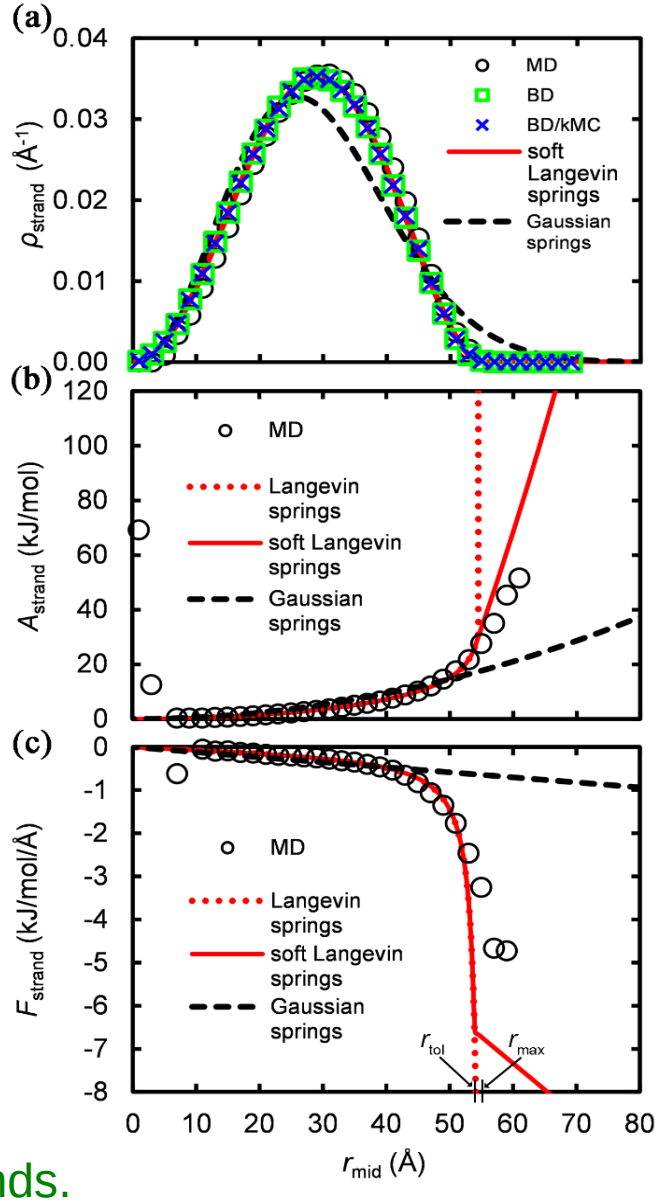

Nonbonded Helmholtz energy in the bulk melt

$$A_{\text{nonbonded}} = \int_{\text{box}} \mathrm{d}^3 r \; a_{\text{vol}}^{\text{ex}} \left[\rho(\mathbf{r}), T \right] = \sum_{k \in \text{cells}} V_{\text{cell}} a_{\text{vol}}^{\text{ex}} \left(\rho_{\text{cell},k}, T \right)$$

Excess Helmholtz energy density $a_{\text{vol}}^{\text{ex}}$ from equation of state.

Sanchez-Lacombe *J. Phys. Chem.* **1976**, *80*, 2352 – 2362

$$a_{\text{vol}}^{\text{ex}}(\rho, T) = -P^* \tilde{\rho}^2 + P^* \tilde{T} (1 - \tilde{\rho}) \ln(1 - \tilde{\rho}) + P^* \tilde{T} \tilde{\rho} \left\{ 1 + \frac{1}{r_{\text{SL}}} \ln \left(\frac{Z_{\text{intra, cg chain}} \prod_i \Lambda_i^3}{Z_{\text{intra}} \Lambda_{\text{bead}}^{3 n_{\text{beads/chain}}}} \right) \right\}$$

$$\tilde{\rho} = \frac{\rho}{\rho^*} \qquad r_{\text{SL}} = \frac{P^* M}{\rho^* R T^*}$$

Mass of each bead uniformly smeared within a voxel of edge length $h = R_{g,\text{bead}}$

Local density distribution $\rho(\mathbf{r})$ accumulated using a grid of cubic cells of edge length l_{cell}=3 to 5 nm

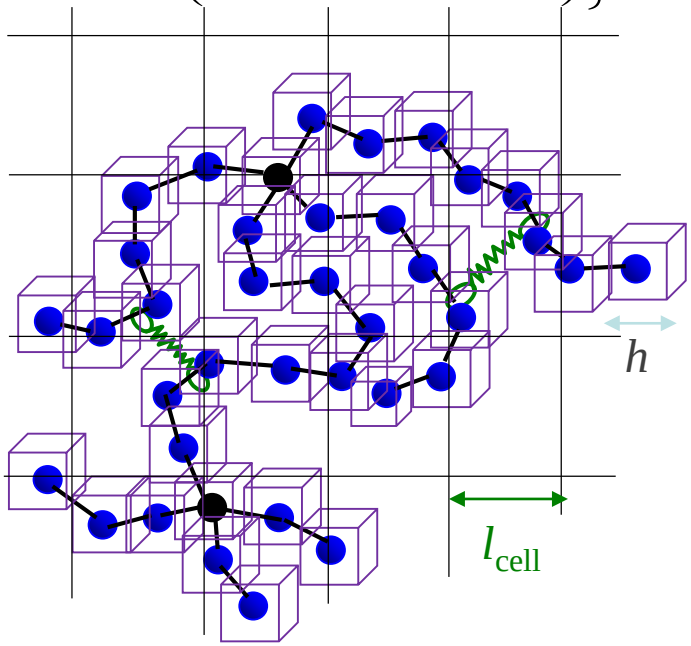

Mesoscopic Brownian Dynamics simulation

$$\mathbf{r}_i\left(t_n+\Delta t\right)=\mathbf{r}_i\left(t_n\right)+\frac{1}{\zeta_{\text{bead}}(T)}\left[\mathbf{F}_i\left(t_n\right)\Delta t+\frac{1}{2}\dot{\mathbf{F}}_i\left(t_n\right)\left(\Delta t\right)^2\right]+\mathbf{R}_i\left(\Delta t\right)$$

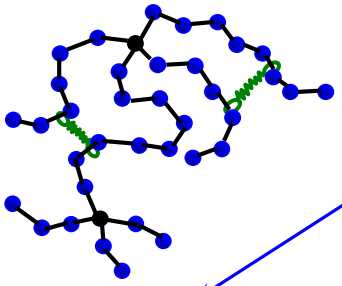

$$\zeta_{\text{bead}}(T)=\zeta_0(T)\frac{m_{\text{bead}}}{m_{\text{monomer}}}$$

ζ_0 obtained from MD simulations (Harmandaris, V.A.; Mavrantzas. V.G.; DNT Macromolecules **1998**, 31, 7934) or from NMR measurements (Klopffer, M-H; Bokobza, L; Monnerie, L. *Polymer* **1998,** *39*, 3445).

$$\log\zeta_0\left(T\right)=\log\zeta_{0,\infty}+\frac{C_1^{\text{g}}C_2^{\text{g}}}{T-T_{\text{g}}+C_2^{\text{g}}}$$

$$\zeta_0\left(\text{PE},450\text{K}\right)=4.15\times10^{-13}\ \text{kg/s}$$

Random displacement vector. Components follow Gaussian distribution:

$$\left\langle R_{i,\alpha}^2\left(\Delta t\right)\right\rangle=2k_{\text{B}}T\frac{\Delta t}{\zeta_{\text{bead}}(T)}\quad(\alpha=1,2,3)$$

$\mathbf{F}_i=-\nabla_{\mathbf{r}_i}A$ including all contributions

Integration time step for PE: Δt=10 ps
Total time simulated: 0.1 s

Slip-springs: discrete hopping dynamics

Density of slip-springs (controlled via z_{activ}): 1.5 that determined from M_e

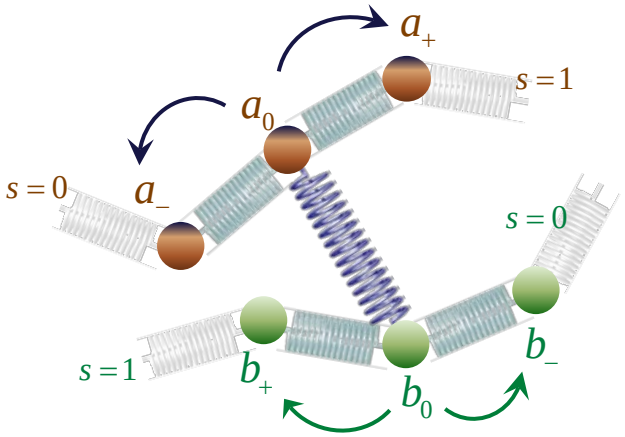

$$k_{\text{hop}} = \nu_0 \exp\left(-\frac{A^{\ddagger}_{\mathcal{O}\to\mathcal{N}} - A_{a_0\wedge b_0}}{k_B T}\right) = \nu_{\text{hop}} \exp\left(\frac{A_{a_0\wedge b_0}}{k_B T}\right)$$

TST picture of hopping over a free energy barrier

Slip-springs move along chain contour by discrete jumps between neighboring beads.

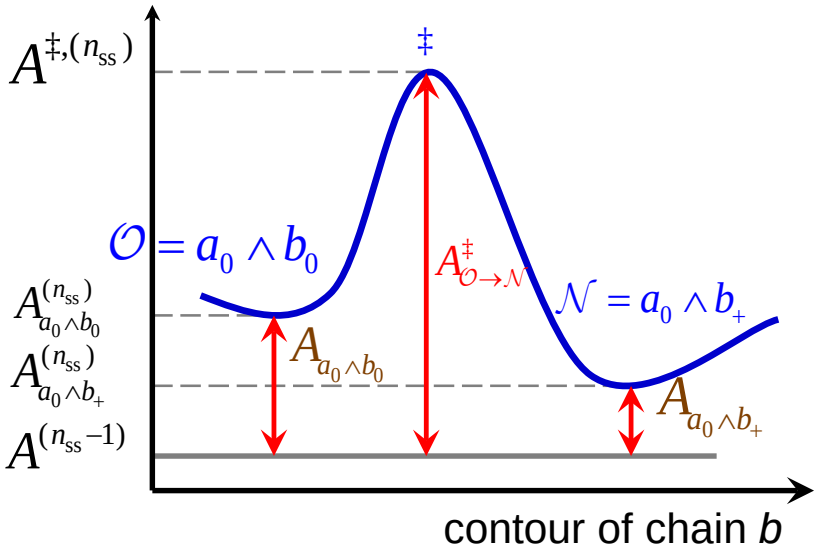

Initial estimate:

$$\nu_{\text{hop}} \approx \frac{k_B T}{\zeta_{\text{bead}}} \frac{\langle N_{ss} \rangle}{N_{\text{beads}}} \frac{1}{\left(n_{\text{Kuhns/bead}} b^2\right)}$$

$$\nu_{\text{hop}}\left(\text{PE}, 450\text{K}\right) = 5\times10^5 \ \text{s}^{-1}$$

Vogiatzis, G.G.; Megariotis, G.; DNT *Macromolecules* **2017**, *50*, 3004.

Formation and destruction of slip-springs

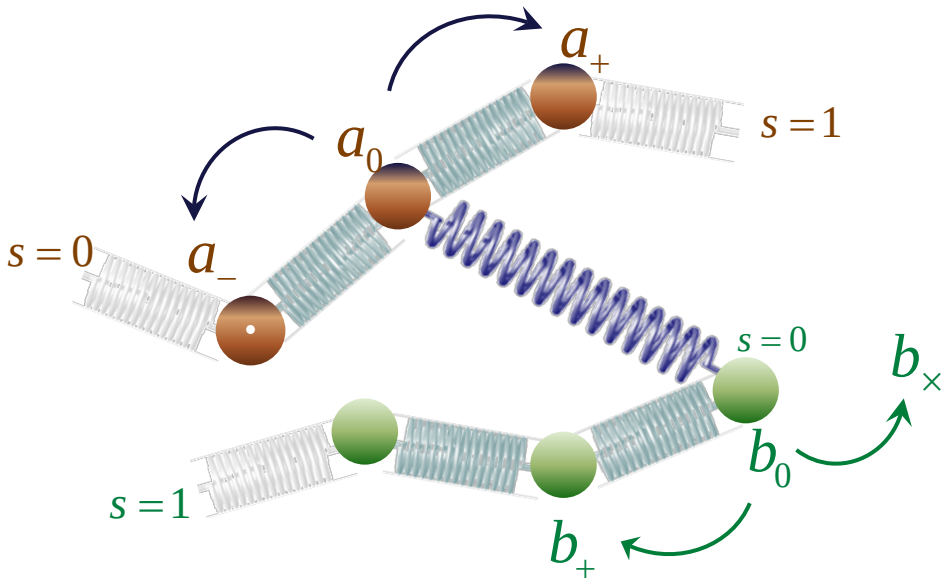

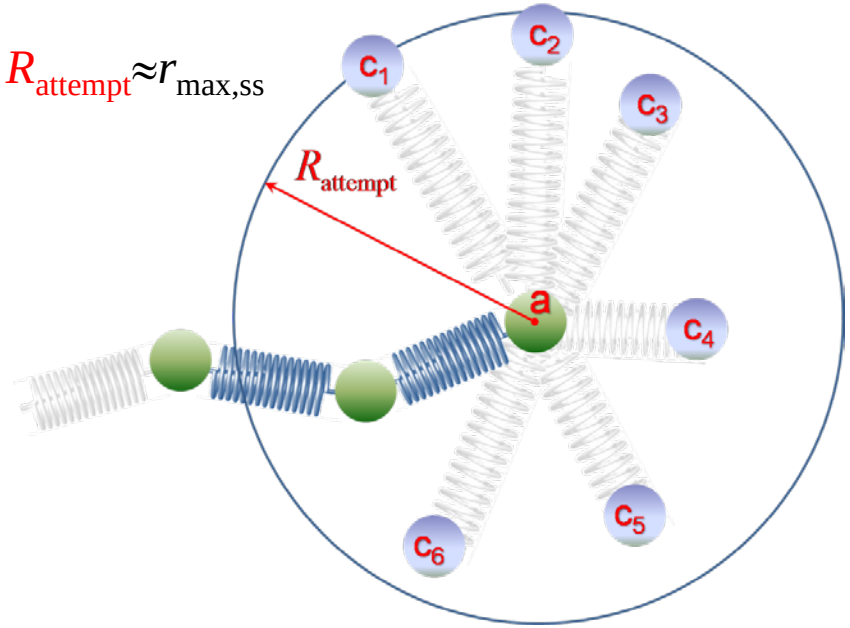

Destruction takes place for slip-springs connected with chain-ends.

Formation is initiated by chain ends.

$$k_{destruction} = k_{hop} \qquad k_{form}$$

Detailed balance: $\underset{destruction}{Rate} = \underset{formation}{Rate} \Rightarrow k_{form,a_0 \wedge b_\times \to a_0 \wedge b_0} = \nu_{hop} \frac{z_{activ}}{n_{ss,a_0 \wedge b_0}}$

Slip-spring formation, destruction, and hopping tracked by

Kinetic Monte Carlo (kMC) simulation

Vogiatzis, G.G.; Megariotis, G.; DNT *Macromolecules* **2017**, *50*, 3004.

Equilibrium melt: Chain conformation

PE 450 K, 1 bar

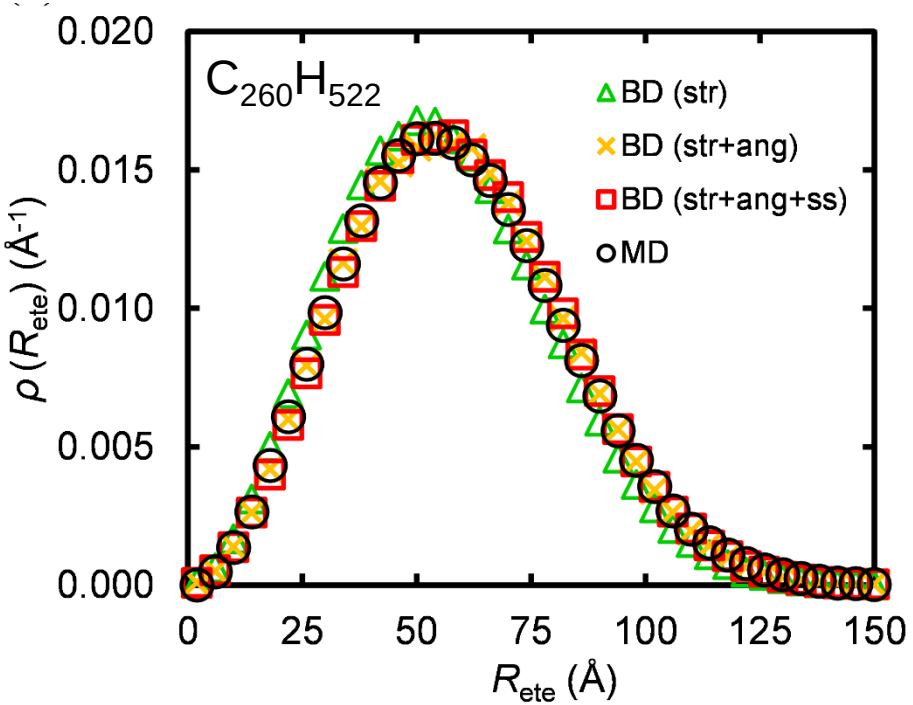

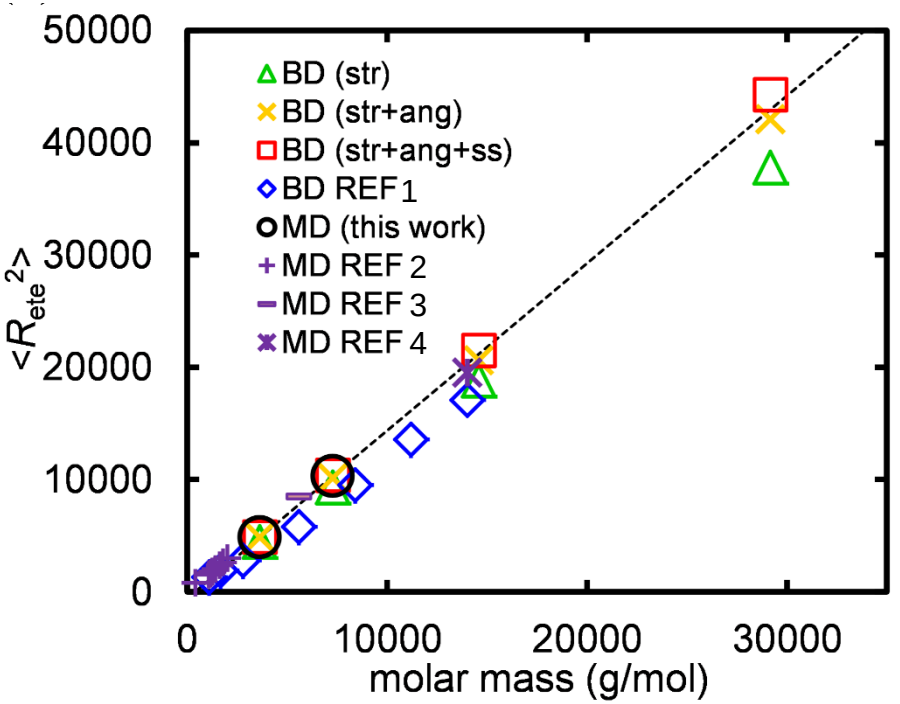

1. Padding, J.T.; Briels, W.J. *J. Chem. Phys.* **2002**, *117*, 925.
2. Harmandaris, V.A.; Mavrantzas, V.G.; DNT *Macromolecules* **1998**, *31*, 7934.
3. Nafar Sefiddashti, M.H.; Edwards, B.J.; Khomami, B. *J. Rheol*. **2015**, *59*, 119.
4. Harmandaris, V.A.; Mavrantzas, V.G. in Terzis, A.F.; Paspalakis, E. (Eds.) *Recent Research Topics and Developments in Chemical Physics: From Quantum Scale to Macroscale;* Research Signpost, 2008; p 179.

Sgouros, A. P.; Megariotis, G.; DNT *Macromolecules* **2017**, *50*, 4524-4541.

Equilibrium melt: Chain dynamics

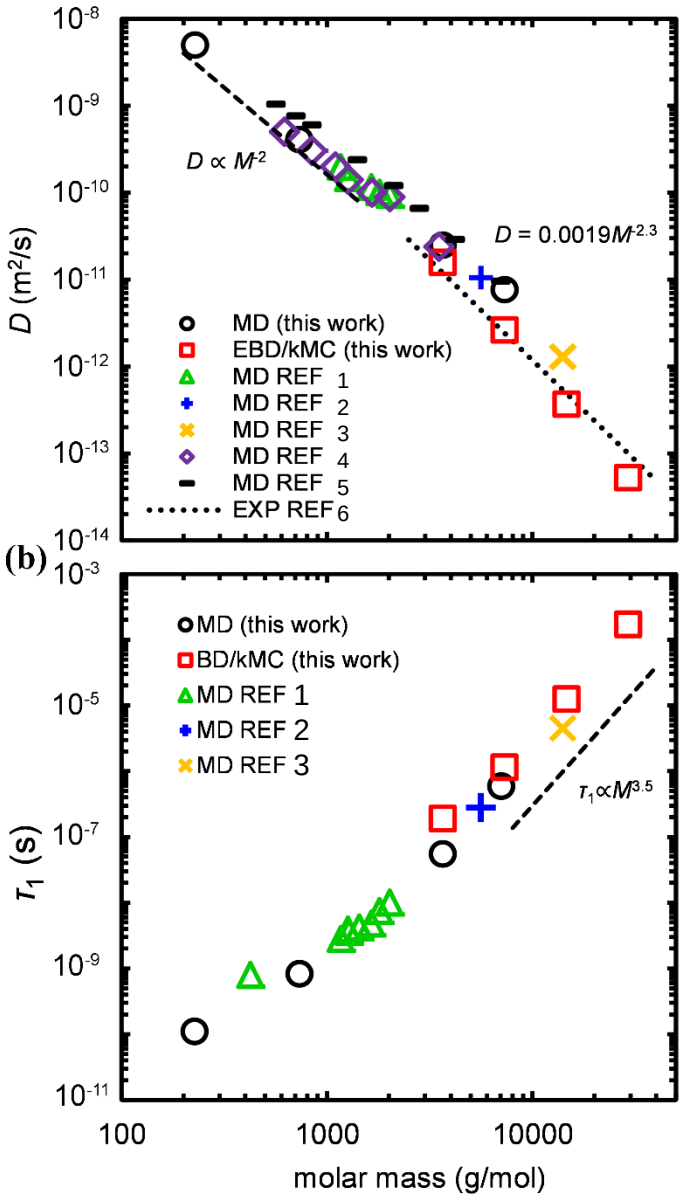

PE 450 K, 1 bar

1. Harmandaris, V.A.; Mavrantzas, V.G.; DNT *Macromolecules* **1998**, *31*, 7934.
2. Nafar Sefiddashti, M.H.; Edwards, B.J.; Khomami, B. *J. Rheol*. **2015**, *59*, 119.
3. Harmandaris, V.A.; Mavrantzas, V.G. in Terzis, A.F.; Paspalakis, E. (Eds.) *Recent Research Topics and Developments in Chemical Physics: From Quantum Scale to Macroscale;* Research Signpost, **2008**, p 179.
4. Hur, K.; Jeong, C.; Winkler, R.G.; Lacevic, N.; Gee, R.H.; Yoon, D.Y.; *Macromolecules* **2011**, *44*, 2311.
5. Harmandaris, V.A.; Mavrantzas, V.G.; DNT; Kröger, M.; Ramírez, J.; Öttinger, H.C.; Vlassopoulos, D. *Macromolecules* **2003**, *36*, 1376.
6. Lodge, T.P. *Phys. Rev. Lett* **1999**, *83*, 3218.

Sgouros, A. P.; Megariotis, G.; DNT *Macromolecules* **2017**, **2017**, *50*, 4524-4541.

Stress relaxation modulus from equilibrium BD/kMC

PE 450 K, 1 bar

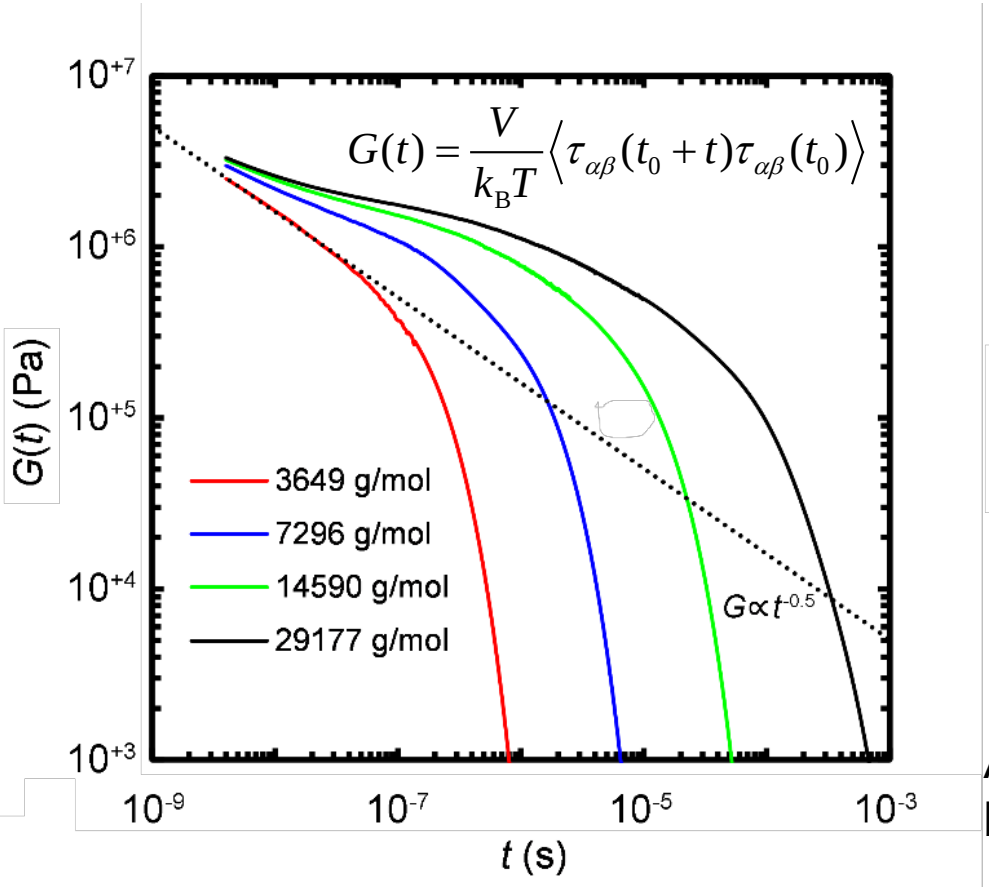

$$\boldsymbol{\tau} = \rho \mathbf{F} \cdot \left(\frac{\partial \left(A\left(\{\mathbf{R}_{ij}\}, \{\rho_{\text{cell}}\}, T \right) / m \right)}{\partial \mathbf{F}} \right)^{\mathrm{T}}$$

Deformation gradient tensor[1]

To improve accuracy, we average over all possible ways of choosing a pair of perpendicular axes:[2]

$$G(t) = \frac{V}{3k_B T} \left[\begin{array}{l} \langle \tau_{xy}(t_0+t)\tau_{xy}(t_0) \rangle \\ + \langle \tau_{xz}(t_0+t)\tau_{xz}(t_0) \rangle \\ + \langle \tau_{yz}(t_0+t)\tau_{yz}(t_0) \rangle \end{array} \right]$$

Autocorrelation functions are calculated by using the multiple tau-correlator.[3]

1. Sgouros, A. P.; Vogiatzis, G.G.; Megariotis, G.; Tzoumanekas, C.; DNT *Macromolecules* **2019**, *52*, 7503.
2. A. Likhtman, *in Polymer Science: A Comprehensive Reference*, edited by K. Matyjaszewski and M. Möller (Elsevier, Amsterdam, 2012) pp. 133-179.
3. Ramirez, J.; Sukumaran, S. K.; Vorselaars, B.; Likhtman, A.E. *J. Chem. Phys.* **2010**, *133*, 154103.

Mesoscopic BD/kMC simulation of Polymer/Solid Interfaces

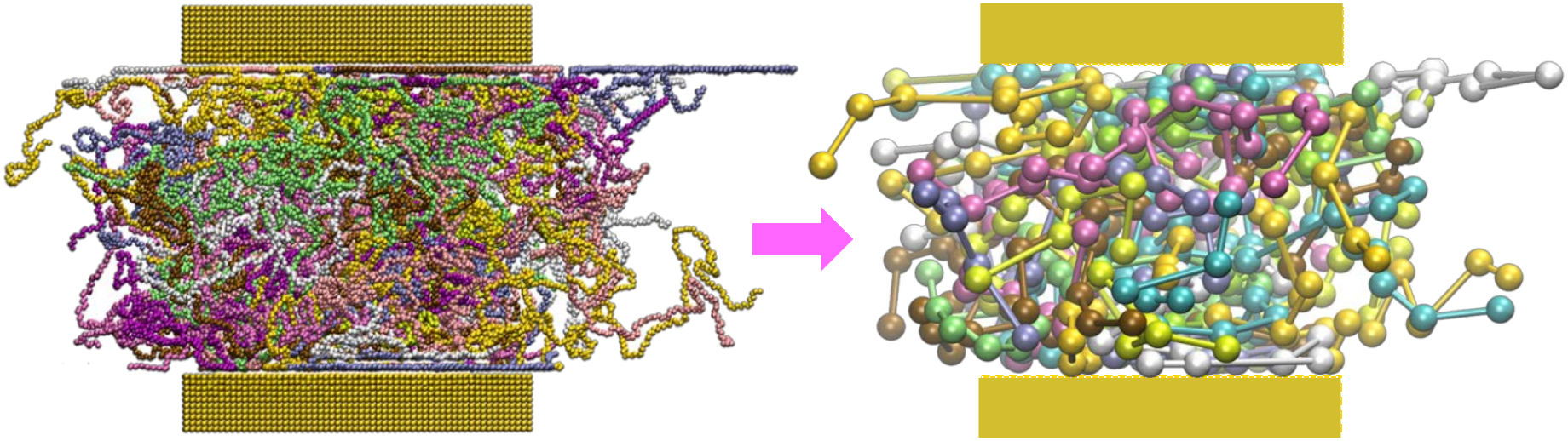

Sgouros, A. P.; Vogiatzis, G.G.; Megariotis, G.; Tzoumanekas, C.; DNT *Macromolecules* **2019**, *52*, 7503.

Sgouros, A.P.; DNT *Molec. Phys*. **2020**, *118*, e1706775.

Sgouros, A.P.; Tsagkalakis, D.; DNT *J. Phys. Chem*. **2021**, *125*, 6681-6696.

Lifetimes of adsorbed chains: PE melt/graphite

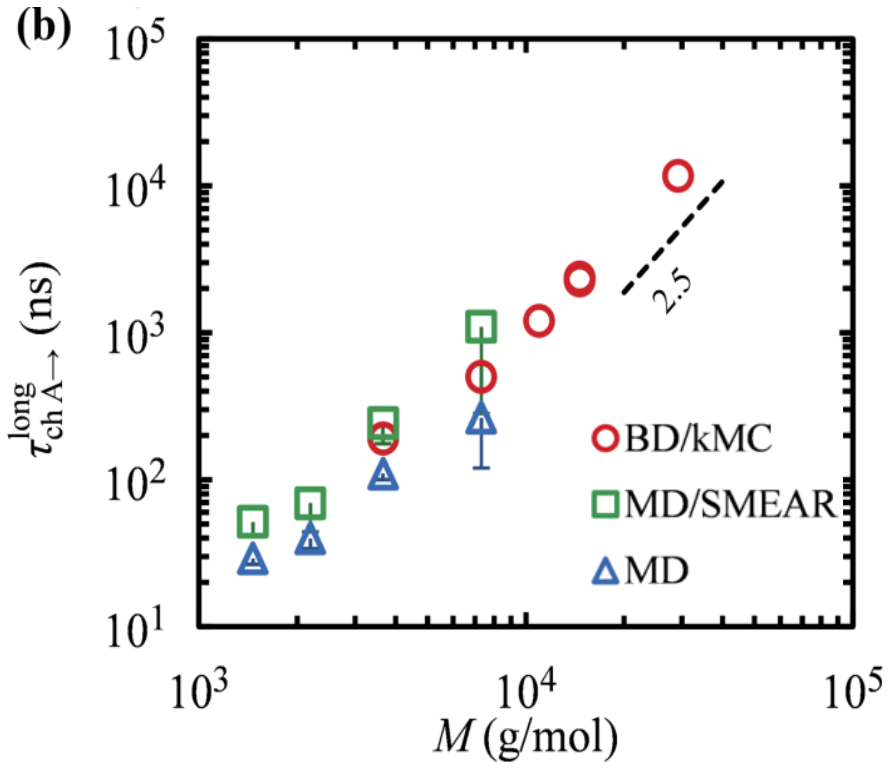

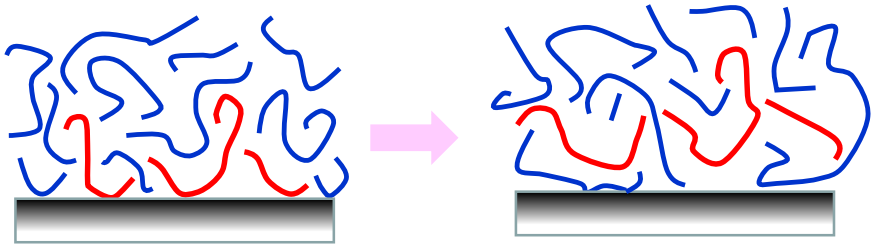

$$\tau^{\text{long}}_{\text{ch,A}\rightarrow} = 1/k^{\text{long}}_{\text{ch,A}\rightarrow}$$

Relaxation time extracted from long-time linear slope of hazard plot for desorption of *entire chain.*

Scaling $\tau^{\text{long}}_{\text{ch,A}\rightarrow} \sim M^{2.5}$ for long chains suggests diffusion-limited desorption.

Chain end-to-end vectors exhibit longer and more strongly M-dependent correlation times.

Douglas, J.F.; Frantz, P.; Johnson, H.E.; Schneider, H.M.; Granick, S. *Colloids Surf*. **1994**, *86*, 251.

Douglas, J.F.; Johnson, H.E.; Granick, S. *Science* **1993**, *262*, 2010.

Sgouros, A. P.; Vogiatzis, G.G.; Megariotis, G.; Tzoumanekas, C.; DNT *Macromolecules* **2019**, *52*, 7503.

Summary

- Coarse-graining is a necessity given the multiplicity of length and time scales in soft matter systems.
- Optimal selection of coarse-grained variables depends on the problem at hand.
- Strategies for approximating many-body potential of mean force: Force Matching, Iterative Boltzmann Inversion, Pretabulation of Interactions.
- Projection Operator Formalism provides a rigorous framework for dynamical coarse-graining. Its implementation in Langevin, Brownian, and Dissipative Particle Dynamics methods calls for judicious approximations.
- Brownian Dynamics/kinetic Monte Carlo with slip springs offers versatile tools for addressing dynamics of entangled polymers.